

6-5-1962

The Determination of Thermal Neutron Density from the Absolute Measurement of the Activity Induced in Gold Foils

Munson M. Thorpe

Follow this and additional works at: https://digitalrepository.unm.edu/phyc_etds



Part of the [Physics Commons](#)

Recommended Citation

Thorpe, Munson M.. "The Determination of Thermal Neutron Density from the Absolute Measurement of the Activity Induced in Gold Foils." (1962). https://digitalrepository.unm.edu/phyc_etds/171

This Thesis is brought to you for free and open access by the Electronic Theses and Dissertations at UNM Digital Repository. It has been accepted for inclusion in Physics & Astronomy ETDs by an authorized administrator of UNM Digital Repository. For more information, please contact disc@unm.edu.

UNIVERSITY OF NEW MEXICO-GENERAL LIBRARY



A14420 866461

378.789

Un30tho

1962

cop. 2

DETERMINATION OF THERMAL NEUTRON DENSITY

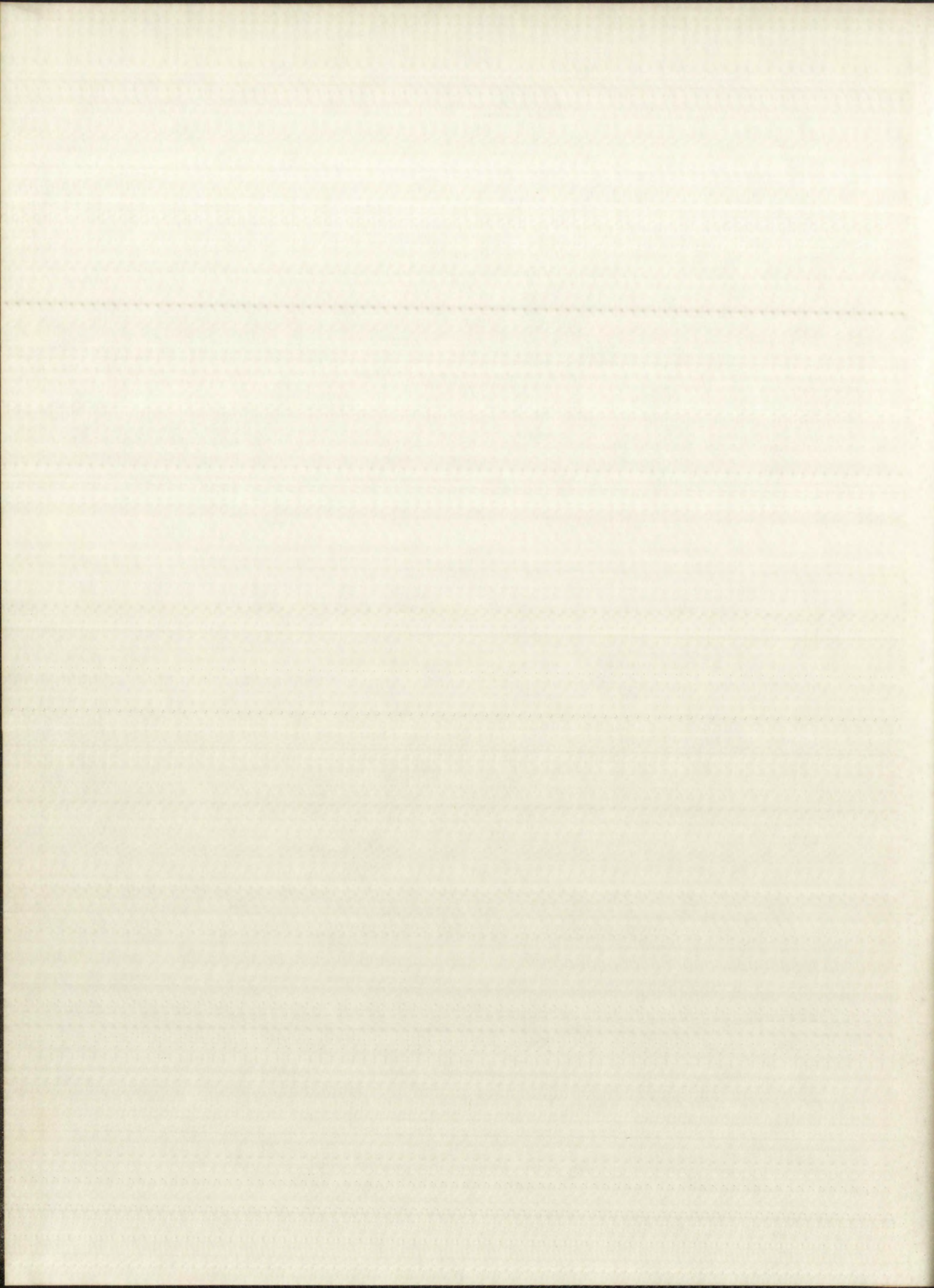
— THEODORE

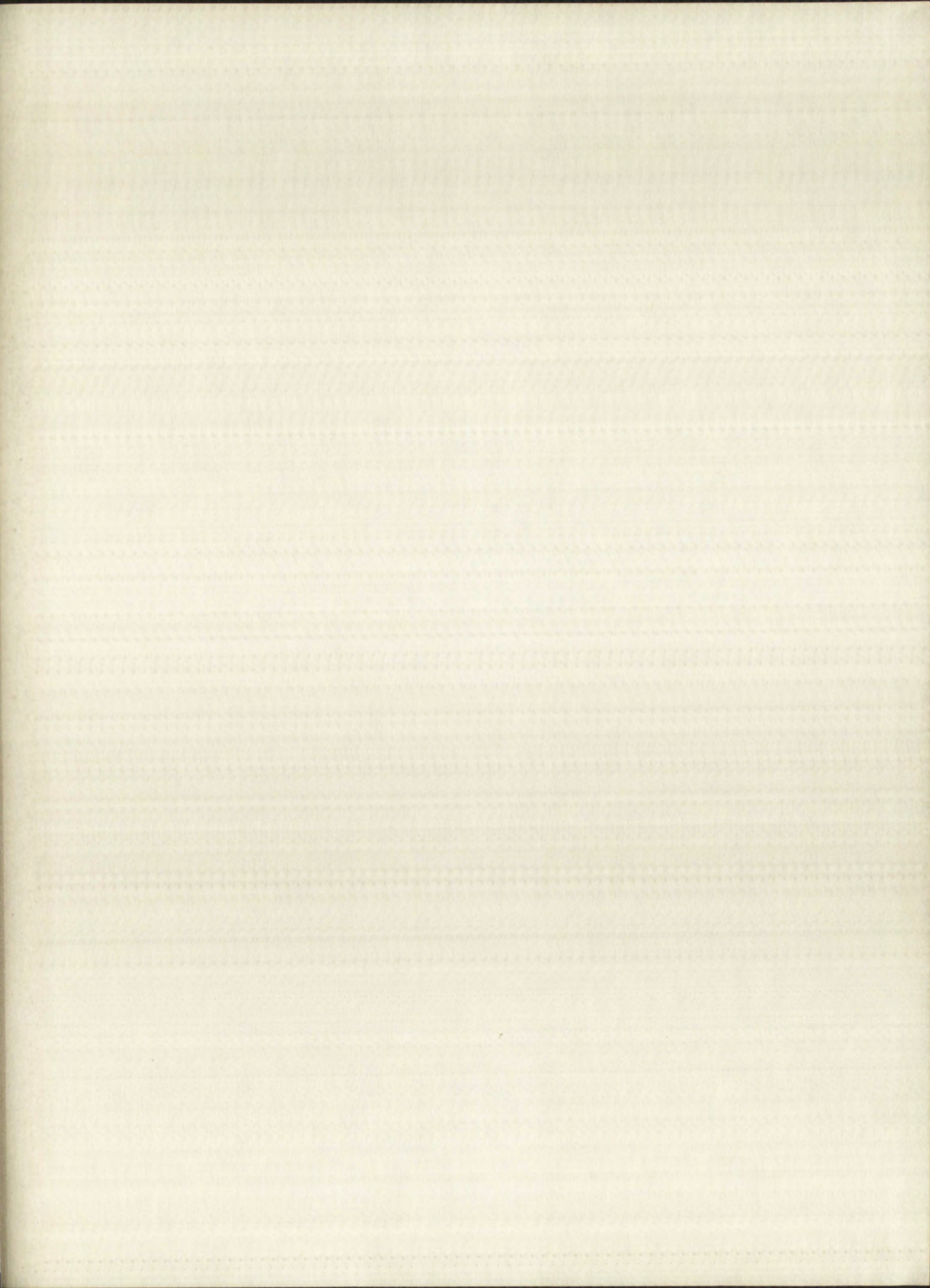
THE LIBRARY
UNIVERSITY OF NEW MEXICO

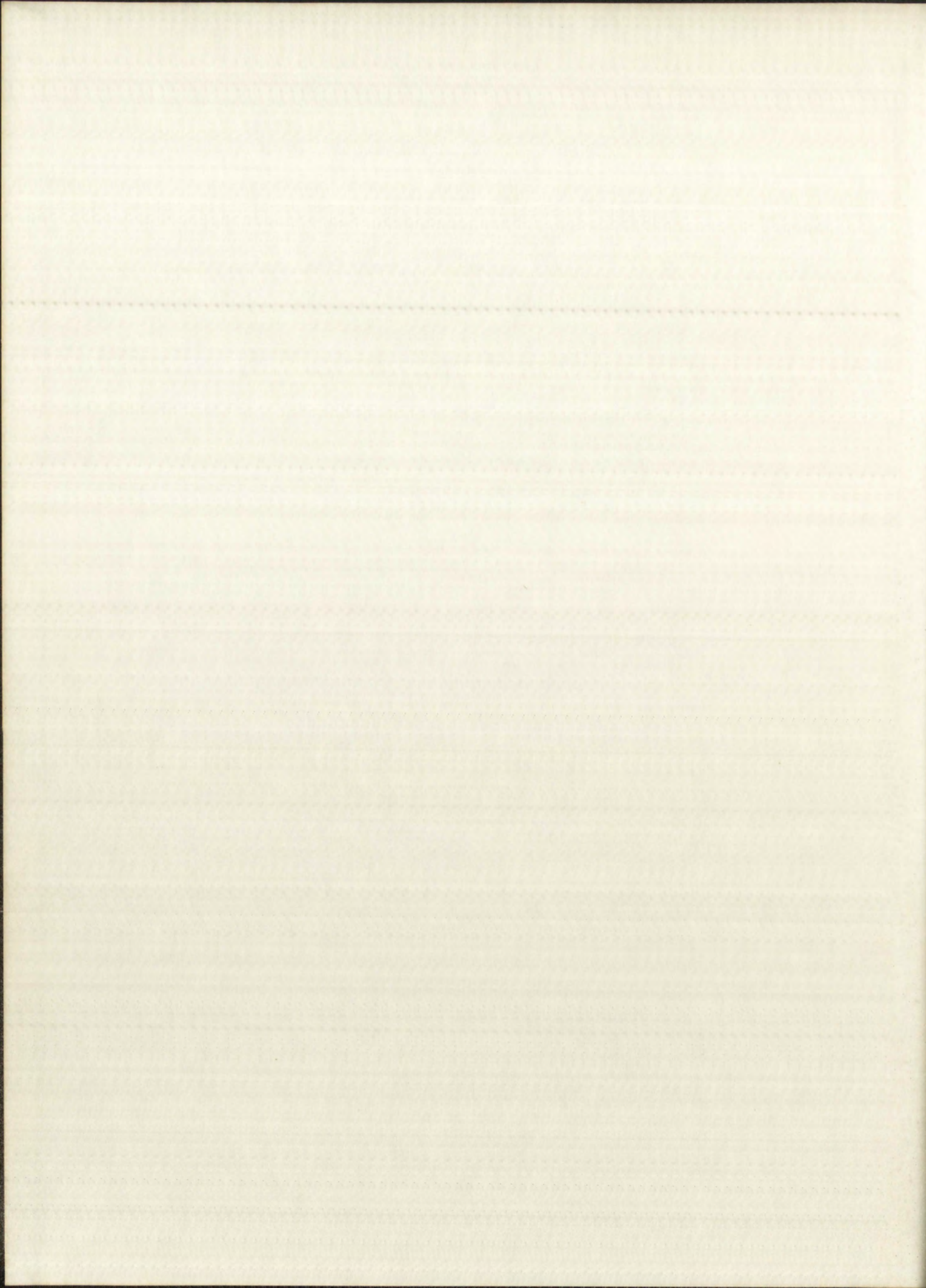


Call No.
378.789
Un30tho
1962
cop.2

Accession
Number
291575







LIBERTY

WASB FOND

OTIOLIBRE

ALBERT
CASE BOND
ON 11/18/75

UNIVERSITY OF NEW MEXICO LIBRARY

MANUSCRIPT THESES

Unpublished theses submitted for the Master's and Doctor's degrees and deposited in the University of New Mexico Library are open for inspection, but are to be used only with due regard to the rights of the authors. Bibliographical references may be noted, but passages may be copied only with the permission of the authors, and proper credit must be given in subsequent written or published work. Extensive copying or publication of the thesis in whole or in part requires also the consent of the Dean of the Graduate School of the University of New Mexico.

This thesis by Munson M Thorpe
has been used by the following persons, whose signatures attest their acceptance of the above restrictions.

A Library which borrows this thesis for use by its patrons is expected to secure the signature of each user.

NAME AND ADDRESS

DATE

ERASE
COPY CONTENT

MANUSCRIPT TERMS

Unpublished theses submitted to the University of New Mexico are deposited in the University of New Mexico Library and are open for inspection, but are not to be copied or otherwise used without the consent of the author. Bibliographical references may be made and passages may be copied only with the permission of the author and proper credit must be given in subsequent written or published work. Extensive copying or publication of theses in whole or in part requires also the consent of the Dean of the Graduate School of the University of New Mexico.

This thesis by Wenon H. George

has been used by the following persons whose names are listed in the acceptance of the above restrictions:

A Library which borrows this thesis has not yet been identified. It is expected to secure the signature of each user.

NAME AND ADDRESS
LIBRARY
UNIVERSITY OF NEW MEXICO
ALBUQUERQUE, N.M.

THE DETERMINATION OF THERMAL NEUTRON DENSITY
FROM THE ABSOLUTE MEASUREMENT OF THE ACTIVITY INDUCED IN GOLD FOILS

By

Munson M. Thorpe



A Thesis

Submitted in Partial Fulfillment of the

Requirements for the Degree of

Master of Science in Physics

//////////

The University of New Mexico

1962



MUNSON MEADE THORPE

This thesis, directed and approved by the candidate's committee, has been accepted by the Graduate Committee of the University of New Mexico in partial fulfillment of the requirements for the degree of

MASTER OF SCIENCE

Stuart A. Thorpe
Dean

June 5, 1962
Date

Thesis committee

C. P. Lemons
Chairman

Howard C Bryant

Donald Spurgeon

This thesis, directed and approved by the committee on
advice, has been accepted by the Graduate Council of the
University of New Mexico in partial fulfillment of the require-
ments for the degree of

MASTER OF SCIENCE

[Signature]

March 21/1942
Date

Thesis committee

[Signature]
Chairman

[Signature]

[Signature]

UCLD

378,789
Un 30tho
1962
cop. 2

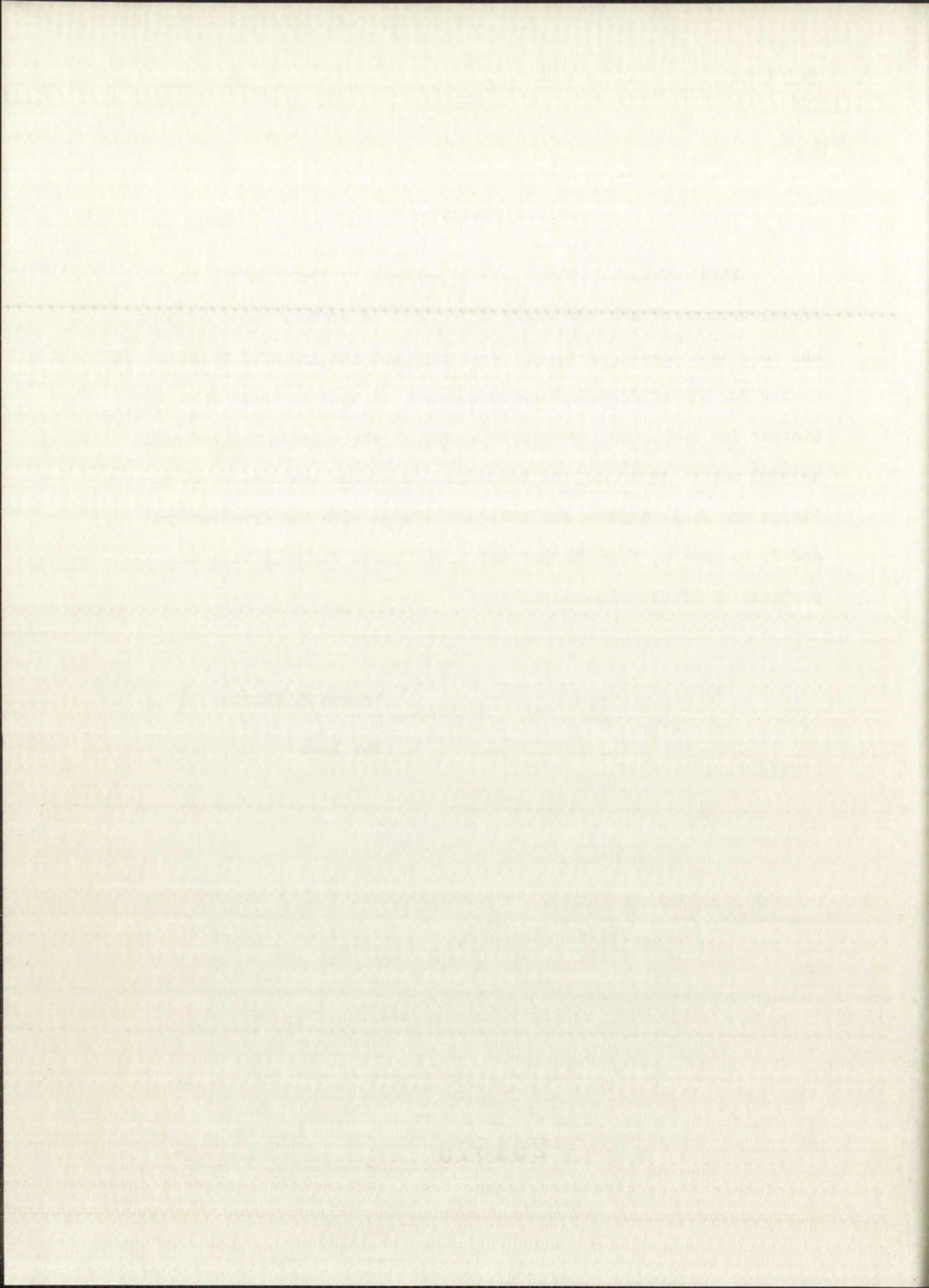
ACKNOWLEDGMENTS

First of all I should like to express my gratitude to the Administration of the Los Alamos Scientific Laboratory whose support has made this thesis possible. I am indebted and grateful to Robert E. Carter for his guidance and encouragement. I wish to thank John W. Starner for supplying the detectors used in the experiment, and much helpful advice regarding the techniques of source evaluation; E. H. Pierce and J. K. Heydorn for their assistance with the irradiations; and F. D. Newcom, K. H. Harper and L. K. Thorpe for help with the preparation of the manuscript.

Munson M. Thorpe

May 1962

291575



ABSTRACT

The interaction of thermal neutrons with a coin shaped detector is discussed in terms of the reaction rate in an infinite sheet of pure absorber irradiated in a void by an isotropic, Maxwell distribution of thermal neutrons. A coincidence method for the evaluation of the decay rate of the neutron induced activity in gold is examined in detail and utilized to measure the relative specific activity of gold foils exposed to neutrons in the graphite thermal column of the Water Boiler Reactor. The relative specific activity was obtained for 3/4" and 1/4" diameter foils as a function of thickness for values of the thickness from 1.5 mg/cm² to a nominal thickness of .010". From the activity of the thinnest foils, the neutron density in the thermal column was obtained relative to the reactor power and the counting rate of a parallel plate fission chamber.

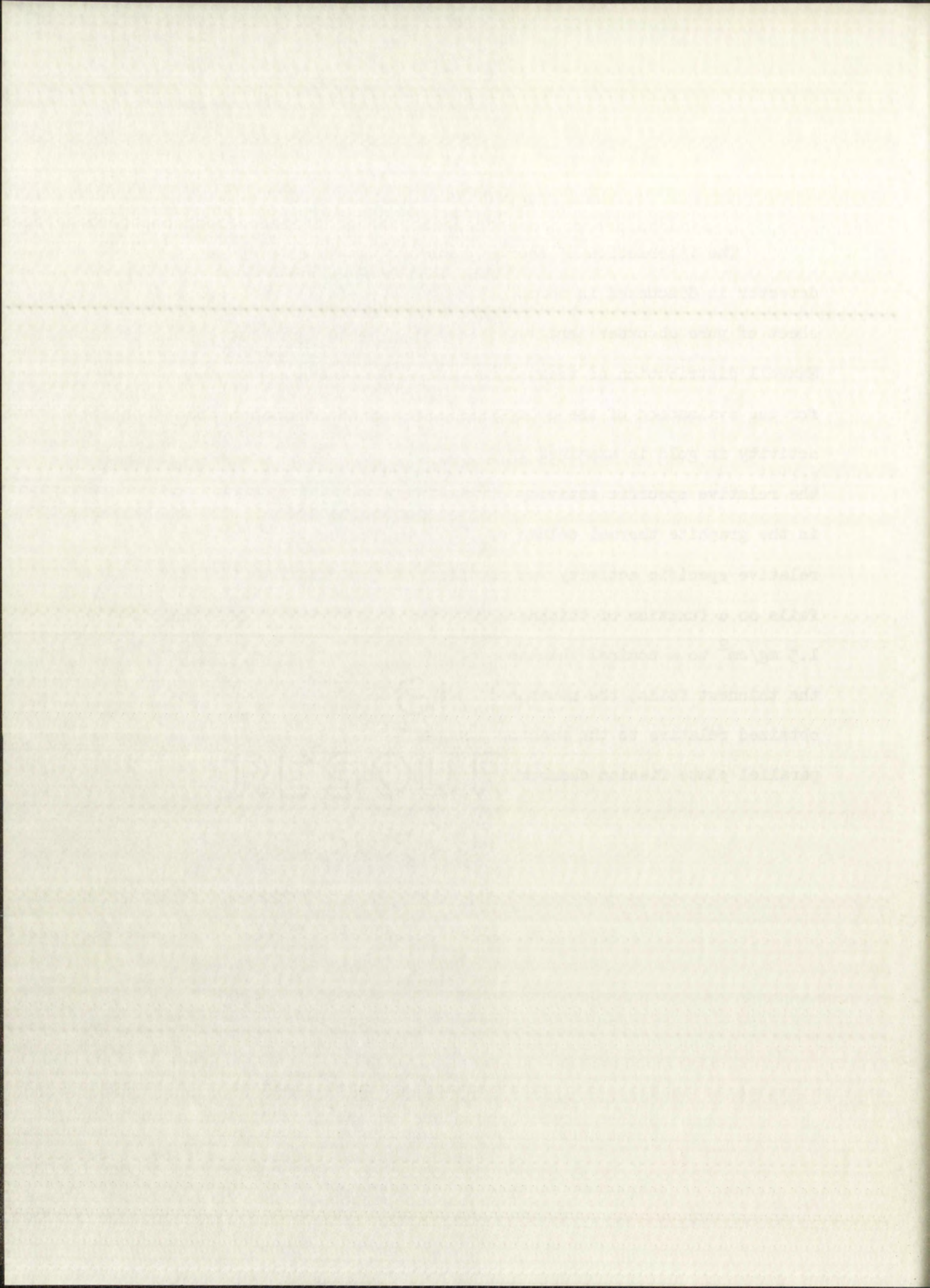
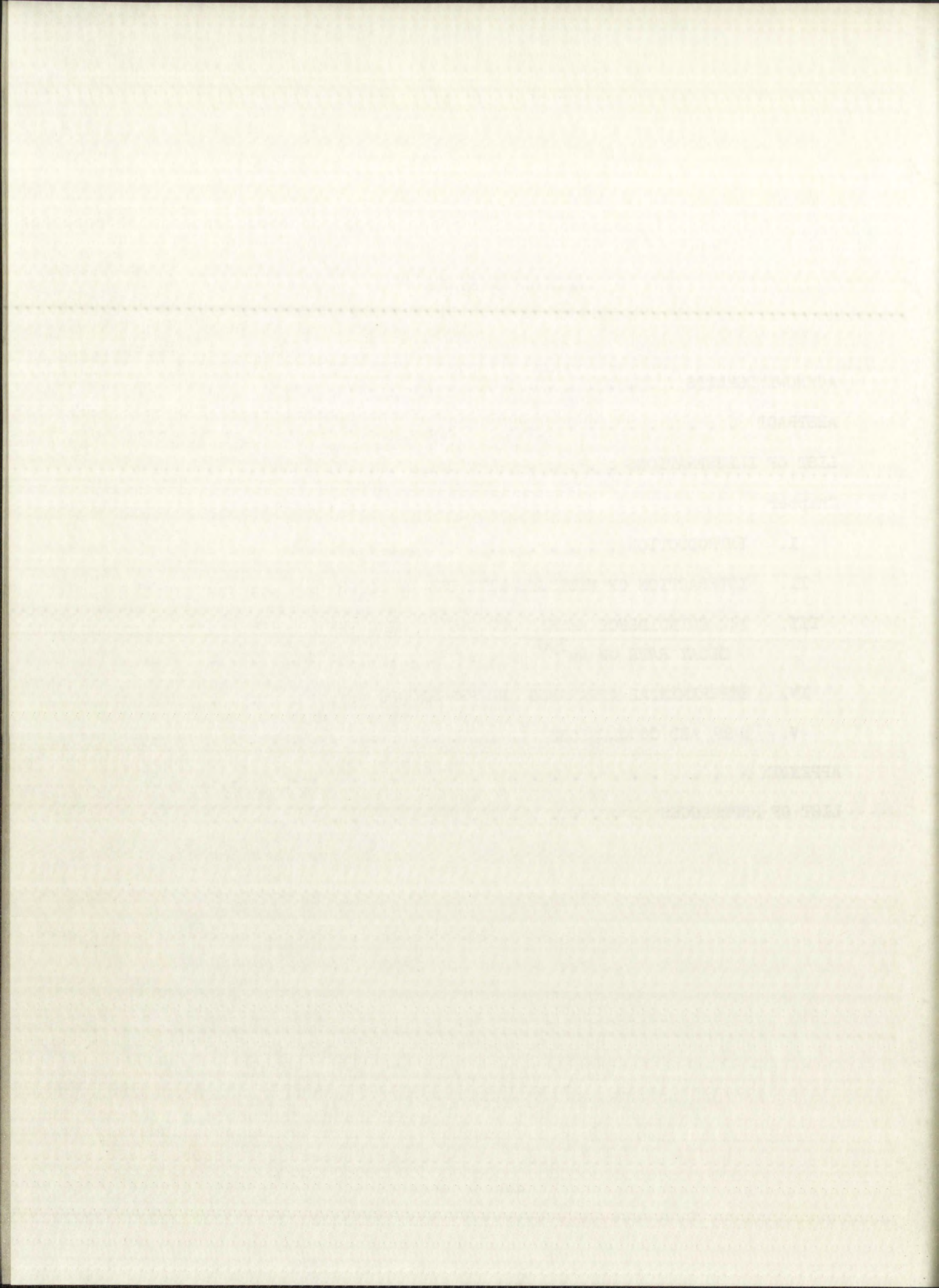


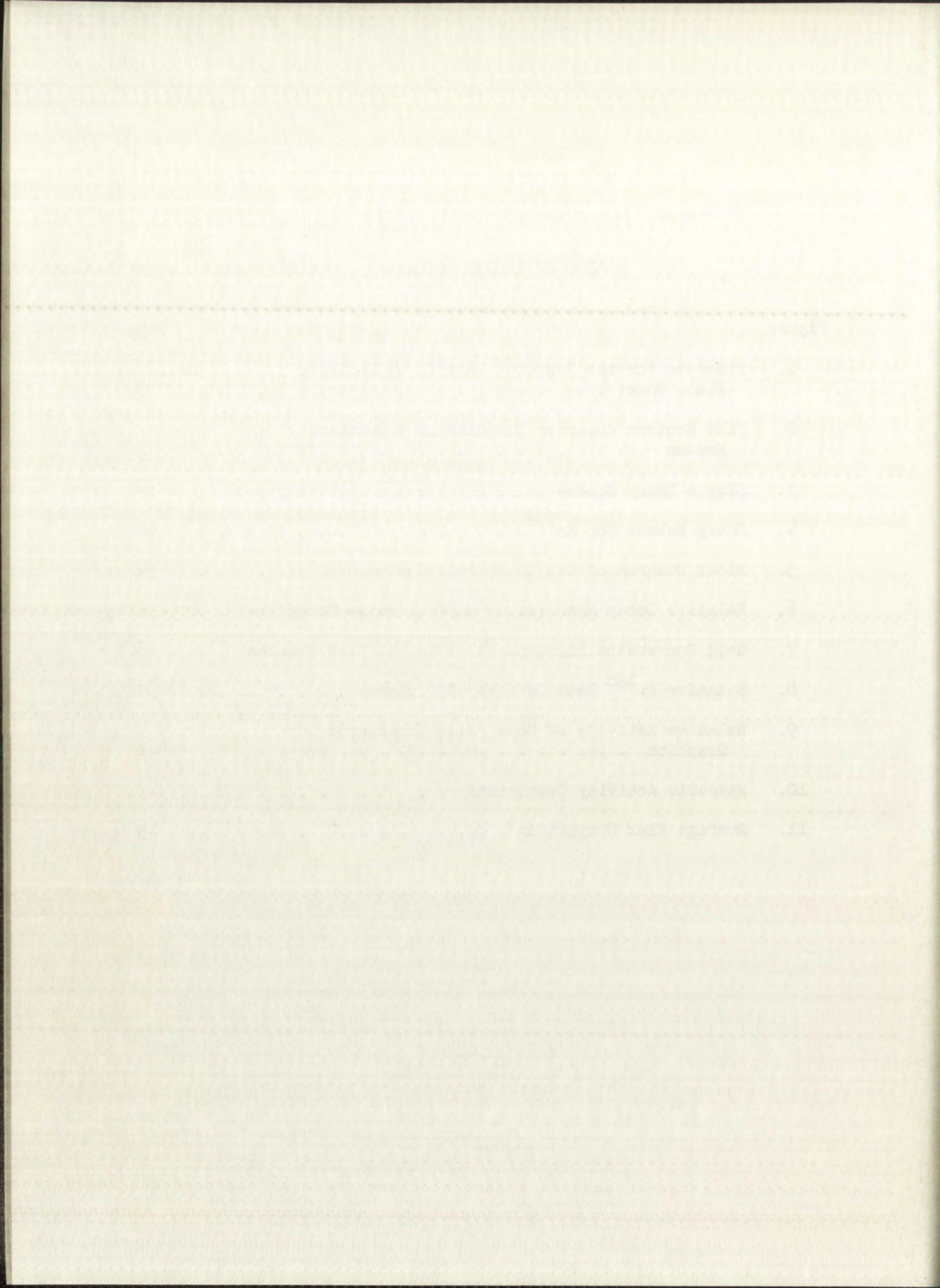
TABLE OF CONTENTS

	Page
ACKNOWLEDGMENTS	ii
ABSTRACT	iii
LIST OF ILLUSTRATIONS	v
Chapter	
I. INTRODUCTION	1
II. INTERACTION OF NEUTRONS WITH THE DETECTOR	5
III. THE COINCIDENCE METHOD FOR DETERMINING THE ABSOLUTE DECAY RATE OF Au ¹⁹⁸	16
IV. EXPERIMENTAL APPARATUS AND PROCEDURES	33
V. DATA AND CONCLUSIONS	39
APPENDIX A	50
LIST OF REFERENCES	53



LIST OF ILLUSTRATIONS

Figure		Page
1.	Diagrams for the Reaction Rate in an Infinite Plane Sheet	8
2.	Disc Neutron Absorber Imbedded in a Scattering Medium	11
3.	Simple Decay Scheme	17
4.	Decay Scheme for Au ¹⁹⁸	26
5.	Block Diagram of the Electronic Equipment	34
6.	Relative Decay Rate Versus Minimum Pulse Height	36
7.	Gold Conversion Electron Pulse Height Distribution	36
8.	Relative Au ¹⁹⁸ Beta Detector Efficiency	37
9.	Relative Activity of Gold Foils Irradiated in Graphite	41
10.	Specific Activity Comparison	43
11.	Average Flux Comparison	45



INTRODUCTION

Since the neutron was discovered by Chadwick in 1932, the study of the neutron and its interaction with matter has constituted a large part of nuclear physics. This study involves not only information about the nuclei under investigation but also requires knowledge of such quantities as the energy, angular and spatial distribution of the incident neutrons. There are many sources of neutrons now available ranging from the interaction of alpha particles with beryllium to the neutrons produced from fission in a nuclear reactor. Further, such sources or distribution of sources may be placed in a single medium or in combinations of various media. This discussion will be mainly concerned with the situation produced when neutrons are introduced into a large quantity of highly scattering and more or less non-absorbing homogeneous media such as graphite, heavy water and ordinary water. When neutrons enter scattering media they lose energy by elastic and inelastic collision with the nuclei of the material. Most neutrons reaching points distant from the source will have suffered many collisions and the energies of the scattered neutrons will have been correspondingly reduced. Not all neutrons will have the same collision history. Even in the case of a mono-energetic source there will exist throughout the medium a spectrum of neutron energies extending from the source energy to energies comparable with the thermal agitation energy of the scattering nuclei. Calculations have shown and experiment has verified that within a weakly

Faint, illegible text, possibly bleed-through from the reverse side of the page.

absorbing material far from sources and boundaries the neutron spectrum will resemble the Maxwell energy distribution for the atoms of an ordinary mono-atomic gas at the temperature of the medium. There will also be present, to a lesser extent, a distribution of neutrons which have not yet reached thermal energies. For media of relatively large atomic mass such as graphite, the angular distribution will be approximately isotropic.

Several types of reactions are available for the detection of thermal neutrons. The reaction cross sections are relatively large and, for many of the substances commonly used, are proportional to the reciprocal of the relative velocity of the neutron and the target nucleus. The reactions may be divided into two groups; those which promptly yield readily detectable radiation such as an alpha particle or fission fragment and those producing an excited nucleus which later decays by the emission of radiation in the form of beta particles, gamma rays or both. The latter type of reaction seems more appropriate for the investigation and exploration of the neutron situation described in the preceding paragraph. A small quantity of neutron detecting material perhaps in the form of a foil or coin may be conveniently placed in the region of interest and, after suitable neutron exposure, removed to an apparatus for determining the induced activity.

The activation of foils by neutrons has been and remains a very satisfactory method of neutron detection. In recent years the measurement of neutron cross sections with high accuracy and the development of gamma and beta ray counting techniques have created even more interest in this method. Of particular importance is the use of gold as a thermal neutron detector. The half-life and decay scheme are well known and the decay scheme is sufficiently uncomplicated that the β - γ coincidence method

The text on this page is extremely faint and illegible. It appears to be a multi-paragraph document, possibly a report or a letter, but the content cannot be discerned. The text is mirrored across the page, suggesting a scanning artifact or bleed-through from the reverse side.

for evaluating absolute decay rates may be used. The neutron activation cross section has been measured as a function of energy¹⁺ and a value of 98.8 ± 0.3 barns is quoted² for the value of the cross section at 2200 m/sec. The behaviour of the cross section is nearly $1/v$ in the thermal region.

If a small enough quantity of $1/v$ material is used as a neutron detector the induced activity is proportional to the neutron density and is independent of the energy and angular distribution. For practical reasons the material should be in a form that can be handled and weighed accurately. Also enough material must be used so that an irradiation for a reasonable length of time will yield a decay rate which may be evaluated with the required degree of precision. The response of a finite detector is not independent of the neutron energy and angular distribution. Further, the presence of the detector perturbs the original distributions. It is necessary then to establish the response of the detector in some manner. The problem of the activation of a neutron absorber placed in a medium has been the object of much theoretical and experimental interest.^{3,4,5,6,7} Accurate calculations of the response of the detector involve a numerical solution of the integro-differential equation of neutron transport. An approximate relationship for a coin or foil shaped detector may be derived in terms of the activation in a void of an infinite sheet of material. The effects of the adjacent scattering media and the finite size of the detector are regarded as corrections which approach zero as the thickness of the foil becomes very small. This relationship, first introduced by Bothe,³ will be considered in the first chapter of this discussion. When sufficient

⁺Superscript numbers in the text refer to items so numbered in the List of References, infra.

The following table shows the results of the survey conducted in 1964. The data is presented in a tabular format, with columns representing different categories and rows representing the years 1964 and 1965. The table is located at the top of the page, above a dashed line.

The first section of the report discusses the overall findings of the survey. It highlights the key trends and provides a summary of the data presented in the table. This section is located in the middle of the page, below the dashed line.

The second section of the report provides a detailed analysis of the data. It examines the various factors that influence the results and discusses the implications of the findings. This section is located in the lower middle part of the page.

The final section of the report concludes the study and offers recommendations for future research. It summarizes the main points and provides a final assessment of the survey's findings. This section is located at the bottom of the page.

neutron intensity and counting system sensitivity are available, it is possible to measure the activity produced per gram of detector as a function of detector thickness. The curve obtained may then be extrapolated to zero thickness where the proportionality between the neutron density and decay rate is applicable.

The twelve-inch diameter spherical vessel constituting the core of the Water Boiler reactor is surrounded by a large region of graphite. Within this region, approximately four feet from the core, less than 10^{-4} of the activity produced in gold will be due to neutrons which have not yet reached thermal energies. At this position the neutron density is great enough that a few hours of irradiation will yield gold decay rates in excess of 3×10^4 dis/sec per milligram. It is the purpose of this research to measure the relationship between the neutron induced activity and the thickness of gold foils irradiated at such a position within the graphite surrounding the reactor core. The data obtained will provide a measurement of the thermal neutron density at the given position. The known neutron density can be used to predict the decay rate of sources made from various materials and can serve as a standard for the calibration of other neutron detectors and counting systems. Also the measured values of the activity per gram of gold foils of varying thickness may be compared to those values obtained by means of different methods of calculation.

...the ... of ...
...the ... of ...
...the ... of ...
...the ... of ...
...the ... of ...

...the ... of ...
...the ... of ...
...the ... of ...
...the ... of ...
...the ... of ...

...the ... of ...
...the ... of ...
...the ... of ...
...the ... of ...
...the ... of ...

...the ... of ...
...the ... of ...
...the ... of ...
...the ... of ...
...the ... of ...

...the ... of ...
...the ... of ...
...the ... of ...
...the ... of ...
...the ... of ...

CHAPTER II

INTERACTION OF NEUTRONS WITH THE DETECTOR

Suppose the probability of interaction per unit neutron path length in a given material is Σ . If the density of neutrons in the material is n and the speed of the neutrons is v then the path length swept out per unit volume per second is nv . The product nv is called the neutron flux. The reaction rate per unit volume may then be expressed by:

$$R_1 = \Sigma nv.$$

Frequently one is concerned with a distribution of neutrons having different velocities. The quantity

$$\phi = \int_v n(v) v dv$$

represents the total path length swept out per unit volume per second by all neutrons in the distribution. The neutron density per unit velocity interval is designated by $n(v)$. The flux may also be written in terms of the average velocity of the distribution and the total neutron density,

$$\phi = n_0 \bar{v} .$$

The average velocity and the total neutron density are defined by:

$$n_0 = \int_v n(v) dv$$

and

$$\bar{v} = \frac{\int_v n(v) v dv}{\int_v n(v) dv} .$$

The reaction rate per unit volume in this instance is given by:

$$R_V = \int_v \Sigma(v) n(v) v dv .$$

Faint, illegible text, possibly bleed-through from the reverse side of the page. The text is mirrored and difficult to decipher.

For many substances $\Sigma(v)$ is proportional to the reciprocal of the relative neutron velocity. That is:

$\Sigma(v) = \Sigma_0 v_0 / v$, where Σ_0 represents the macroscopic cross section of the material for neutrons having velocity v_0 . The reaction rate per unit volume for this type of material is:

$$R_0 = \int_v \Sigma_0 v_0 n(v) dv = \Sigma_0 n v_0 .$$

If one introduces into a uniform neutron flux distribution a quantity of $1/v$ neutron detector substance so small that the presence of the detector does not perturb the original distribution one can obtain the total neutron density from:

$$R_V = \int_v \int_V \Sigma(v) n(v) v dv dV = V \Sigma_0 n v_0 .$$

The total volume of detector material is given by V . Σ , the probability of interaction per unit neutron path length, is found to be proportional to the density of nuclei.

$$\Sigma = N\sigma .$$

The proportionality constant σ is designated the microscopic cross section for the reaction considered. The density of nuclei is given by:

$$N = N_0 \rho / A.$$

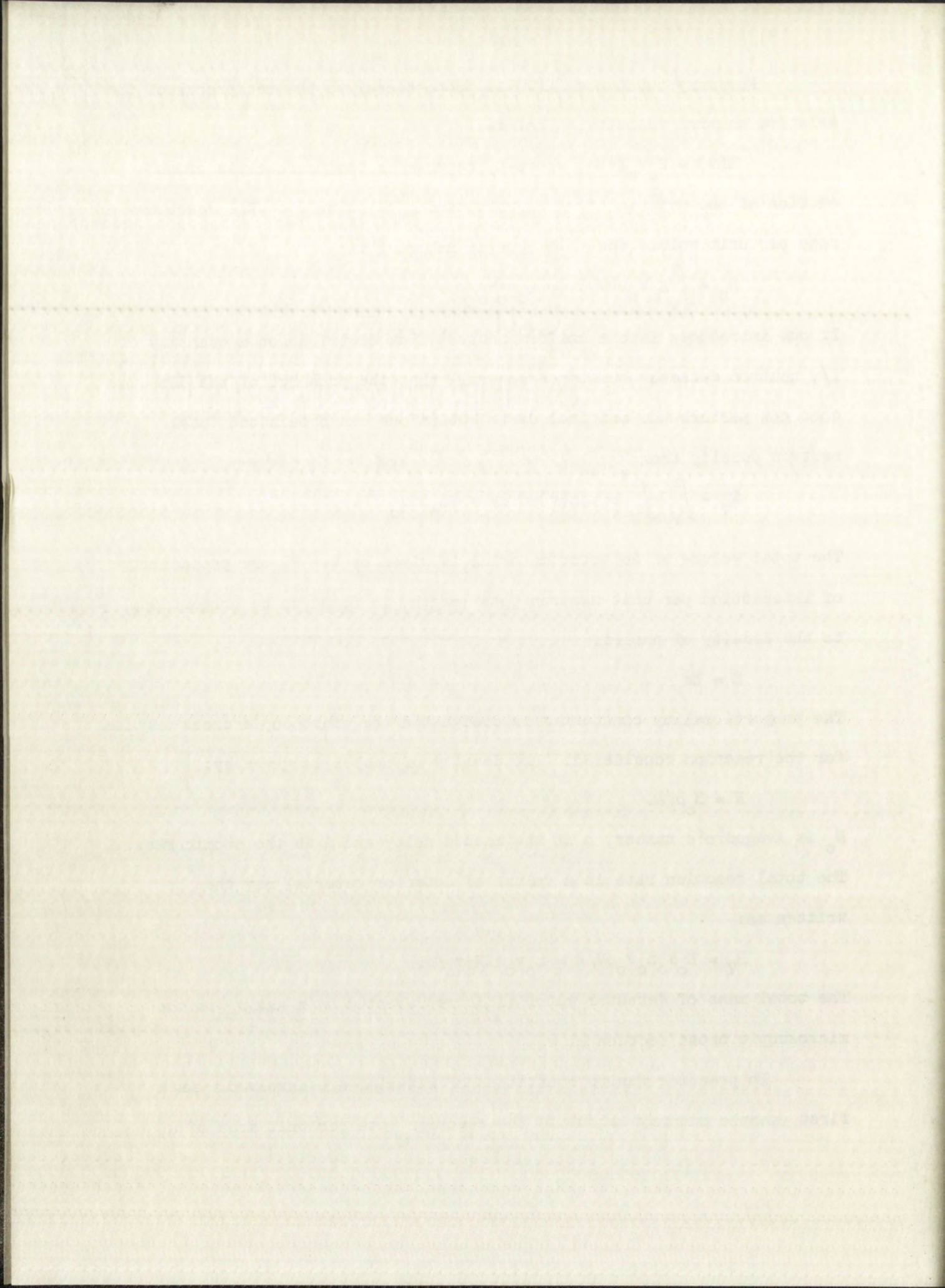
N_0 is Avagadro's number, ρ is the mass density and A is the atomic mass.

The total reaction rate in a volume of detector material may then be written as:

$$R_V = N_0 \sigma_0 n v_0 \rho V / A = n v_0 m N_0 \sigma_0 / A.$$

The total mass of detector material is represented by m and σ_0 is the microscopic cross section at v_0 .

In practice finite quantities of material are involved. As a first example one may calculate the reaction rate per unit area of a



large thin sheet of purely absorbing material. For this example the incident neutron distribution is assumed to be mono-energetic, isotropic and uniform over the surface of the sheet. The number of captures due to neutrons incident on a unit area of foil from the solid angle $d\Omega$ is given by (Appendix A, Sect. 1):

$$nv/4\pi \left\{ 1 - \exp[-\Sigma t/|\cos\theta|] \right\} |\cos\theta| d\Omega .$$

The term $(1 - \exp[-\Sigma t/|\cos\theta|])$ represents the probability that a neutron incident from the direction defined by the angles (θ, ϕ) (Fig. 1a) will be captured while traversing the distance $l = t/|\cos\theta|$ (Fig. 1b). Integrating over the entire solid angle yields the total rate of capture per unit area.

$$R_{\theta} = nv/4\pi \int_0^{\pi} \int_0^{2\pi} \left\{ 1 - \exp[-\Sigma t/|\cos\theta|] \right\} |\cos\theta| \sin\theta d\theta d\phi .$$

The integration may be performed, yielding the result (Appendix A, Sect. 2):

$$R_{\theta} = \frac{1}{2}nv \left[1 - e^{-\Sigma t} (1 - \Sigma t) - (\Sigma t)^2 E_1(\Sigma t) \right] .$$

The function $E_1(\Sigma t)$ is defined by:

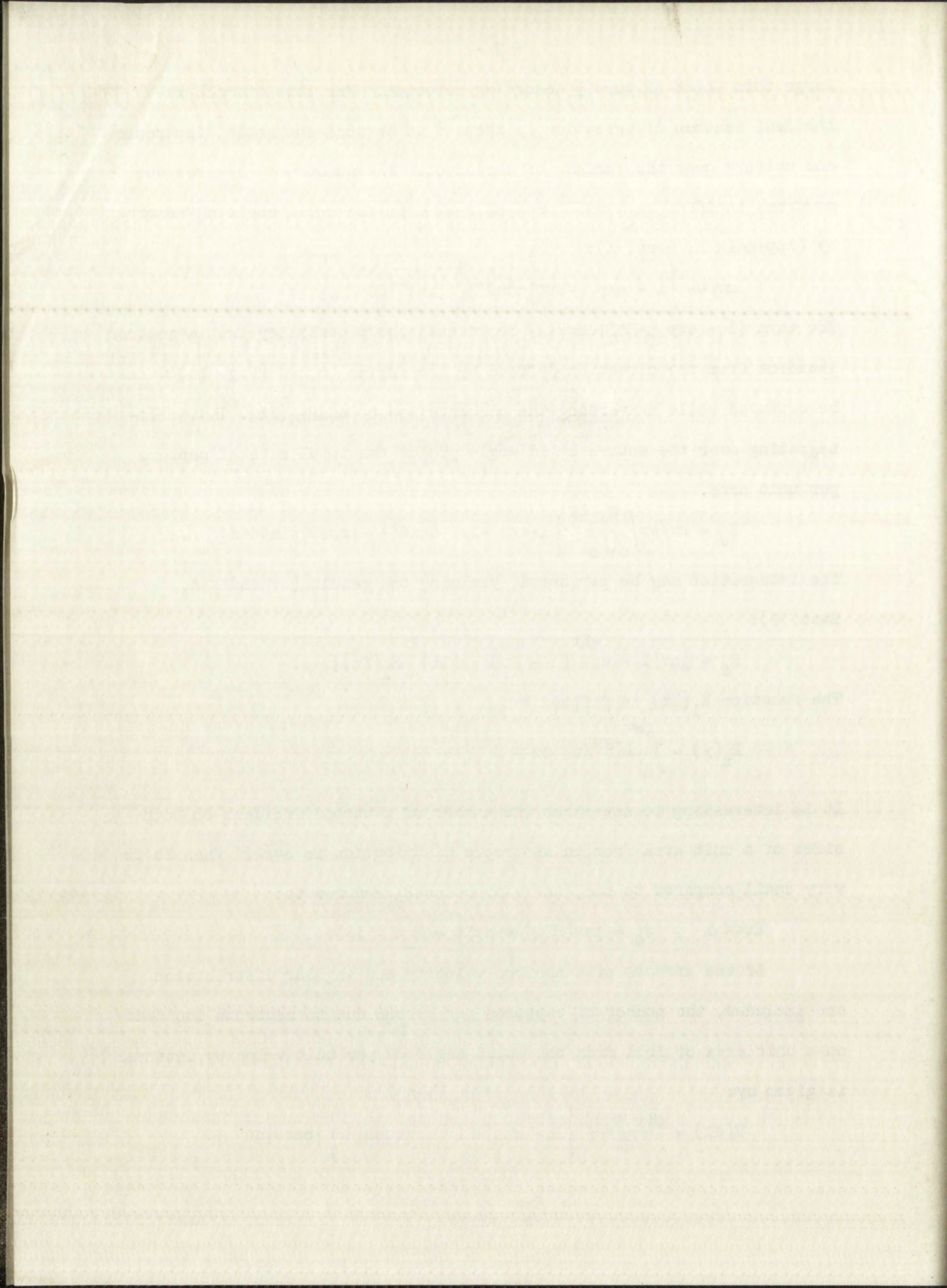
$$E_n(y) = \int_1^{\infty} e^{-yu}/u^n du .$$

It is interesting to note that the number of neutrons incident on both sides of a unit area from an isotropic distribution is $nv/2$. When Σt is very small compared to one, the expression R_{θ} reduces to:

$$\Sigma t \ll 1 , \quad R_{\theta} = \frac{1}{2}nv(2\Sigma t) = nv\Sigma t = R_1 t .$$

If the effects of a neutron velocity and angular distribution are included, the number of captures per second due to neutrons incident on a unit area of foil from the solid angle $d\Omega$ per unit velocity interval is given by:

$$R(d\Omega) = \frac{\phi(v, \theta, \phi)}{4\pi} \left\{ 1 - \exp[-\Sigma(v)t/|\cos\theta|] \right\} |\cos\theta| d\Omega .$$



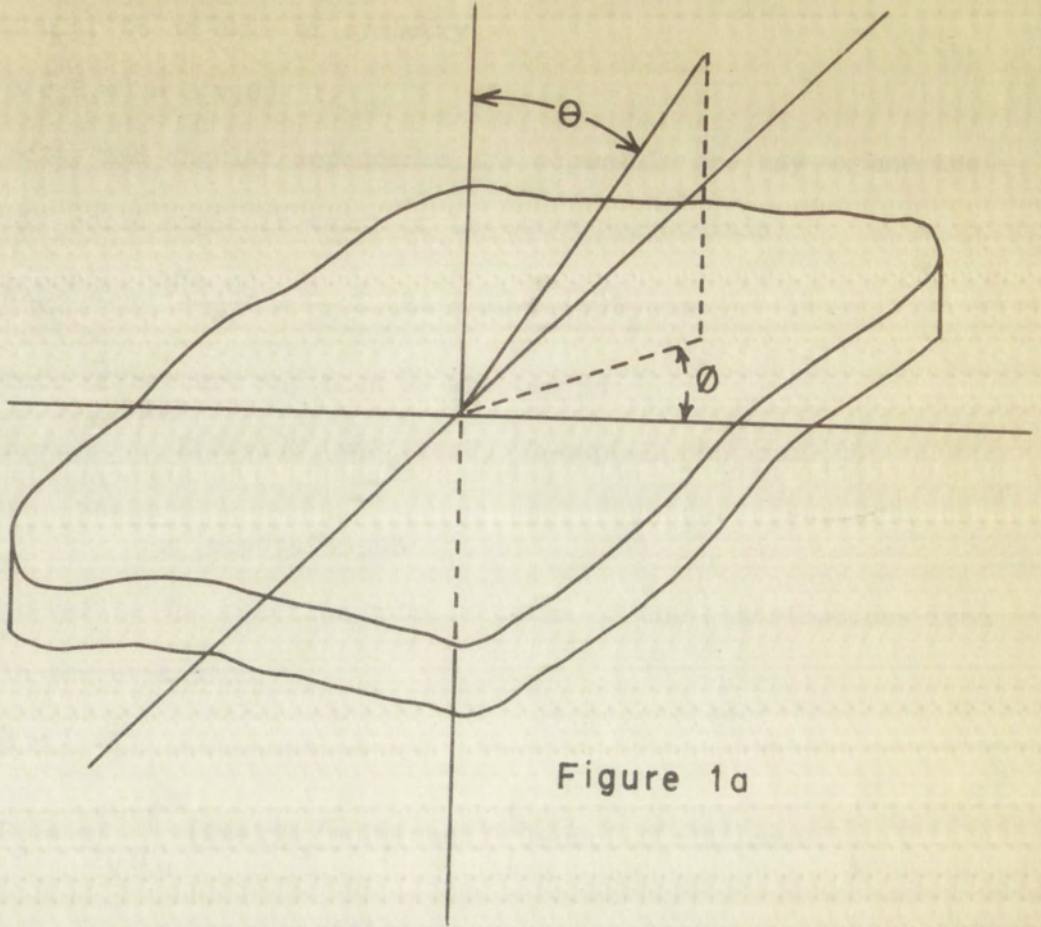


Figure 1a

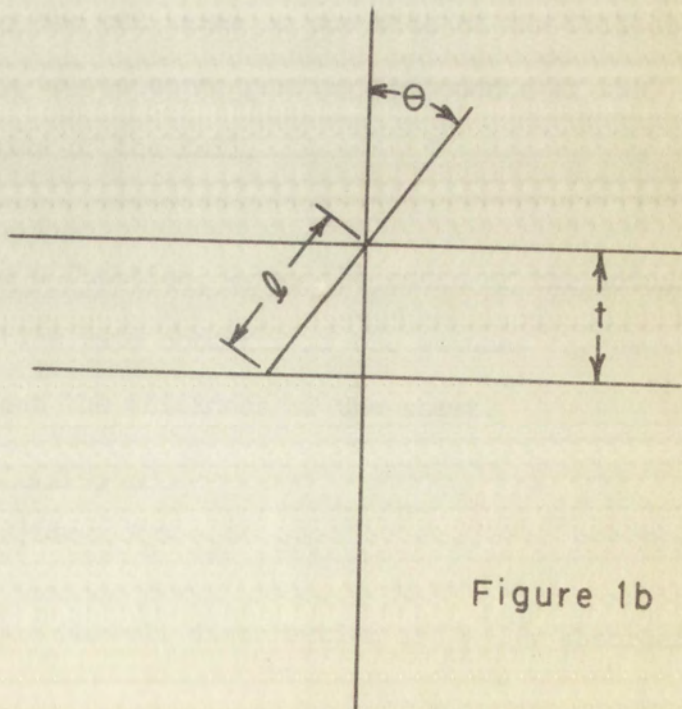
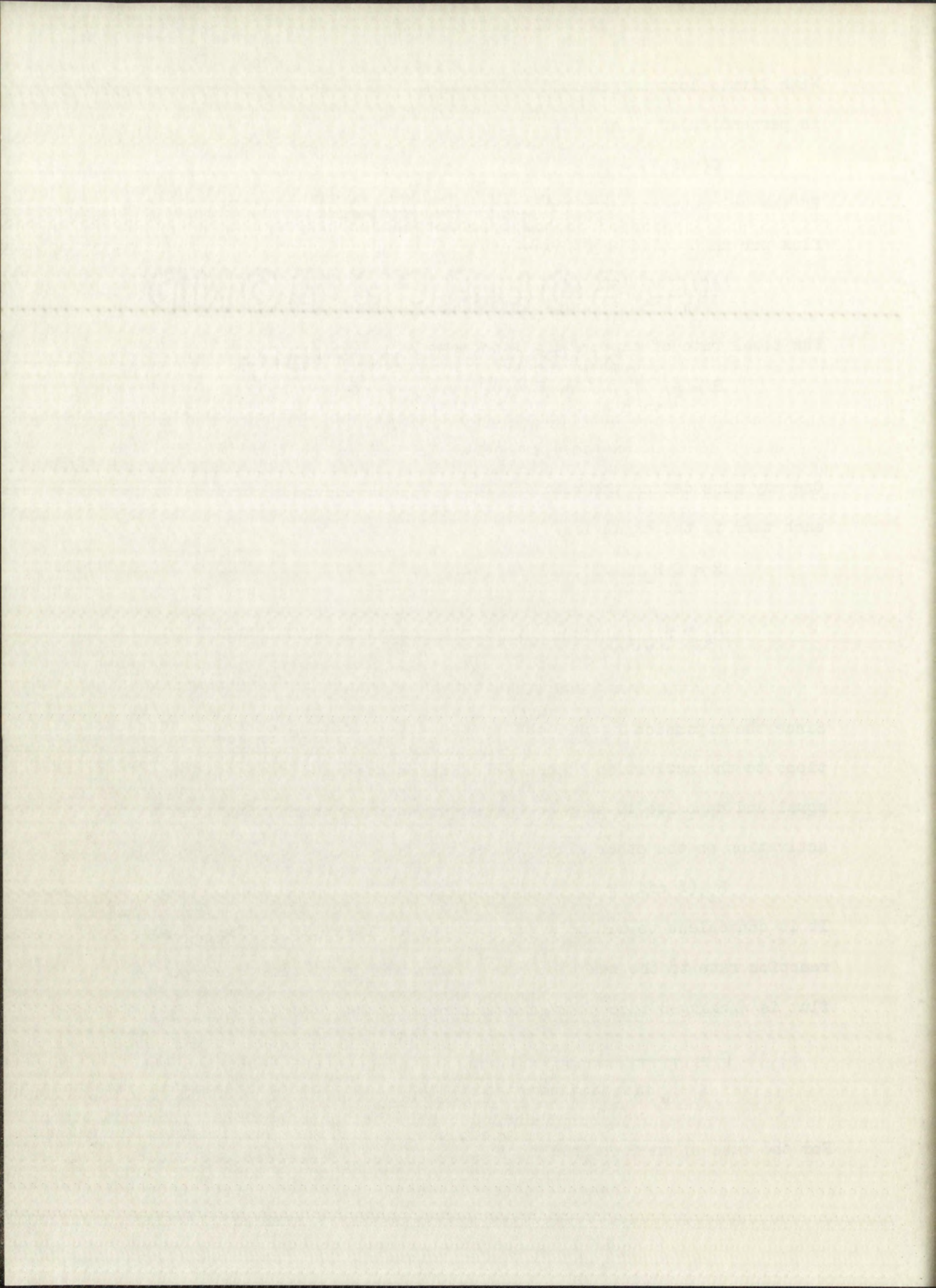


Figure 1b



is given by:

$$R_M = \int_0^\infty \int_0^{\pi/2} \frac{4n_0}{\sqrt{\pi}} (v/v_0)^3 \exp[-(v/v_0)^2] \\ \times \left\{ 1 - \exp[-\Sigma_0 t v_0/v \cos\theta] \right\} \cos\theta \sin\theta d\theta dv .$$

The quantity R_M may be evaluated (Appendix A, Sect. 3) in terms of one of a class of integrals investigated by C. T. Zahn.⁸

$$R_M = \frac{n_0 v_0}{\sqrt{\pi}} (1 - f_0(\Sigma_0 t)) .$$

$f_0(\Sigma_0 t)$ is defined by:

$$f_n(x) = \int_0^\infty y^n e^{-y-x/\sqrt{y}} dy .$$

If the reaction rate is given by R_M then the function G is expressed as:

$$G_M = 1/\sqrt{\pi} \Sigma_0 t (1 - f_0(\Sigma_0 t))$$

and

$$R_M = n_0 v_0 \Sigma_0 t G_M .$$

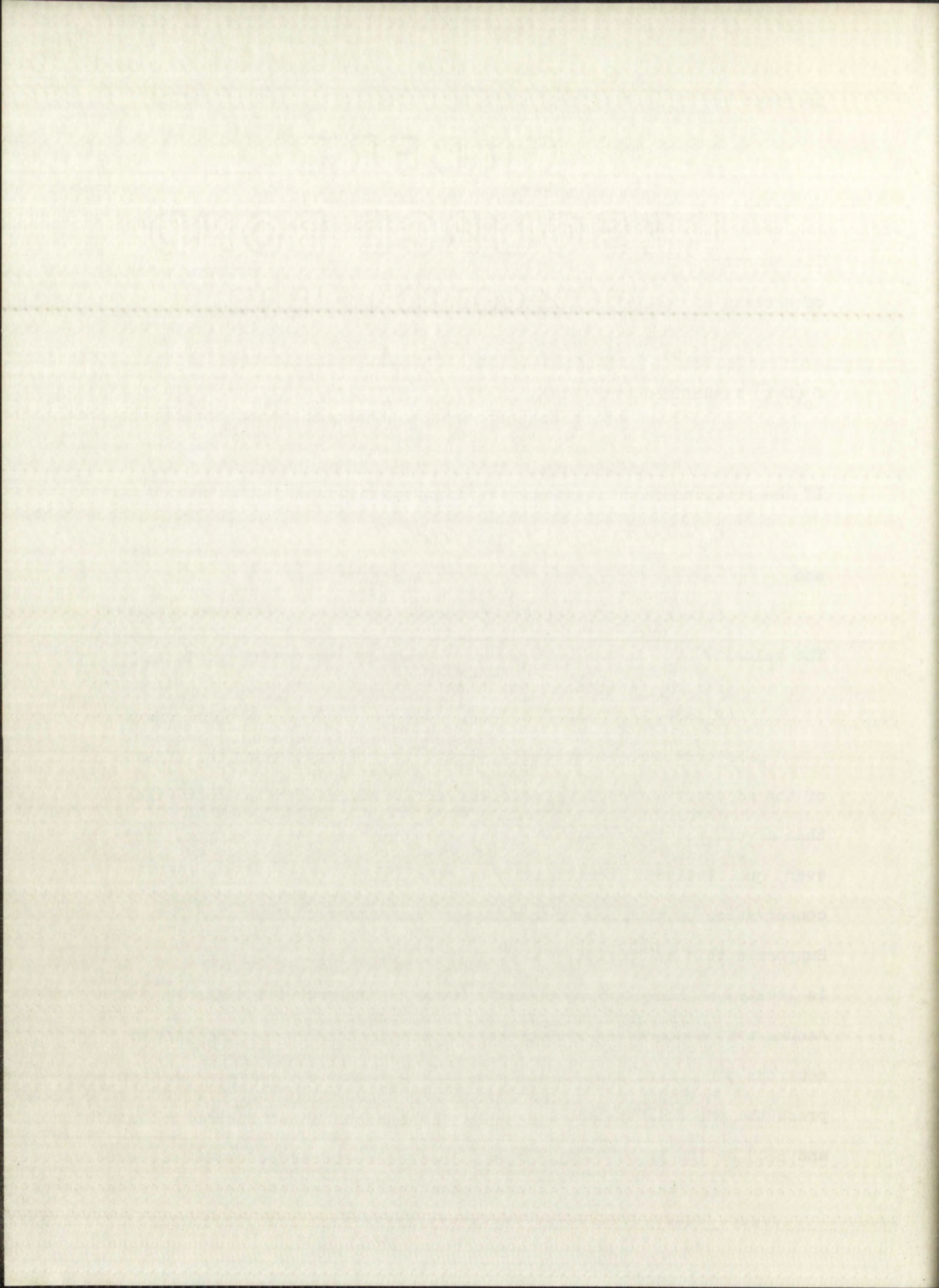
The velocity, v_0 , is the most probable velocity for the distribution

$$(v_0 = \sqrt{\frac{\pi}{2}} \bar{v}) .$$

As previously mentioned, quantitative discussion of the effects of the adjacent material when an absorber is irradiated in media other than a void require a solution of the neutron transport equation. However, qualitative information may be obtained by considering the conservation of neutrons in a simple system with and without an absorber.

Suppose a thin cylindrical box surrounding an absorber of equal diameter is located within a region of neutron scattering material (Fig. 2).

Assume that a source of neutrons is present in this region and that γS neutrons per second are supplied to the box from this source. Let α express the probability that a neutron entering the absorber will be captured and $\beta(\alpha)$ be the probability that a neutron incident on the inner surface



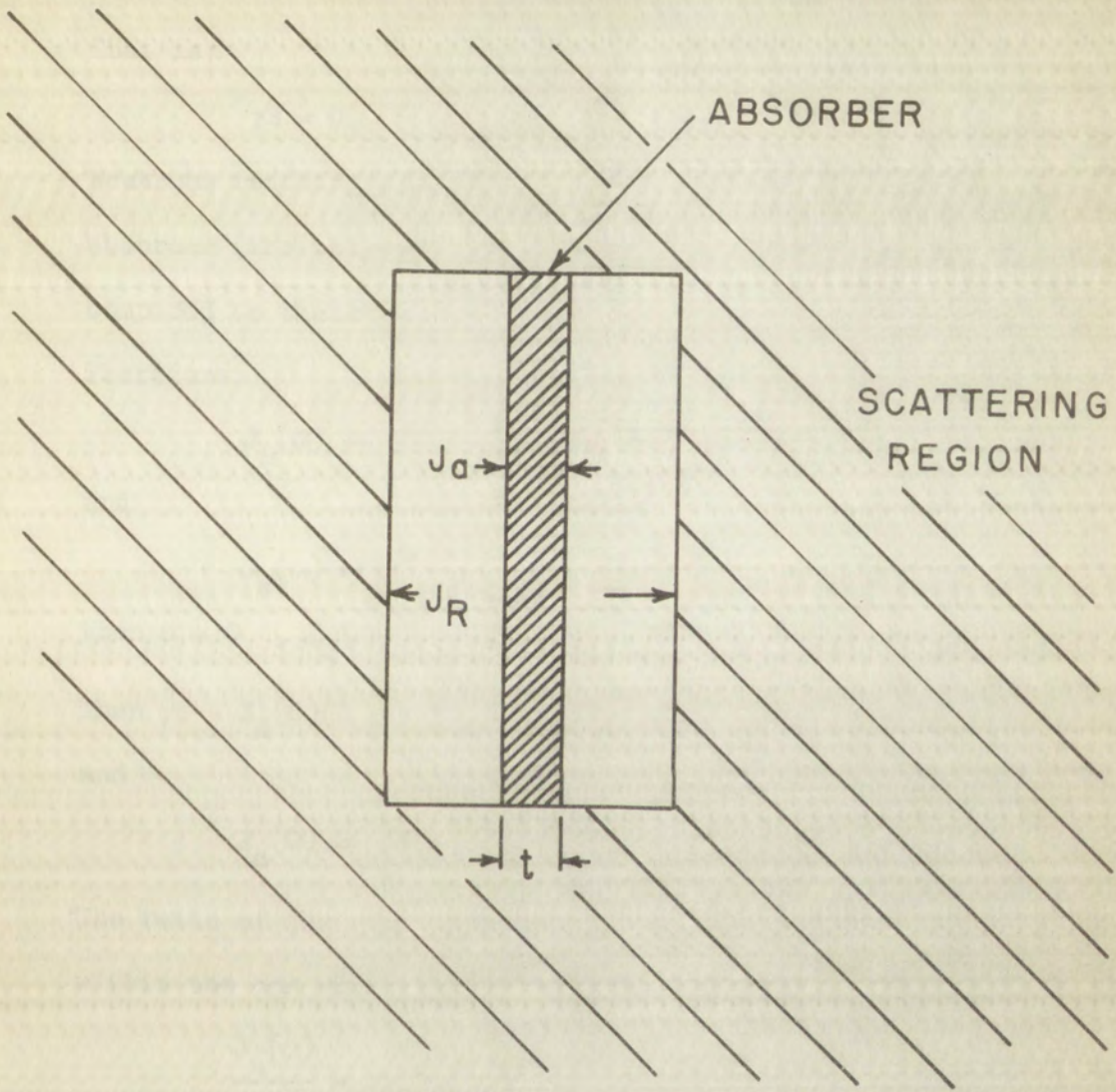


Figure 2

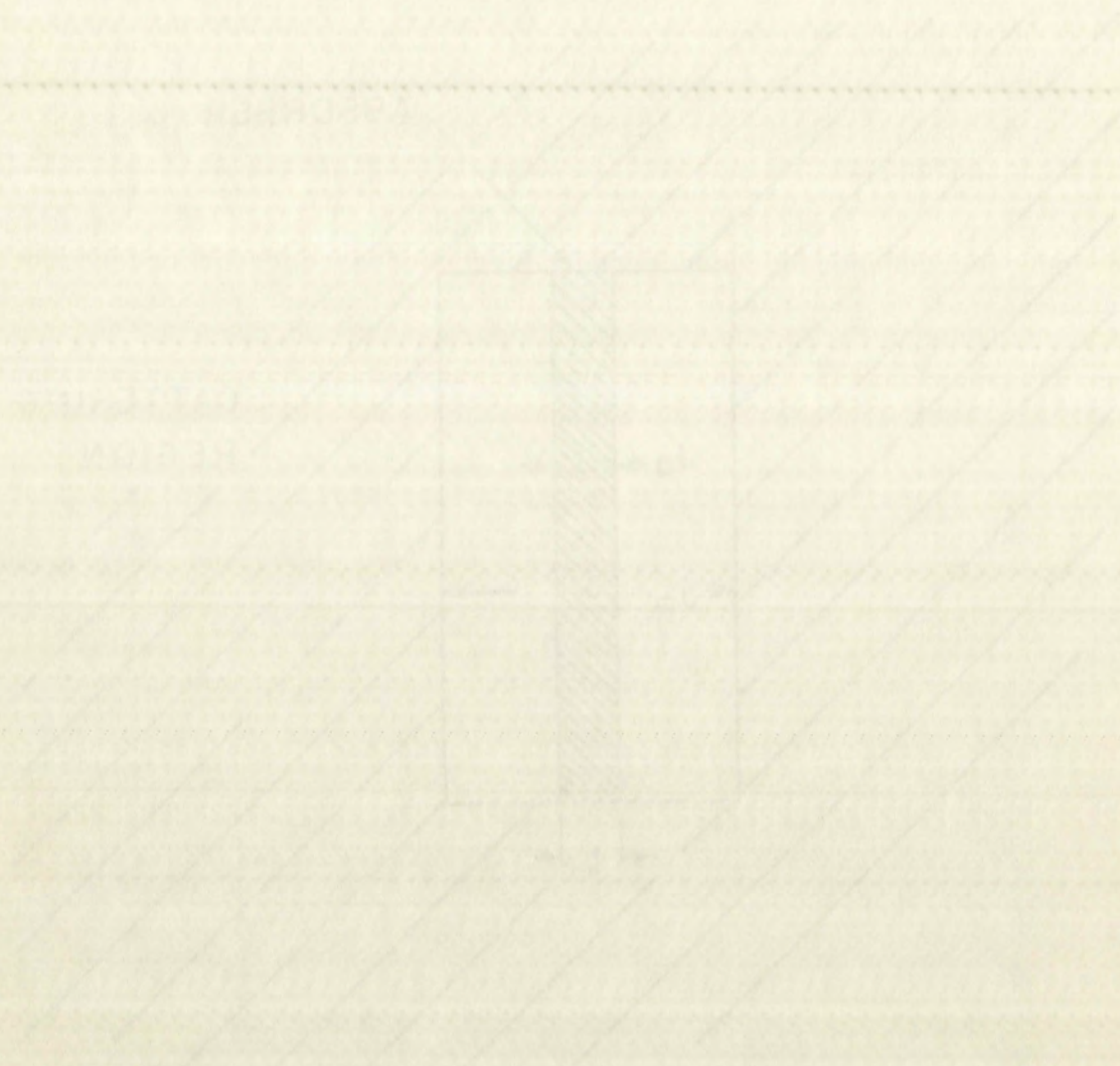


Figure 2

of the box will scatter in the surrounding material and eventually be returned to the box. Also let $J_R(\alpha)$ and $J_a(\alpha)$ represent respectively, the number of neutrons incident per second on the inner surface of the box and on the surface of the absorber. At equilibrium the rate of supply of neutrons to the box is equal to the rate of loss.

That is:

$$\gamma S = J_R(\alpha) (1 - \beta(\alpha)) + \alpha J_a(\alpha).$$

Neutrons reaching the inner surface of the box must pass through the absorber (the thicknesses of the box and absorber are considered small compared to their diameter so that edge effects may be neglected).

Therefore:

$$J_R(\alpha) = (1 - \alpha) J_a(\alpha)$$

and

$$J_a(\alpha) = \frac{\gamma S}{(1 - \alpha) (1 - \beta(\alpha)) + \alpha} .$$

When $\alpha = 0$, $J_a(0) = J_R(0)$.

Then $\gamma S = J_R(0)(1 - \beta(0)) = J_a(0)(1 - \beta(0))$,

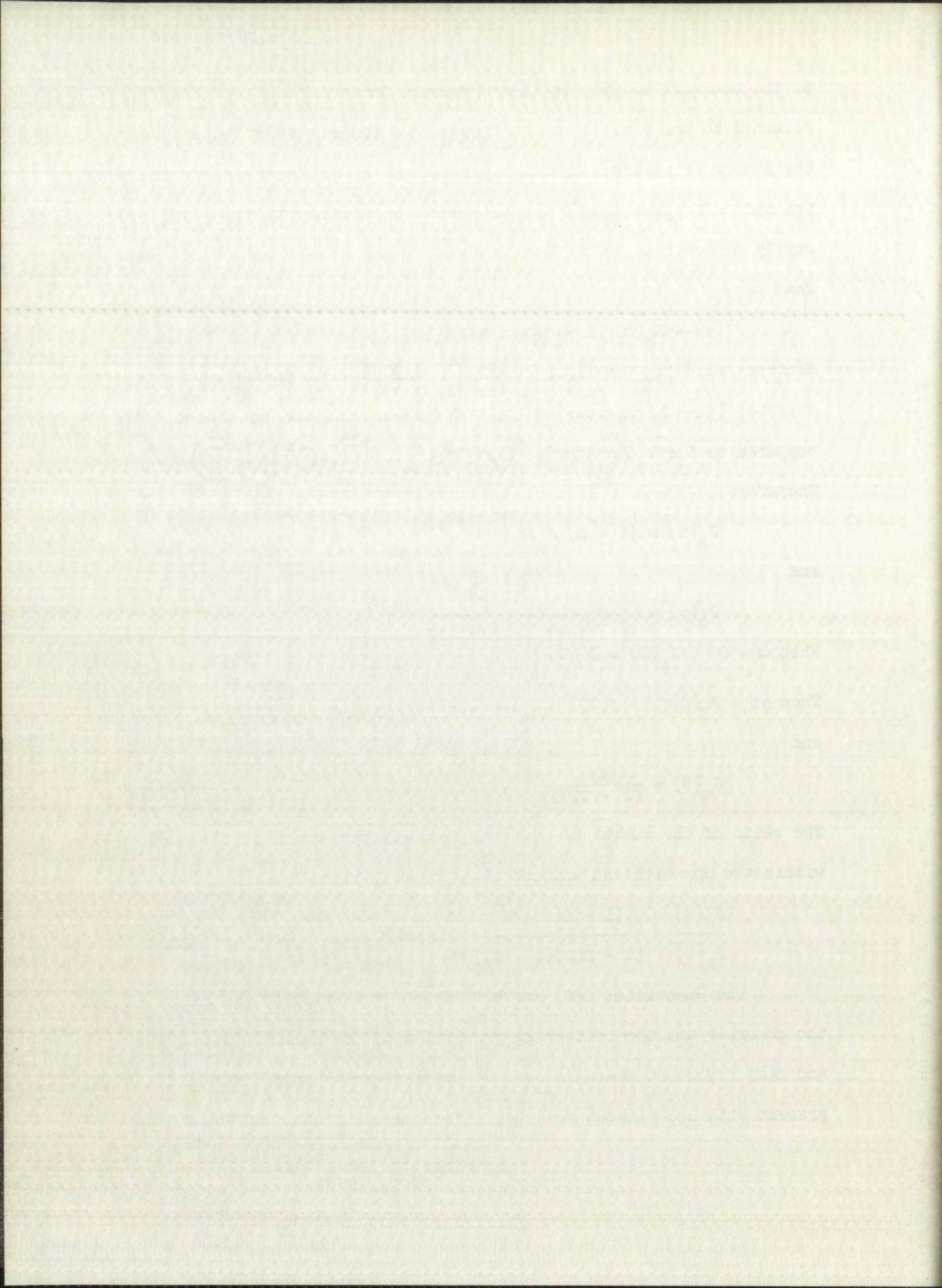
and

$$J_a(0) = \frac{\gamma S}{(1 - \beta(0))} .$$

The ratio of the number of neutrons incident per second on the surface within the box with and without absorption is given by:

$$\frac{J_a(\alpha)}{J_a(0)} = \frac{[1 - \beta(0)]}{[1 - \beta(\alpha)(1 - \alpha)]} .$$

The quantities $\beta(0)$ and $\beta(\alpha)$ depend primarily on the radius of the absorber and the scattering properties of the medium. Also $\beta(0)$ and $\beta(\alpha)$ represent averages over the angular and energy distributions present with and without absorber. The preceding ratio may be written



generally in terms of a function $g(a, \Sigma_s, \alpha)$ defined by:

$$\frac{J_a(\alpha)}{J_a(0)} = \frac{(1 - \beta(0))}{[1 - \beta(\alpha)(1 - \alpha)]} = \frac{1}{[1 + \alpha g(a, \Sigma_s, \alpha)]}$$

The inclusion of α in the argument of g does not imply specific dependence on α but is meant to signify that the function g will be affected by a change in α . Similarly, Σ_s denotes the dependence of g on the cross sections of the scattering medium while a is the radius of the disc. The reaction rate in an absorber surrounded by a scattering medium may be written in terms of the function g and the number of neutrons incident without absorption as:

$$R(\alpha) = J_a(0) \frac{\alpha}{[1 + \alpha g(a, \Sigma_s, \alpha)]}$$

It must be emphasized that α is the absorption probability calculated for the perturbed energy and angular distributions. If the foil is thin ($\alpha \ll 1$), the distributions will be essentially unchanged and $\beta(\alpha)$ will be approximately equal to $\beta(0)$. Also α will be closely equal to α_0 , where α_0 is defined as the capture probability of the absorber averaged over the distributions present in the medium without the absorber.

For $\alpha \ll 1$,

$$\frac{J_a(\alpha)}{J_a(0)} = \frac{1}{1 + \alpha_0 \frac{\beta}{\beta - 1}} \quad \beta = \beta(0)$$

Further, if the return probability is small enough $\alpha(\beta/(1 - \beta))$ will also be small compared to one and

$$(\alpha \ll 1), \quad \frac{J_a(\alpha)}{J_a(0)} = 1 - \alpha_0 \frac{\beta}{1 - \beta} + \left(\frac{\alpha_0 \beta}{1 - \beta} \right)^2 - \dots$$

The capture rate in the foil may be written in terms of the capture

Consider in turn the two cases $\alpha < \beta$ and $\alpha > \beta$.

The function $f(x)$ is defined as $f(x) = \frac{1}{x}$ for $x > 0$ and $f(x) = 0$ for $x = 0$.

It is clear that $f(x)$ is continuous at $x = 0$ if and only if $\lim_{x \rightarrow 0} f(x) = f(0)$.

Since $f(x) = \frac{1}{x}$, we have $\lim_{x \rightarrow 0} f(x) = \lim_{x \rightarrow 0} \frac{1}{x}$.

It can be shown that $\lim_{x \rightarrow 0} \frac{1}{x}$ does not exist.

For the present, let us assume that $\lim_{x \rightarrow 0} \frac{1}{x} = L$.

Then, for any $\epsilon > 0$, there exists a $\delta > 0$ such that $0 < |x| < \delta$ implies $|\frac{1}{x} - L| < \epsilon$.

But, if $\epsilon = 1$, we can choose $\delta = \frac{1}{2}$. Then, for $x = \frac{1}{2}$, we have $|\frac{1}{x} - L| = |2 - L|$.

The right-hand side of the inequality is $|2 - L|$.

probability and distributions present without absorption.

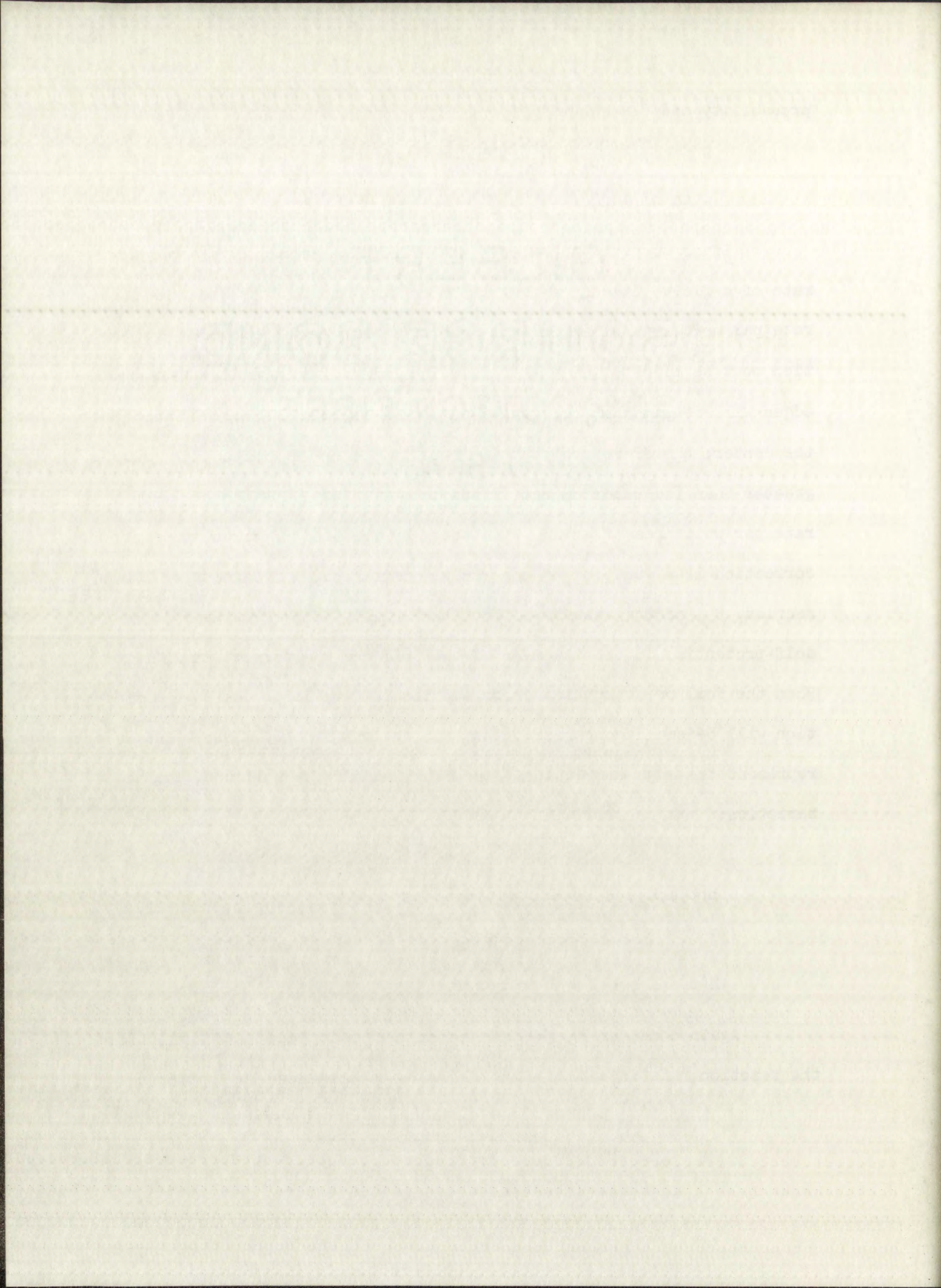
$$\alpha \ll 1, R(\alpha_0) = J_a(0)\alpha_0 [1 - \alpha_0\beta/(1-\beta) + (\alpha_0\beta/(1-\beta))^2 - (\alpha_0\beta/(1-\beta))^3 + \dots]$$

It is possible to express the absorption probability and reaction rate of a finite disc in terms of the capture probability and reaction rate per unit area of an infinite sheet of absorber. However a correction must be made for edge effects. The interior of the disc near the edges will be somewhat less shielded than a portion of the disc near the center; therefore the reaction rate in a disc of finite size will be greater than the reaction rate predicted by multiplying the reaction rate per unit area of an infinite sheet by the area of the disc. The correction is a function of the radius, thickness, and absorption cross section, Σ_a , of the absorber. When the foil is very thin there is no self-protection in the interior of the foil and the correction is zero. When the foil or absorption cross section is very large the edge correction will be small compared to the total reaction rate. Let $[h(t,a,\Sigma_a)+1]$ represent the edge correction. The function has the following characteristics:

$$h(t,a,\Sigma_a) + 1 = 1 \text{ for } \begin{cases} t = 0 \\ a = \infty \\ \frac{1}{\Sigma_a} \ll a \end{cases}$$

$$h(t,a,\Sigma_a) + 1 > 1 \text{ otherwise.}$$

Again considering the case of an isotropic Maxwell distribution, the reaction rate in a thin disc of radius a surrounded by scattering



material may be written as:

For $\Sigma_0 t \ll 1$,

$$R(\alpha_M, a) = \pi a^2 \frac{n_0 v_0}{\sqrt{\pi}} [1 - f_0(\Sigma_0 t)] \frac{[1 + h(t, \Sigma_a, a)]}{[1 + \alpha_M g(a, \Sigma_s, \alpha_M)]}$$

Alternatively, $R(\alpha_M, a)$ may be expressed in terms of G_M , the microscopic cross section, and the mass of the disc.

$$R(\alpha_M, a) = n_0 v_0 \frac{N_0 \sigma_0}{A} m G_M \frac{[1 + h_M(t, \Sigma_a, a)]}{[1 + \alpha_M g(a, \Sigma_s, \alpha_M)]}$$

The capture probability for the disc is given by:

$$\alpha_M = [1 - f_0(\Sigma_0 t)] [1 + h_M(t, \Sigma_a, a)]$$

When the absorption of a neutron causes the formation of an excited state which decays with a mean life λ , an irradiation for a time t_0 will yield a decay rate of:

$$S(\alpha_M, m) = n_0 v_0 \frac{N_0 \sigma_0}{A} m G_M \frac{[1 + h_M(t, \Sigma_a, a)]}{[1 + \alpha_M g(a, \Sigma_s, \alpha_M)]} [1 - e^{-\lambda t_0}]$$

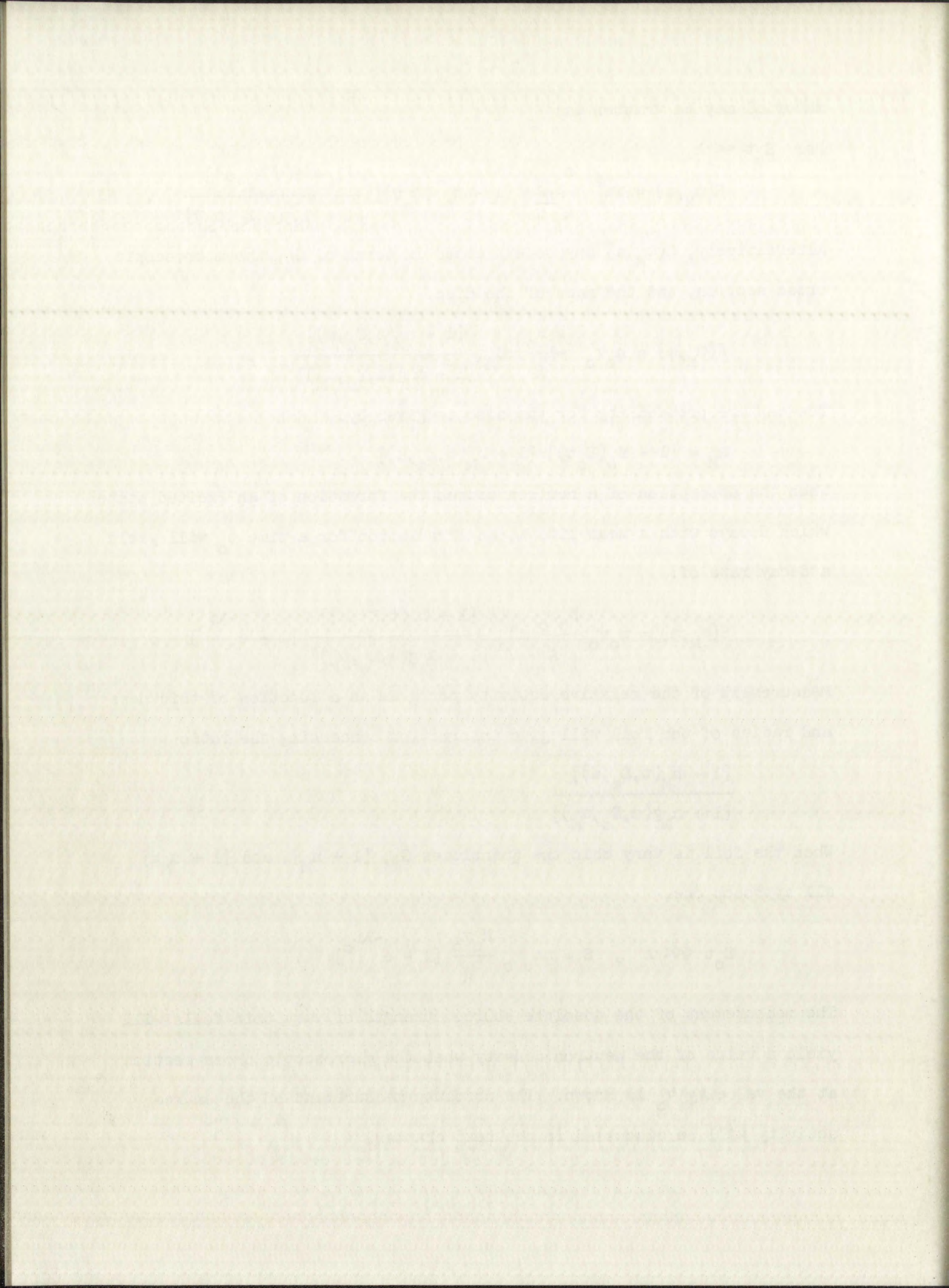
Measurement of the relative activity per gram as a function of thickness and radius of the foil will give information concerning the ratio

$$\frac{[1 + h_M(t, \Sigma_a, a)]}{[1 + \alpha_M g(a, \Sigma_s, \alpha_M)]}$$

When the foil is very thin the quantities G_M , $[1 + h_M]$, and $[1 + \alpha_M g]$ all approach one.

$$\Sigma_0 t \lll 1, \quad S = m n_0 v_0 \frac{N_0 \sigma_0}{A} [1 - e^{-\lambda t_0}]$$

The measurement of the absolute source strength of very thin foils will yield a value of the neutron density when the microscopic cross section at the velocity v_0 is known. The absolute measurement of the source activity will be discussed in the next chapter.



CHAPTER III

THE COINCIDENCE METHOD FOR

DETERMINING THE ABSOLUTE DECAY RATE OF Au¹⁹⁸

In order to introduce the method one may consider an idealized counting system and source. Suppose one has a point source which emits a beta particle followed immediately by a single gamma ray (Fig. 3). Also assume two idealized detectors; each sensitive to only one type of radiation. Associated with each detector is a means of scaling the number of events in the detector. Further, a circuit is provided which registers the number of times a coincidence occurs between the two detectors. The number of beta events registered will be the product of the source strength and the probability that the beta ray causes a detectable event in the beta detector. The same reasoning applies to the gamma detector. The counting rate from the respective detectors is given by:

$$N_{\beta} = \epsilon_{\beta} S$$

and

$$N_{\gamma} = \epsilon_{\gamma} S .$$

Here ϵ_{β} and ϵ_{γ} represent the efficiency or probability of detection. If there is no angular correlation between the beta particle and the gamma ray, the coincidence counting rate will be the product of the probabilities of detection and the source strength.

$$N_{\beta\gamma} = \epsilon_{\beta} \epsilon_{\gamma} S .$$

THE UNIVERSITY OF CHICAGO

PHYSICS DEPARTMENT

In order to understand the nature of the interaction between the electron and the nucleus, it is necessary to consider the structure of the nucleus. The nucleus is composed of protons and neutrons, which are held together by the strong nuclear force. This force is much stronger than the electromagnetic force, but it has a very short range. The strong force is responsible for the stability of the nucleus, and it is also responsible for the energy released in nuclear reactions. The energy released in nuclear reactions is due to the difference in the binding energy of the nucleus before and after the reaction. The binding energy of a nucleus is the energy required to separate the nucleus into its constituent protons and neutrons. The binding energy per nucleon is a measure of the stability of the nucleus. The binding energy per nucleon is highest for nuclei with a mass number between 2 and 60, and it decreases for nuclei with a mass number greater than 60. The energy released in nuclear reactions is due to the difference in the binding energy per nucleon of the reactants and the products. The energy released in nuclear reactions is a very large amount of energy, and it is the source of the energy of the sun and of nuclear power plants.

$$E = mc^2$$

and

$$E = hf$$

where E is the energy, m is the mass, c is the speed of light, h is Planck's constant, and f is the frequency. The energy released in nuclear reactions is a very large amount of energy, and it is the source of the energy of the sun and of nuclear power plants. The energy released in nuclear reactions is due to the difference in the binding energy of the nucleus before and after the reaction. The binding energy of a nucleus is the energy required to separate the nucleus into its constituent protons and neutrons. The binding energy per nucleon is a measure of the stability of the nucleus. The binding energy per nucleon is highest for nuclei with a mass number between 2 and 60, and it decreases for nuclei with a mass number greater than 60. The energy released in nuclear reactions is due to the difference in the binding energy per nucleon of the reactants and the products. The energy released in nuclear reactions is a very large amount of energy, and it is the source of the energy of the sun and of nuclear power plants.

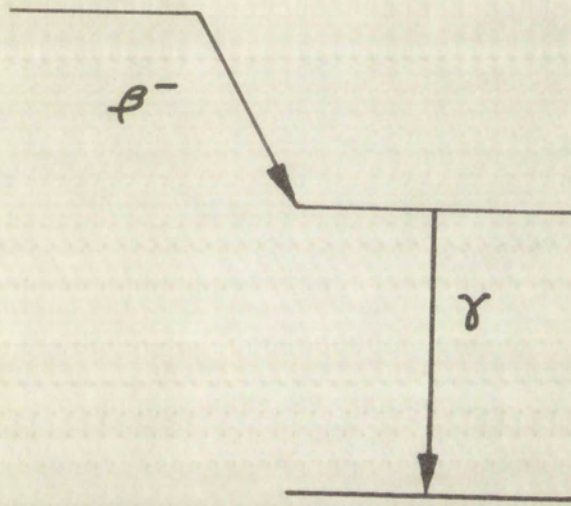
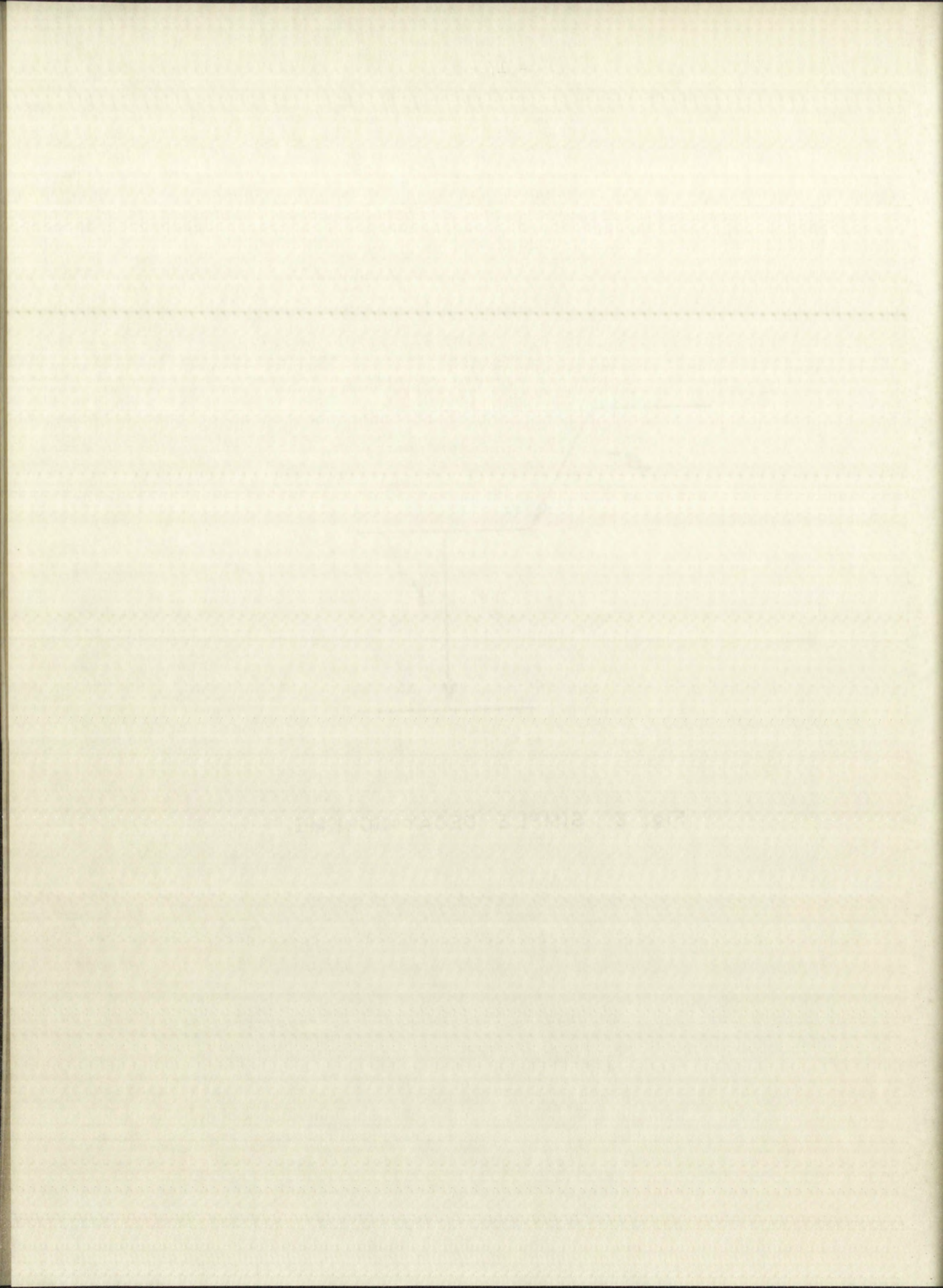


Fig. 3 SIMPLE DECAY SCHEME



Thus there are three equations in the three unknown quantities ϵ_β , ϵ_γ and S. Solving the system of equations yields:

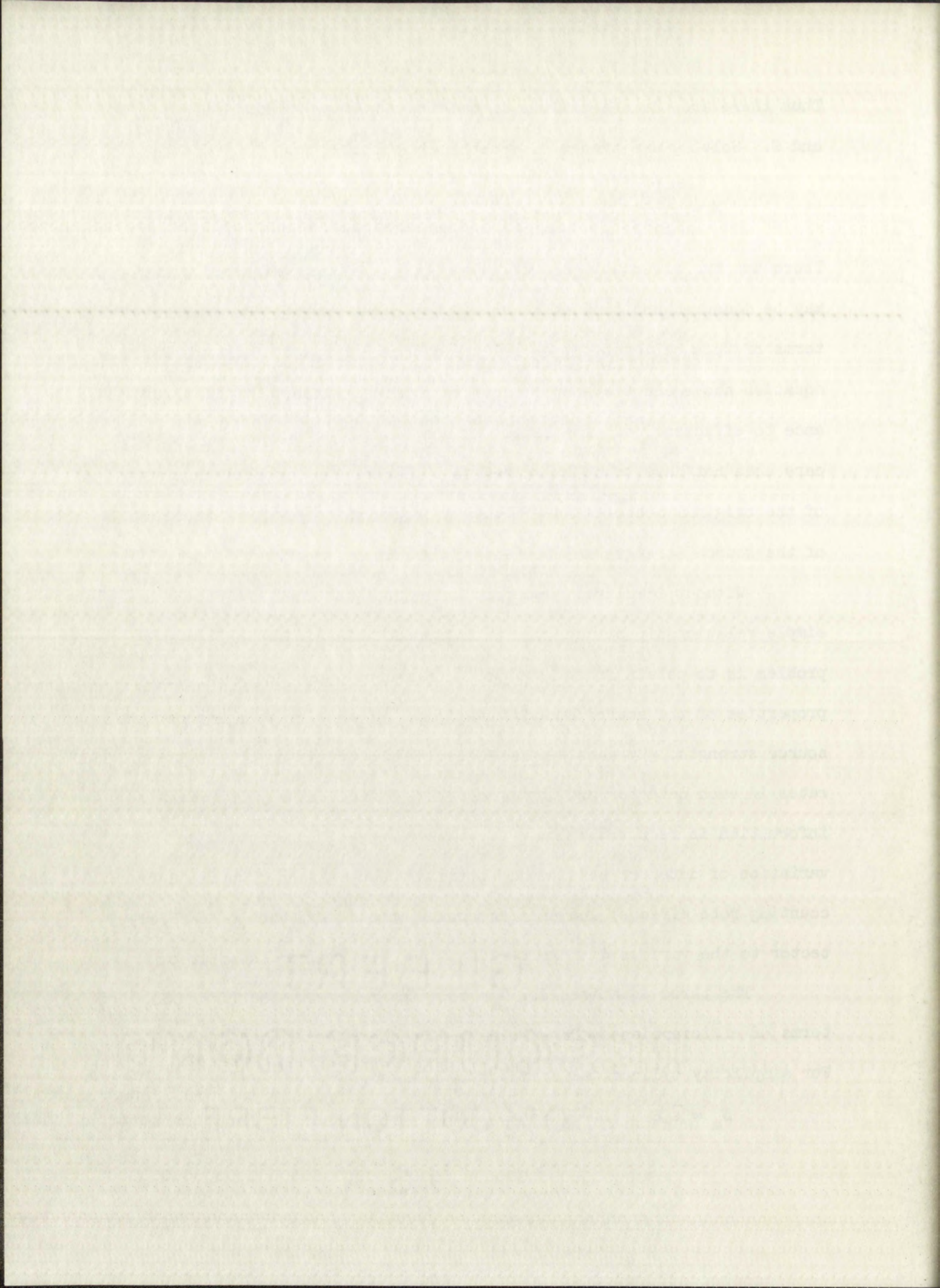
$$S = \frac{N_\gamma N_\beta}{N_{\beta\gamma}} , \quad \epsilon_\gamma = \frac{N_{\beta\gamma}}{N_\beta} , \quad \epsilon_\beta = \frac{N_{\beta\gamma}}{N_\gamma} .$$

There are two alternatives available. The counting system efficiency may be measured and then each succeeding source strength derived in terms of this calibration, or all the data may be used as in the first equation above and the source strength obtained without explicit reference to efficiencies. The latter method has the advantage that great care does not have to be exercised to duplicate the precise conditions of the original measurement. Either approach gives an absolute value of the source strength independent of an external calibration.

Without idealized detectors and source one does not have a simple relationship between the detection efficiencies. The central problem is to obtain from the experimental conditions and known decay properties of the source enough additional information to solve for the source strength. By considering in detail the origin of the counting rates in each detector and the coincidence system one may learn what information is required. There are three areas of interest: the variation of detector sensitivity over the volume of an extended source; counting rate effects; and most important, the sensitivity of each detector to the various different radiations emitted from the source.

The three equations for the counting rates may be written in terms of efficiencies averaged over the volume of an extended source. For simplicity cylindrical symmetry is assumed.

$$N_a = \bar{\epsilon}_a S , \quad N_b = \bar{\epsilon}_b S , \quad N_c = \bar{\epsilon}_c S .$$



The various averages are defined by:

$$\epsilon_i = \frac{\int_V \epsilon_i(r,z) S(r,z) dv}{\int_V S(r,z) dv} .$$

Since either detector may respond to both gamma rays and beta particles, the detectors are not here distinguished as to sensitivity. The true coincidence counting rate is given by N_c . The efficiencies as a function of position within the source may be expressed as a fractional deviation from the average.

$$\bar{\epsilon}_a g(r,z) = \bar{\epsilon}_a - \epsilon_a(r,z) .$$

$$\bar{\epsilon}_b h(r,z) = \bar{\epsilon}_b - \epsilon_b(r,z) .$$

When the coincidence efficiency is the product of the two detection efficiencies one obtains:

$$\text{If } \epsilon_c(r,z) = \epsilon_a(r,z) \epsilon_b(r,z)$$

$$\text{then } \epsilon_c(r,z) = \bar{\epsilon}_a \bar{\epsilon}_b [1 - g(r,z) - h(r,z) + g(r,z) h(r,z)]$$

$$\text{and } \bar{\epsilon}_c = \int_V \epsilon_c(r,z) S(r,z) dv = \bar{\epsilon}_a \bar{\epsilon}_b (1 + \overline{gh}) S_o .$$

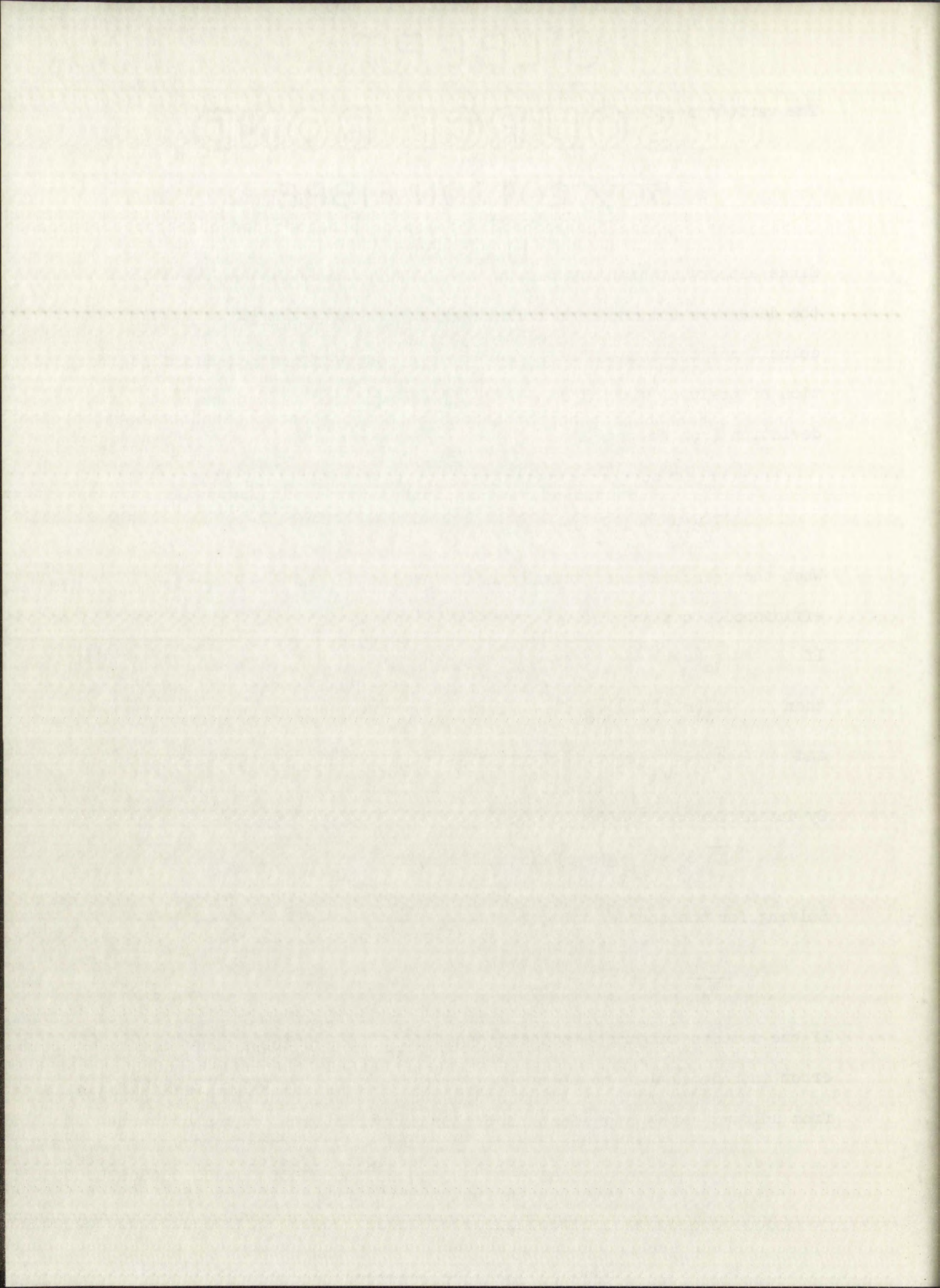
By definition $\bar{g} = \bar{h} = 0$ therefore:

$$\overline{gh} S_o = \int_V g(r,z) h(r,z) S(r,z) dv .$$

Solving for the source strength yields:

$$\frac{N_a N_b}{N_c} (1 + \overline{gh}) = S_o .$$

If one assumes uniform sensitivity over the volume of the source, the error introduced will be the average product of the fractional deviations from uniform sensitivity for each detector.⁹



There is a variety of possible arrangements of detector and counting systems each having different behaviour concerning counting rate effects. The particular system to be considered here has the following properties (see also Fig. 5):

a) Interaction with the detector produces an electrical pulse. The amplitude of the pulse is proportional to the energy deposited in the detector and the width is equal to τ . If two pulses overlap in time, the shape of the resulting pulse will be the sum of the individual amplitudes.

b) A gate pulse of width τ_c and constant amplitude is sent to a scaler and to a coincidence circuit at the time when a pulse amplitude exceeds a given minimum value corresponding to an energy minimum, E_m . The time required between successive gate pulses is τ .

c) Any time two gate pulses overlap in the coincidence circuit for a time τ_e a count will be registered in the coincidence scaler. The overlap time is small compared to the coincidence gate width τ_c .

d) The scaling circuit resolving times are less than τ .

A source disintegration will be registered in the singles scaler and a gate pulse sent to the coincidence circuit if the following conditions are met:

Either:

a) The source disintegration deposits enough energy to exceed the minimum and no source disintegration during the preceding interval τ deposited enough energy to exceed the minimum

or:

b) The source disintegration does not deposit enough energy to

There is a number of ...

... the ...

... the ...

... the ...

... the ...

... the ...

... the ...

... the ...

... the ...

... the ...

... the ...

... the ...

... the ...

... the ...

exceed the minimum but combines with a below-minimum pulse in the preceding interval τ such that the sum of the amplitudes of the two pulses does exceed the minimum.

The singles counting rate is given by:

$$N_i = [Q_i S_o (1 - \tau Q_i S_o) + \tau S_o^2 Q_i^2 ((1-F_i)^2 / F_i^2) P_i(i,i)] .$$

The quantities Q_i , Q_i/F_i , F_i , $P_i(i,i)$ represent respectively: the probability that a source disintegration deposits enough energy to exceed the minimum, the probability that a source disintegration interacts with the detector, the fraction of the interactions which exceed the minimum, and the probability that two below-minimum pulses will combine to yield a pulse greater than the minimum. The first term in the square brackets is the contribution from greater-than-minimum events in the detector while the second term represents the increase in sensitivity as a result of combination pulses. The source strength is assumed to be small enough that the approximate expression, $(1 - \tau Q_i S_o)$, for the probability of no above-minimum pulse occurring in the interval may be used, and that the possibility of combinations involving more than two source disintegrations may be neglected. The counting rates are assumed to be corrected for background.

The coincidence counting rate is more complicated since coincidences may be gained or lost by combinations in either or both detectors. A source disintegration will be registered in the coincidence scaler if:

a) The source disintegration deposits enough energy in both detectors to exceed the minimum and no disintegration during the preceding interval τ deposited enough energy in either detector to exceed the minimum.

Section 101 of the Internal Revenue Code provides that the term "charitable contribution" includes any property placed by an individual at the disposal of an organization described in section 170(c) for the use and possession of such organization.

The above definition of charitable contribution is broad and includes contributions of property other than cash, such as stocks, bonds, real estate, and personal property.

Section 170(e) provides that the amount of a charitable contribution is reduced by the amount of any tax imposed on the property at the time of the contribution. This rule applies to contributions of property other than cash.

Section 170(e)(1)(B) provides that the amount of a charitable contribution is reduced by the amount of any tax imposed on the property at the time of the contribution. This rule applies to contributions of property other than cash.

Section 170(e)(1)(B) provides that the amount of a charitable contribution is reduced by the amount of any tax imposed on the property at the time of the contribution. This rule applies to contributions of property other than cash.

Section 170(e)(1)(B) provides that the amount of a charitable contribution is reduced by the amount of any tax imposed on the property at the time of the contribution. This rule applies to contributions of property other than cash.

Section 170(e)(1)(B) provides that the amount of a charitable contribution is reduced by the amount of any tax imposed on the property at the time of the contribution. This rule applies to contributions of property other than cash.

Section 170(e)(1)(B) provides that the amount of a charitable contribution is reduced by the amount of any tax imposed on the property at the time of the contribution. This rule applies to contributions of property other than cash.

Section 170(e)(1)(B) provides that the amount of a charitable contribution is reduced by the amount of any tax imposed on the property at the time of the contribution. This rule applies to contributions of property other than cash.

Section 170(e)(1)(B) provides that the amount of a charitable contribution is reduced by the amount of any tax imposed on the property at the time of the contribution. This rule applies to contributions of property other than cash.

Section 170(e)(1)(B) provides that the amount of a charitable contribution is reduced by the amount of any tax imposed on the property at the time of the contribution. This rule applies to contributions of property other than cash.

Section 170(e)(1)(B) provides that the amount of a charitable contribution is reduced by the amount of any tax imposed on the property at the time of the contribution. This rule applies to contributions of property other than cash.

Section 170(e)(1)(B) provides that the amount of a charitable contribution is reduced by the amount of any tax imposed on the property at the time of the contribution. This rule applies to contributions of property other than cash.

b) The source disintegration deposits enough energy in detector a to exceed the minimum and combines with a previous disintegration which did not deposit enough energy in either detector to give a pulse from detector b which does exceed the minimum.

c) The same as (b) above with the roles of the detectors interchanged.

d) The source disintegration does not deposit enough energy in either detector and combines with a previous disintegration, which also did not deposit enough energy in either detector, to give a pulse from each detector which does exceed the minimum.

e) The source disintegration gives an above-minimum pulse in one detector and a disintegration during the preceding interval τ_c yields an above-minimum pulse in the other detector.

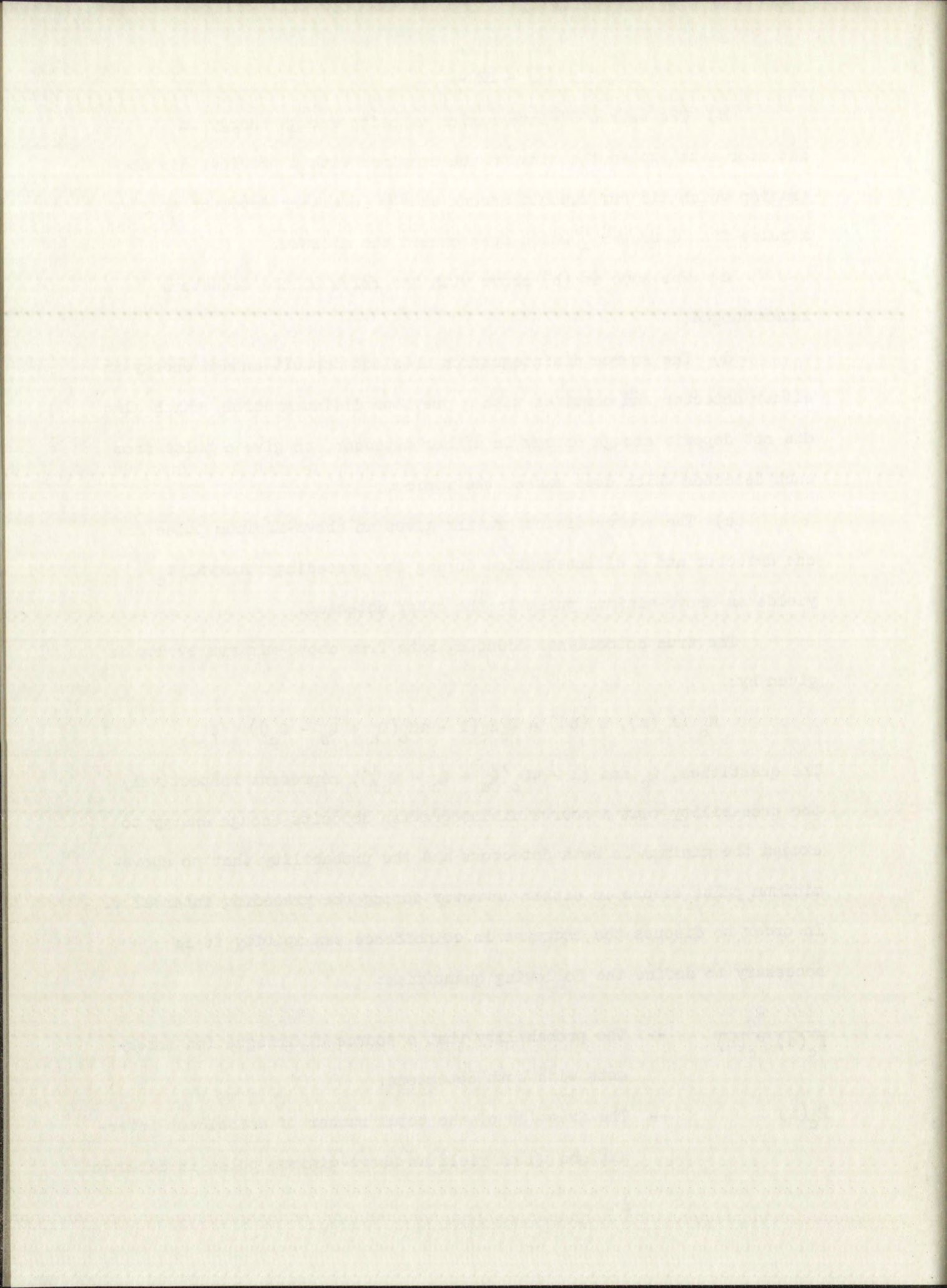
The true coincidence counting rate from above-minimum events is given by:

$$N_c (E_m(a), E_m(b)) = Q_c S_o (1 - \tau S_o (Q_a + Q_b - Q_c))$$

The quantities, Q_c and $(1 - \tau S_o (Q_a + Q_b - Q_c))$, represent respectively the probability that a source disintegration deposits enough energy to exceed the minimum in both detectors and the probability that no above-minimum pulse occurs in either detector during the preceding interval τ .

In order to discuss the increase in coincidence sensitivity it is necessary to define the following quantities:

- | | | |
|-----------------------------|----|-----------------------------------------------------------------------------------------------------------------------|
| $\frac{Q_c}{F_c(a) F_c(b)}$ | -- | The probability that a source disintegration interacts with both detectors. |
| $F_c(i)$ | -- | The fraction of the total number of coincident interactions which yield an above-minimum pulse in detector <u>i</u> . |



- $P_c(i,i)$ -- The probability that a below-minimum pulse in detector i from a coincidence interaction will combine with another below-minimum pulse in detector i to give an above-minimum pulse.
- $P_c(a,a;b,b)$ -- The probability that a below-minimum coincidence interaction will combine with a similar event to yield an above-minimum pulse from both detectors.
- $N_c(i,i)$ -- The additional coincidence counting rate resulting from combinations in detector i.
- $N_c(a,a;b,b)$ -- The additional coincidence counting rate resulting from combinations in both detectors.

Using the above definitions one obtains the increase in coincidence sensitivity resulting from combinations in detector a;

$$N_c(a,a) = \tau Q_c S_o^2 \frac{(1 - F_c(a))}{F_c(a)} (1 - F_c(a)F_c(b))$$

$$\times [Q_a \frac{(1 - F_c(a))}{(1 - F_c(a))} - Q_c \frac{(1 - F_c(a)F_c(b))}{F_c(a)F_c(b)}$$

$$\times (1 - F_c(a)F_c(b))] P_c(a,a) .$$

The term in square brackets is the probability that a source disintegration will give a below-minimum pulse in detector a and a pulse no greater than minimum in detector b. This probability has two terms; the probability that a source disintegration deposits below-minimum energy in detector a, $Q_a(1 - F_a)/F_a$, less the probability that a below-minimum pulse in detector a was accompanied by an above-minimum pulse in detector b,

$$Q_c \frac{(1 - F_c(a)F_c(b))}{F_c(a)F_c(b)} \times (1 - F_c(a)F_c(b)).$$

The first part of the paper is devoted to a general discussion of the problem. It is shown that the problem is well-posed in the sense of Hadamard. The second part is devoted to the construction of the solution. The third part is devoted to the numerical solution of the problem. The fourth part is devoted to the application of the method to the solution of the problem.

The first part of the paper is devoted to a general discussion of the problem. It is shown that the problem is well-posed in the sense of Hadamard. The second part is devoted to the construction of the solution. The third part is devoted to the numerical solution of the problem. The fourth part is devoted to the application of the method to the solution of the problem.

The first part of the paper is devoted to a general discussion of the problem. It is shown that the problem is well-posed in the sense of Hadamard. The second part is devoted to the construction of the solution. The third part is devoted to the numerical solution of the problem. The fourth part is devoted to the application of the method to the solution of the problem.

The first part of the paper is devoted to a general discussion of the problem. It is shown that the problem is well-posed in the sense of Hadamard. The second part is devoted to the construction of the solution. The third part is devoted to the numerical solution of the problem. The fourth part is devoted to the application of the method to the solution of the problem.

One obtains the additional counting rate from combinations in detector b by interchanging the roles of a and b.

$$N_c(b,b) = \tau Q_c S_o^2 \frac{(1 - F_c(b))}{F_c(b)} (1 - F_c(a)F_c(b)) \left[Q_b \frac{(1 - F_b)}{F_b} - Q_c \frac{(1 - F_c(a)F_c(b))}{F_c(a)F_c(b)} (1 - F_c(b)F_c(a)) \right] P_c(b,b) .$$

Similarly the additional counting rate resulting from combinations in both detectors is:

$$N_c(a,a;b,b) = Q_c^2 S_o^2 \frac{(1 - F_c(a))^2 (1 - F_c(b))^2}{F_c(a)^2 F_c(b)^2} \times (1 - F_c(a)F_c(b))^2 P_c(a,a;b,b) .$$

The probability that a gate pulse will appear in the coincidence circuit from single events in detector b during the time a gate pulse from a single event in detector a is present in the coincidence circuit is $\tau_c(N_b - N_c)$. Multiplying this probability by the single event rate in detector a then gives the contribution to the accidental rate from detector a. Similar reasoning applies to detector b. The total accidental coincidence rate is then given by:

$$N_{AC} = 2\tau_c(N_a - N_c)(N_b - N_c) .$$

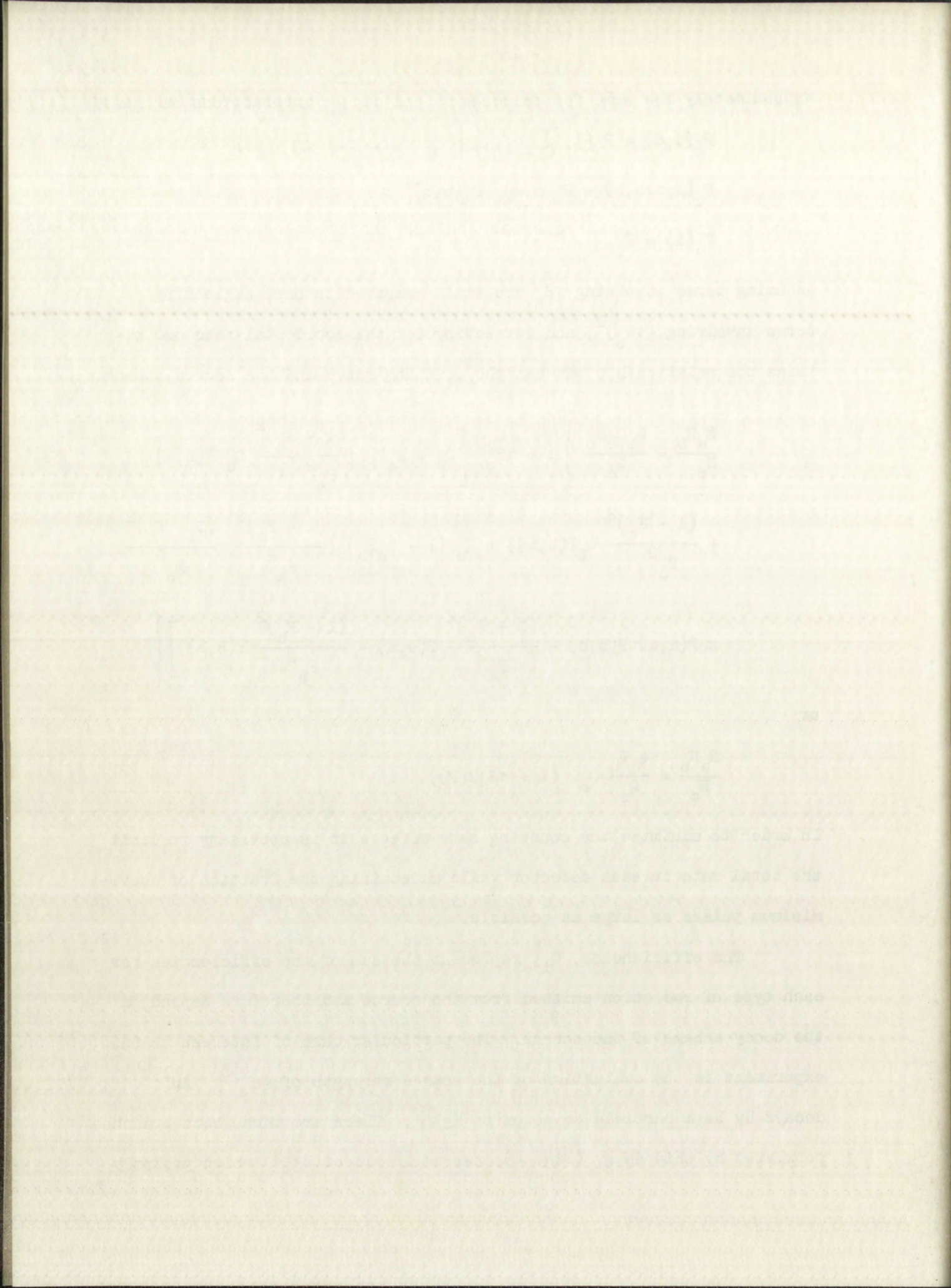
Summing the various contributions to the coincidence counting rate, one obtains the total rate.

$$N_c(T) = N_c(E_m(a), E_m(b)) + N_c(a,a) + N_c(b,b) + N_c(a,a;b,b) + N_{AC}$$

or

$$N_c(T) = N_c + N_{AC} .$$

For simple decay schemes where the pulse height distributions are



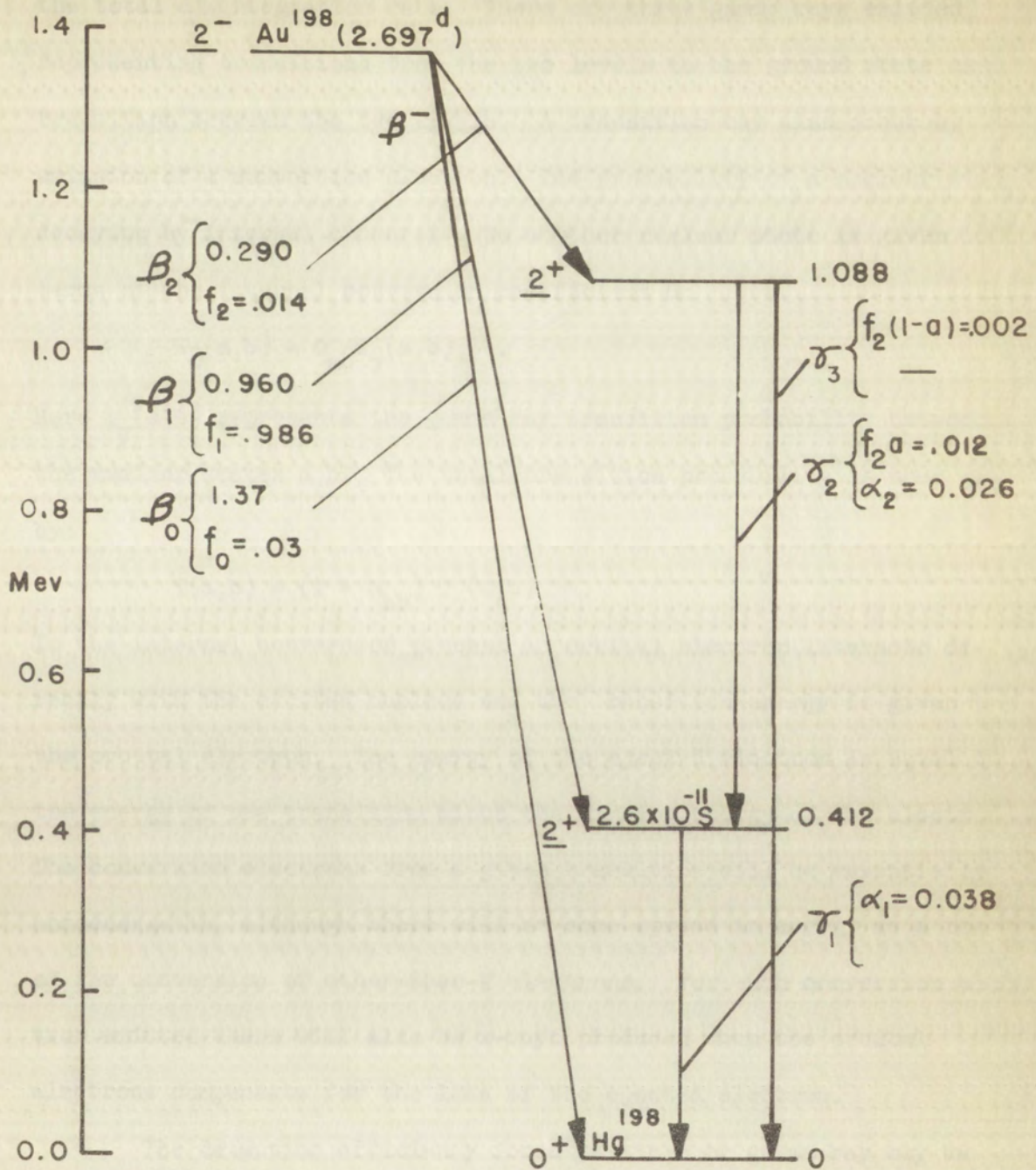
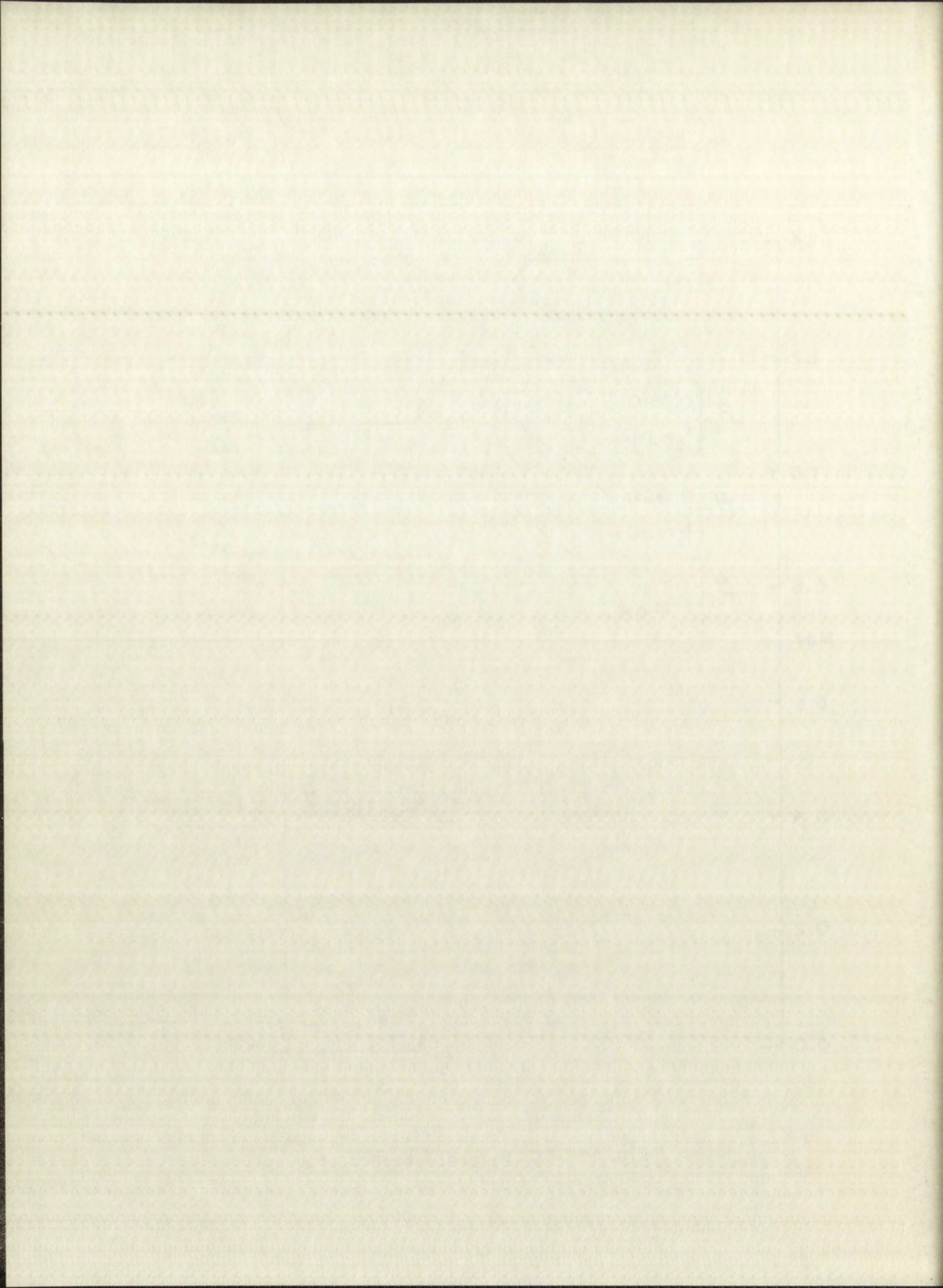


Fig. 4 DECAY SCHEME FOR Au^{198}



decay by the emission of a gamma ray or a conversion electron and the third branch to the ground state of Hg^{198} . The decay to the ground state and the second level of Hg^{198} represent less than two percent of the total disintegration rate. There are three gamma rays emitted, representing transitions from the two levels to the ground state and a transition between the two levels. A transition may also occur by the emission of a conversion electron. The probability of a nuclear state decaying by internal conversion to another nuclear state is given in terms of the internal conversion coefficient α :

$$T_{\alpha}(a,b) = \alpha_{ab} T_{\gamma}(a,b) \quad .$$

Here $T_{\gamma}(a,b)$ represents the gamma ray transition probability between the nuclear states a,b. The total transition probability is then given by:

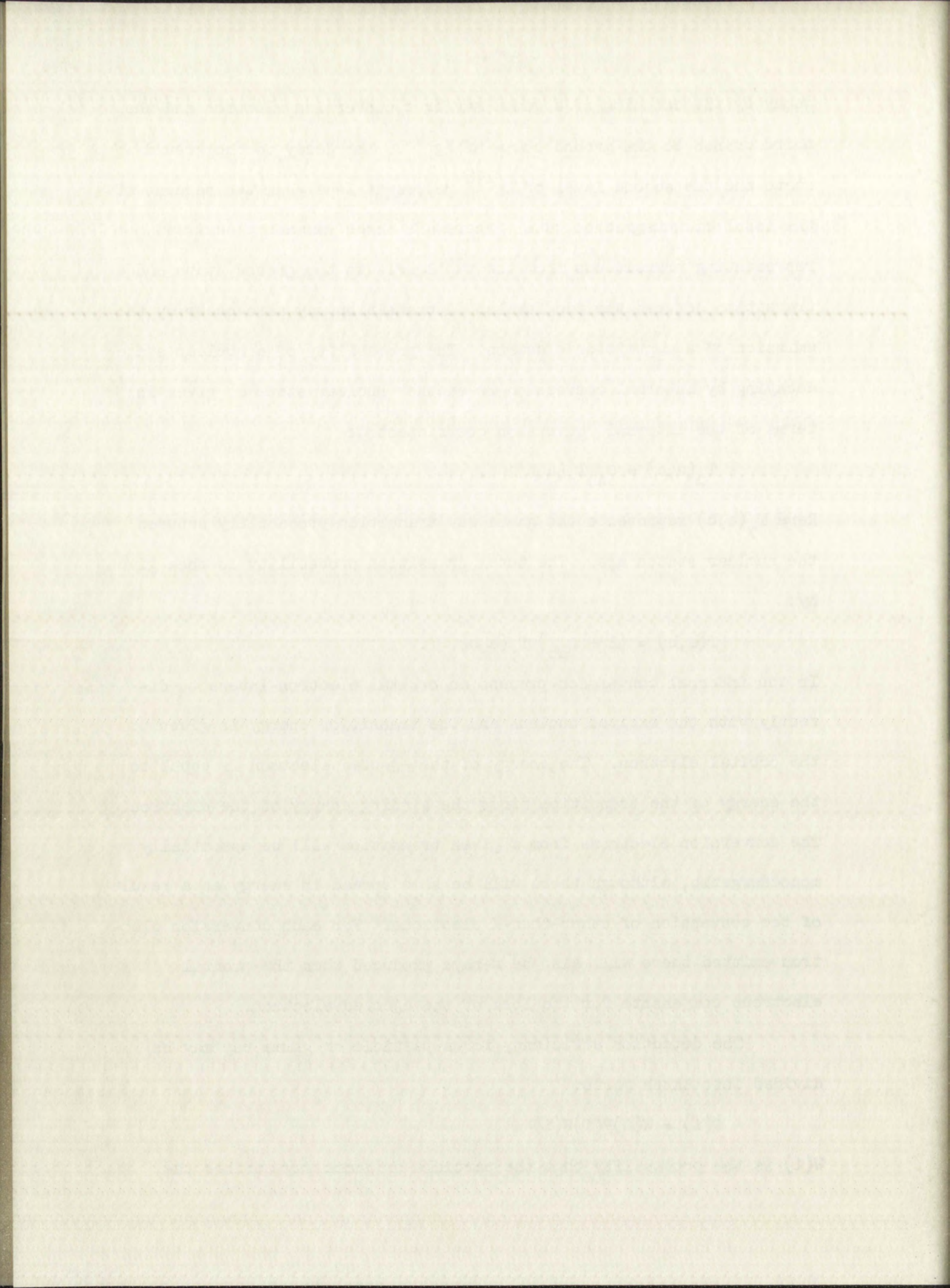
$$T(a,b) = (1 + \alpha_{ab}) T_{\gamma}(a,b) \quad .$$

In the internal conversion process an orbital electron interacts directly with the excited nucleus and the transition energy is given to the orbital electron. The energy of the ejected electron is equal to the energy of the transition minus the binding energy of the electron. The conversion electrons from a given transition will be essentially monoenergetic, although there will be some spread in energy as a result of the conversion of other-than-K electrons. For each conversion electron emitted there will also be x-rays produced when the orbital electrons compensate for the loss of the ejected electron.

The detection efficiency for a particle or gamma ray may be divided into three parts:

$$Q(i) = W(i)P(i)F(i) \quad .$$

$W(i)$ is the probability that the particle or gamma ray strikes the



detector; $P(i)$ is the probability that the particle or gamma ray interacts with the detector; and $F(i)$ is the fraction of interactions which deposit enough energy to exceed the minimum. An above-minimum pulse may also be produced when more than one particle or gamma ray enters the detector, each separately yielding not enough energy to exceed the minimum.

$$Q(i,j) = W(i)P(i)W(j)P(j)(1 - F(i))(1 - F(j))P(i,j) .$$

$P(i,j)$ represents the probability that the sum of the energy deposited from the individual interactions will exceed the minimum energy. There will also be a counting loss as a result of more than one particle or gamma ray entering the detector simultaneously, each having enough energy to exceed the minimum. One may list the contribution to the total counting rate from each branch.

$$N_0 = Q(\beta_0)f_0 S_0 .$$

$$N_1 = \frac{f_1 S_0}{(1+\alpha_1)} \left\{ \begin{aligned} & Q(\beta_1)(1 + \alpha_1) + Q(\gamma_1) + Q(e_1)\alpha_1 + Q(x_1)\alpha_1 \\ & + Q(\beta_1, e_1)(1 - W(x_1)P(x_1))\alpha_1 + Q(\beta_1, \gamma_1) \\ & + Q(\beta_1, x_1)(1 - W(e_1)P(e_1))\alpha_1 + Q(e_1, x_1)(1 - W(\beta_1)P(\beta_1))\alpha_1 \\ & + Q(\beta_1, e_1, x_1)\alpha_1 - [Q(\beta_1)Q(e_1)\alpha_1 + Q(\beta_1)Q(\gamma_1) + Q(\beta_1)Q(x_1)\alpha_1 \\ & + Q(e_1)Q(x_1)\alpha_1 (1 - Q(\beta_1))] \end{aligned} \right\} .$$

The expression for the contribution to the counting rate from the third branch contains more than eighty terms; therefore only terms involving one detection efficiency are listed. Further discussion of the terms not listed will be presented later.

The first part of the proof is to show that the function $f(x)$ is continuous at x_0 . To do this, we need to show that for any $\epsilon > 0$, there exists a $\delta > 0$ such that if $|x - x_0| < \delta$, then $|f(x) - f(x_0)| < \epsilon$.

Let $\epsilon > 0$ be given. We want to find a $\delta > 0$ such that if $|x - x_0| < \delta$, then $|f(x) - f(x_0)| < \epsilon$. We start by noting that $f(x) = \frac{1}{x}$ is continuous at $x_0 \neq 0$. Therefore, there exists a $\delta_1 > 0$ such that if $|x - x_0| < \delta_1$, then $|f(x) - f(x_0)| < \frac{\epsilon}{2}$.

$$\begin{aligned}
 & \text{We also need to ensure that } |f(x)| < \frac{2}{\delta_1} \text{ for } |x - x_0| < \delta_1. \\
 & \text{Since } f(x) = \frac{1}{x}, \text{ we have } |f(x)| = \frac{1}{|x|}. \\
 & \text{If } |x - x_0| < \delta_1, \text{ then } |x| > |x_0| - \delta_1. \\
 & \text{Choose } \delta_2 < |x_0| \text{ such that } |x_0| - \delta_2 > \frac{2}{\epsilon}. \\
 & \text{Let } \delta = \min\{\delta_1, \delta_2\}. \\
 & \text{If } |x - x_0| < \delta, \text{ then } |x - x_0| < \delta_1 \text{ and } |x - x_0| < \delta_2. \\
 & \text{Therefore, } |f(x) - f(x_0)| < \frac{\epsilon}{2} \text{ and } |f(x)| < \frac{2}{\delta_1}. \\
 & \text{Hence, } |f(x) - f(x_0)| < \frac{\epsilon}{2} + \frac{\epsilon}{2} = \epsilon.
 \end{aligned}$$

The expansion for the function $f(x)$ is given by the Taylor series around x_0 . The expansion is valid for $|x - x_0| < \delta$, where δ is the radius of convergence.

$$\begin{aligned}
 N_2 = f_2 S_0 \left\{ Q(\beta_2) + Q(\gamma_1) \frac{a}{1 + \alpha_1} + Q(\gamma_2) \frac{a}{1 + \alpha_2} + Q(\gamma_3) \frac{(1 - a)}{1 + \alpha_3} \right. \\
 + Q(e_1) \frac{\alpha_1 a}{1 + \alpha_1} + Q(e_2) \frac{\alpha_2 a}{1 + \alpha_2} + Q(e_3) \frac{\alpha_3 (1 - a)}{1 + \alpha_3} + Q(x_1) \frac{\alpha_1 a}{1 + \alpha_1} \\
 \left. + Q(x_2) \frac{\alpha_2 a}{1 + \alpha_2} + Q(x_3) \alpha_3 \frac{(1 - a)}{1 + \alpha_3} + \dots \dots \dots \right\} .
 \end{aligned}$$

The quantity, \underline{a} , is the fraction of the transitions from the second level which decay to the first level. So far there has been no distinction made between the two detectors nor has a minimum energy been specified. Suppose now that one detector is sensitive only to gamma rays and the minimum energy is slightly less than the energy of γ_1 . The choice of minimum energy sharply decreases the sensitivity of this detector to scattered gamma rays and x-rays. Under the above conditions the counting rate in the gamma detector is given by:

$$\begin{aligned}
 N_1(\gamma) = f_1 S_0 Q_\gamma(\gamma_1) \frac{1}{1 + \alpha_1} . \\
 N_2(\gamma) = f_2 S_0 a \left\{ Q_\gamma(\gamma_1) \frac{1}{1 + \alpha_1} + Q_\gamma(\gamma_2) \frac{1}{1 + \alpha_2} \right. \\
 + Q_\gamma(\gamma_3) \frac{1}{1 + \alpha_3} \frac{(1 - a)}{a} + \frac{1}{(1 + \alpha_1)(1 + \alpha_2)} [Q_\gamma(\gamma_1, \gamma_2) \\
 \left. + Q_\gamma(\gamma_1, x_2) \alpha_2 + Q_\gamma(x_1, \gamma_2) \alpha_1 - Q_\gamma(\gamma_1) Q_\gamma(\gamma_2)] \right\} .
 \end{aligned}$$

The second detector may be made primarily sensitive to beta particles. The interaction probability for gamma rays is assumed to be small compared to the interaction probability of beta particles. For this detector one may choose a minimum energy greater than the energy of γ_1 . This choice of minimum energy markedly reduces the total detector efficiency. However, for small W_β , the detector will be primarily

1. The first part of the paper is devoted to the study of the asymptotic behavior of the solutions of the system of equations (1) as $t \rightarrow \infty$. It is shown that the solutions of this system tend to zero as $t \rightarrow \infty$ if and only if the matrix A is stable.

2. In the second part of the paper, we consider the problem of the asymptotic stability of the solutions of the system of equations (1) with respect to the initial conditions. It is shown that the solutions of this system are asymptotically stable with respect to the initial conditions if and only if the matrix A is stable and the matrix B is nonsingular.

3. In the third part of the paper, we consider the problem of the asymptotic stability of the solutions of the system of equations (1) with respect to the parameters. It is shown that the solutions of this system are asymptotically stable with respect to the parameters if and only if the matrix A is stable and the matrix B is nonsingular.

4. In the fourth part of the paper, we consider the problem of the asymptotic stability of the solutions of the system of equations (1) with respect to the control. It is shown that the solutions of this system are asymptotically stable with respect to the control if and only if the matrix A is stable and the matrix B is nonsingular.

sensitive to beta particles from the second branch and only an estimate of the remaining sensitivity to other radiations will be required. When the energy is greater than the energy of γ_1 , the counting rate from each branch in the beta detector is given by:

$$N_0(\beta) = Q_\beta(\beta_0) f_0 S_0 \quad ;$$

$$N_1(\beta) = \frac{f_1 S_0}{1 + \alpha_1} [Q_\beta(\beta_1)(1 + \alpha_1) + Q_\beta(\beta_1, e_1)(1 - W_\beta(x_1)P_\beta(x_1))\alpha_1$$

$$+ Q_\beta(\beta_1, \gamma_1) + Q_\beta(\beta_1, x_1)(1 - W(e_1)P_\beta(e_1))\alpha_1$$

$$+ Q_\beta(e_1, x_1)(1 - W_\beta(\beta_1)P_\beta(\beta_1))\alpha_1 + Q_\beta(\beta_1, e_1, x_1)\alpha_1] \quad ;$$

$$N_2(\beta) = f_2 S_0 a \left\{ Q_\beta(\gamma_2) \frac{1}{1 + \alpha_2} + Q_\beta(\gamma_3) \frac{1}{1 + \alpha_3} \frac{(1 - a)}{a} \right.$$

$$+ Q_\beta(\beta_2, e_2)\alpha_2 \frac{1}{1 + \alpha_2} (1 - W_\beta(e_1)P_\beta(e_1))$$

$$+ Q_\beta(\beta_2, e_1) \frac{1}{1 + \alpha_1} \alpha_1 (1 - W_\beta(e_2)P_\beta(e_2)) + Q_\beta(\beta_2, e_3)\alpha_3$$

$$\times \frac{1}{1 + \alpha_3} \frac{(1 - a)}{a} + Q_\beta(e_1, e_2)\alpha_1 \alpha_2 \frac{1}{(1 + \alpha_1)(1 + \alpha_2)}$$

$$\times (1 - W_\beta(\beta_2)P_\beta(\beta_2)) + \dots \text{ other terms involving gamma ray efficiencies } \left. \vphantom{N_2(\beta)} \right\} .$$

The coincidence counting rate from each branch is:

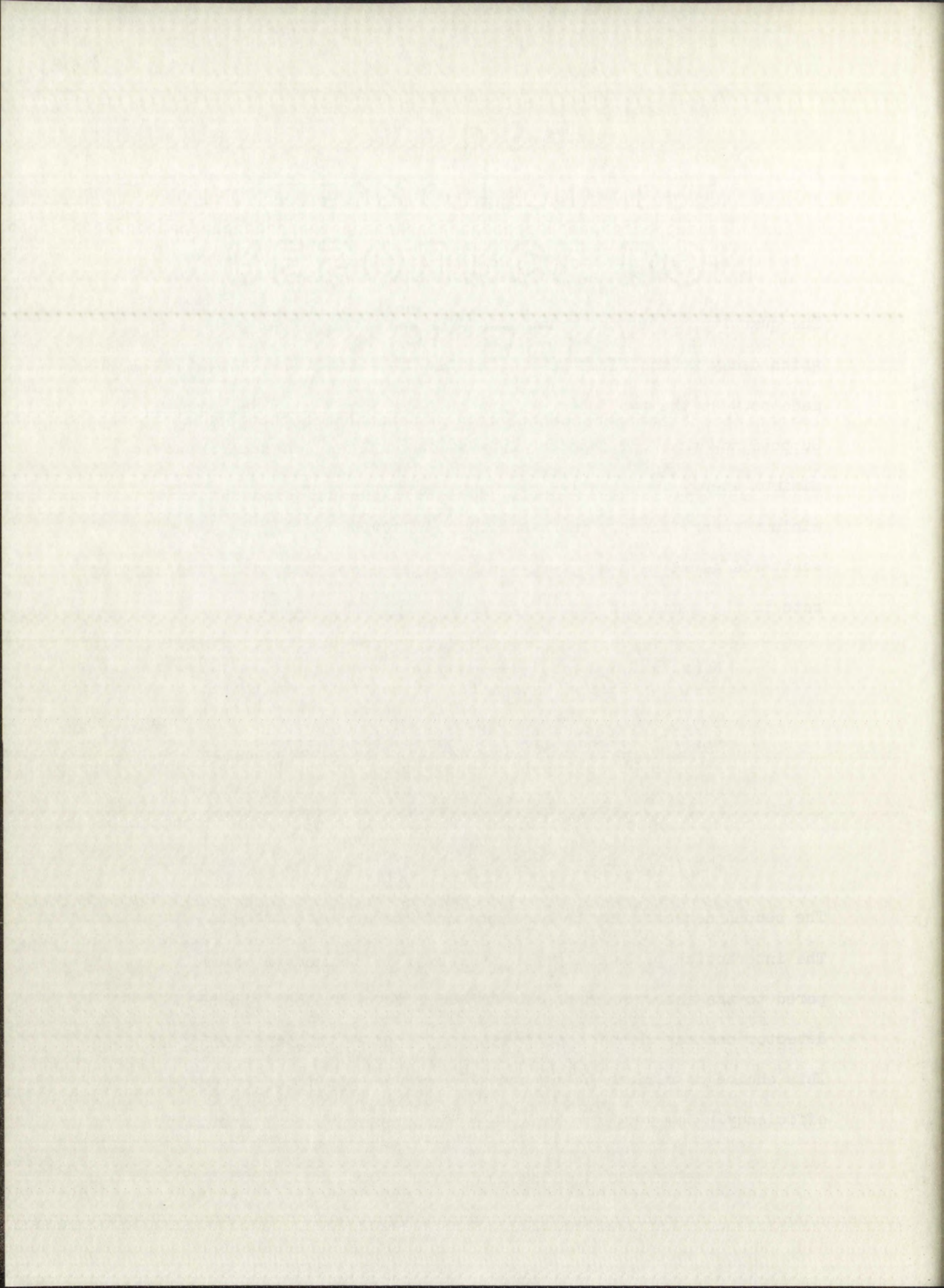
$$N_0(\beta\gamma) = 0 \quad ,$$

$$N_1(\beta\gamma) = \frac{f_1 S}{1 + \alpha_1} Q_\beta(\beta_1) Q_\gamma(\gamma_1) \quad ,$$

and

$$N_2(\beta\gamma) = \frac{f_2 a}{(1 + \alpha_2)(1 + \alpha_1)} [Q_\beta(\gamma_2) Q_\gamma(\gamma_1) + Q_\beta(\beta_2, \gamma_1) Q_\gamma(\gamma_2)$$

$$+ Q_\beta(\beta_2, \gamma_2) Q_\gamma(\gamma_1)] \quad .$$



sensitive to beta particles from the second branch and only an estimate of the remaining sensitivity to other radiations will be required. When the energy is greater than the energy of γ_1 , the counting rate from each branch in the beta detector is given by:

$$N_0(\beta) = Q_\beta(\beta_0) f_0 S_0 \quad ;$$

$$N_1(\beta) = \frac{f_1 S_0}{1 + \alpha_1} [Q_\beta(\beta_1)(1 + \alpha_1) + Q_\beta(\beta_1, e_1)(1 - W_\beta(x_1)P_\beta(x_1))\alpha_1 + Q_\beta(\beta_1, \gamma_1) + Q_\beta(\beta_1, x_1)(1 - W(e_1)P_\beta(e_1))\alpha_1 + Q_\beta(e_1, x_1)(1 - W_\beta(\beta_1)P_\beta(\beta_1))\alpha_1 + Q_\beta(\beta_1, e_1, x_1)\alpha_1] \quad ;$$

$$N_2(\beta) = f_2 S_0 a \left\{ Q_\beta(\gamma_2) \frac{1}{1 + \alpha_2} + Q_\beta(\gamma_3) \frac{1}{1 + \alpha_3} \frac{(1 - a)}{a} + Q_\beta(\beta_2, e_2)\alpha_2 \frac{1}{1 + \alpha_2} (1 - W_\beta(e_1)P_\beta(e_1)) + Q_\beta(\beta_2, e_1) \frac{1}{1 + \alpha_1} \alpha_1 (1 - W_\beta(e_2)P_\beta(e_2)) + Q_\beta(\beta_2, e_3)\alpha_3 \times \frac{1}{1 + \alpha_3} \frac{(1 - a)}{a} + Q_\beta(e_1, e_2)\alpha_1 \alpha_2 \frac{1}{(1 + \alpha_1)(1 + \alpha_2)} \times (1 - W_\beta(\beta_2)P_\beta(\beta_2)) + \dots \text{other terms involving gamma ray efficiencies} \right\} .$$

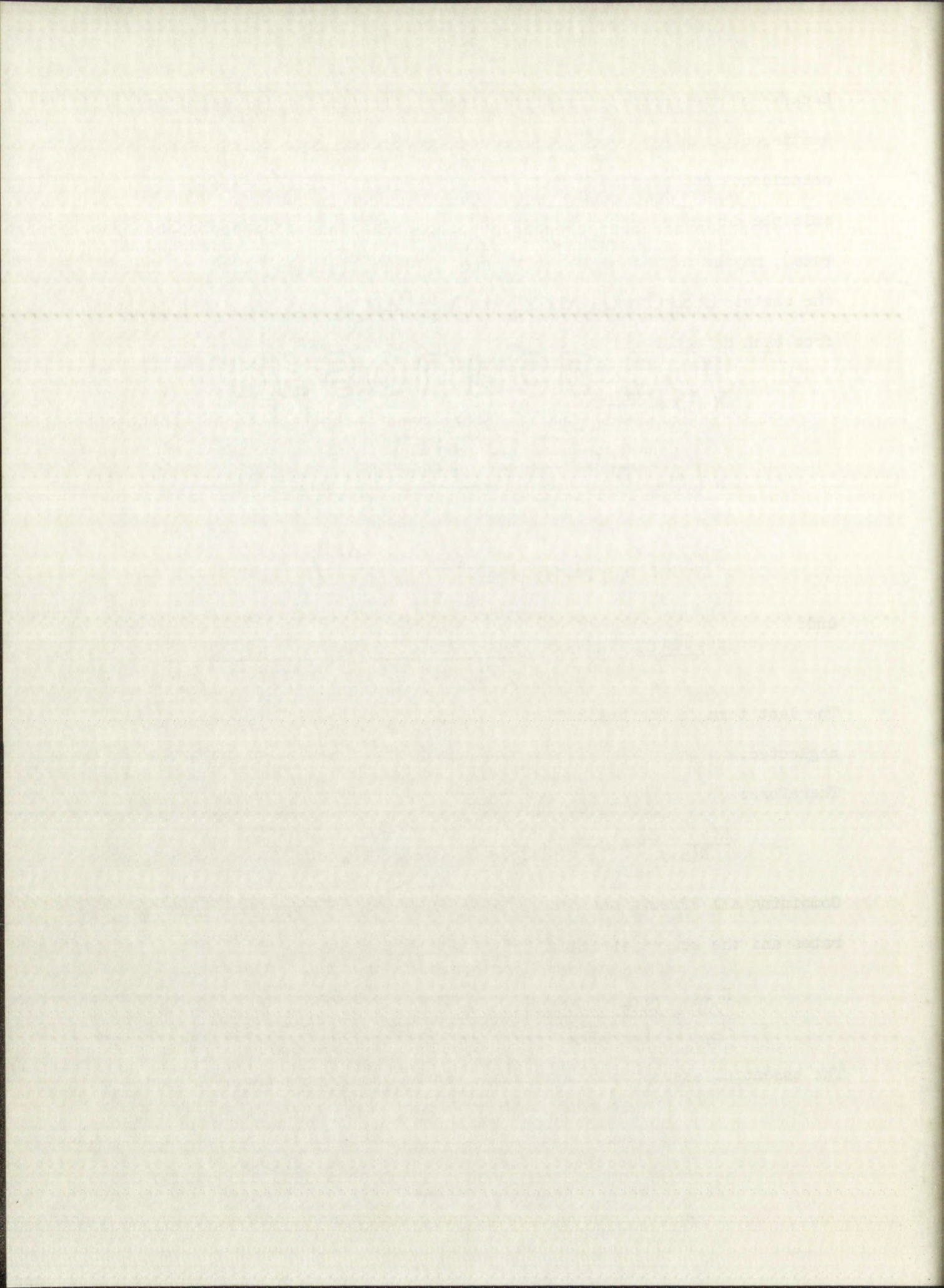
The coincidence counting rate from each branch is:

$$N_0(\beta\gamma) = 0 \quad ,$$

$$N_1(\beta\gamma) = \frac{f_1 S}{1 + \alpha_1} Q_\beta(\beta_1) Q_\gamma(\gamma_1) \quad ,$$

and

$$N_2(\beta\gamma) = \frac{f_2 a}{(1 + \alpha_2)(1 + \alpha_1)} [Q_\beta(\gamma_2) Q_\gamma(\gamma_1) + Q_\beta(\beta_2, \gamma_1) Q_\gamma(\gamma_2) + Q_\beta(\beta_2, \gamma_2) Q_\gamma(\gamma_1)] \quad .$$



above equation may be summarized as follows:

- 1) The coincidence efficiency is approximately equal to the product of the detector efficiencies.
- 2) $\tau S \ll 1$.
- 3) The energy distributions are approximately the same for coincidence and single interactions.
- 4) $E_m(\beta) > .411$ Mev, $E_m(\gamma)$ slightly less than .411 Mev.
- 5) The solid angle subtended by the detectors is small enough that the contributions from terms involving multiple detection efficiencies may be neglected.
- 6) The counting rates have been corrected for background and accidental coincidences.
- 7) There are no angular correlations.

shows equation (1) is satisfied in (10)

1) The relations (10) and (11) are satisfied in the domain of the

the domain of the function

1) $\forall x \in D$

2) The energy distribution is given by the equation

and a similar equation

3) $\forall x \in D$, $\forall t \in T$, $\forall y \in Y$

4) The solid angle subtended by the surface of the sphere is

consequently from (10) and (11) it follows that

may be replaced

5) The density of the mass is given by the equation

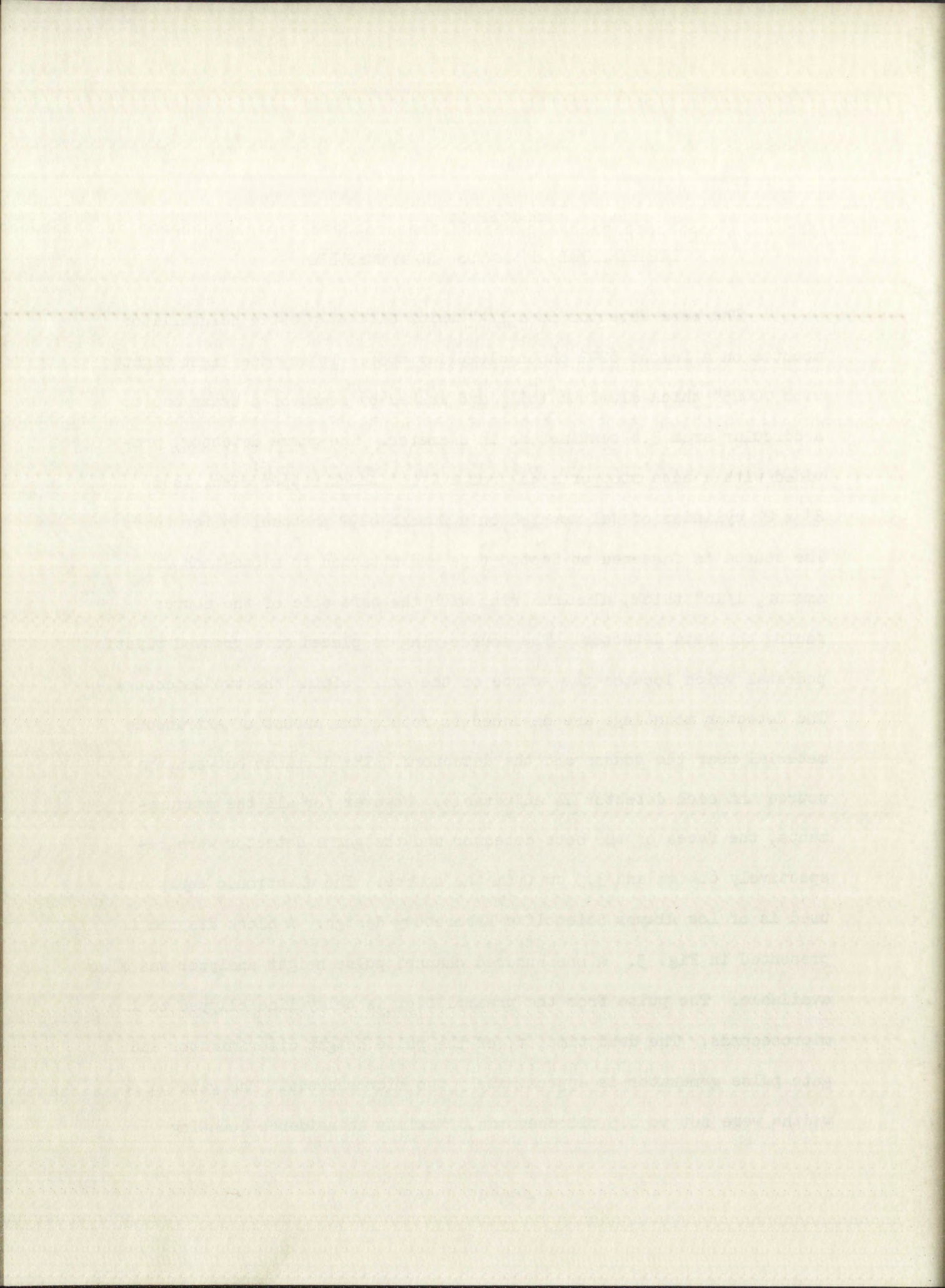
consequently

6) There are no singular points in

CHAPTER IV

EXPERIMENTAL APPARATUS AND PROCEDURES

The beta detector is a $1/4$ " thick disc of plastic scintillator mounted on a Dumont 6292 photomultiplier tube. It is made light tight with $.0025$ " thick aluminum foil, and masked by means of a brass cap to a circular area 3.4 centimeters in diameter. The gamma detector, provided with a beta stopper made from a $1/16$ " thick copper disc, is a 2" x 2" cylinder of NaI mounted on a Dumont 6292 photomultiplier tube. The source is fastened on Scotch tape and attached to a one-inch diameter, $1/16$ " thick, aluminum ring with the bare side of the source facing the beta detector. The source ring is placed on a grooved plastic pedestal which locates the source on the axis joining the two detectors. The detector mountings are designed to reduce the amount of extraneous material near the source and the detectors. The distance between the source and each detector is adjustable. However for all the measurements, the faces of the beta detector and the gamma detector were respectively 6.4 cm and 3.5 cm from the source. The electronic equipment used is of Los Alamos Scientific Laboratory design. A block diagram is presented in Fig. 5. A one hundred channel pulse height analyzer was also available. The pulse from the preamplifier is delay line clipped to 1.6 microseconds. The dead time, τ , of the pulse height discriminator and gate pulse generator is approximately two microseconds. The gate pulse widths were set to 0.5 microseconds. Maximum coincidence counting



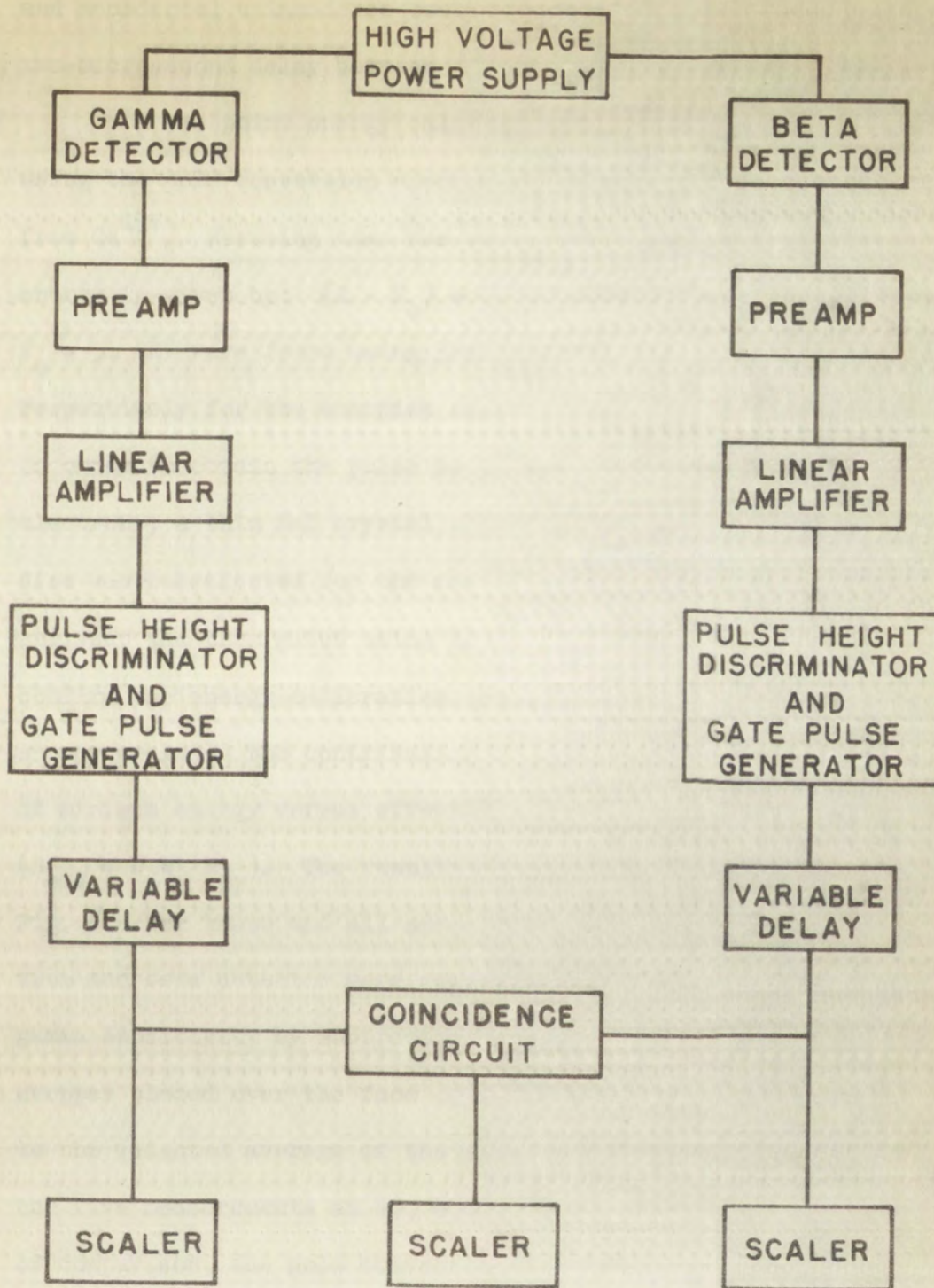


Fig. 5 BLOCK DIAGRAM OF THE ELECTRONIC EQUIPMENT

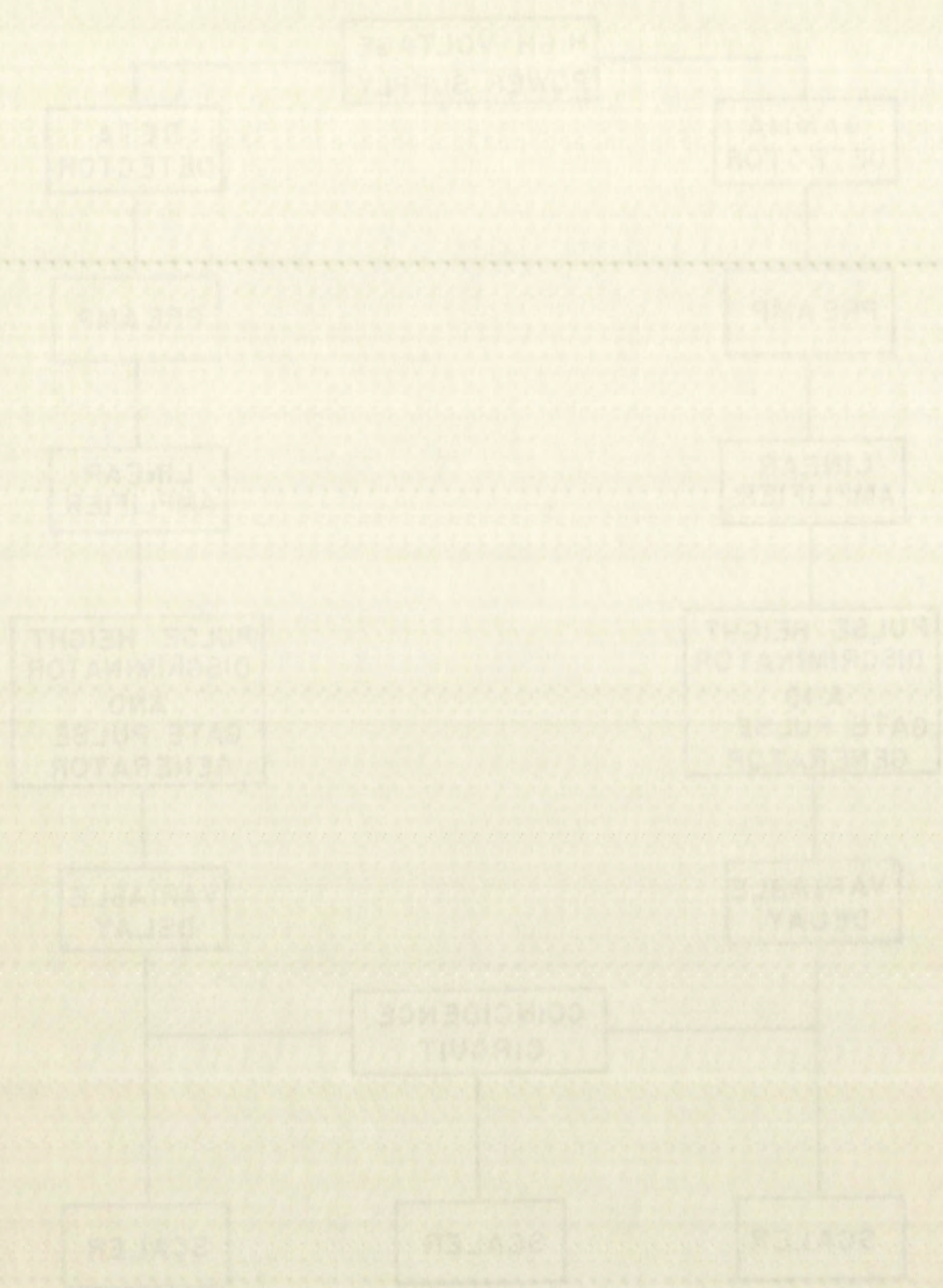
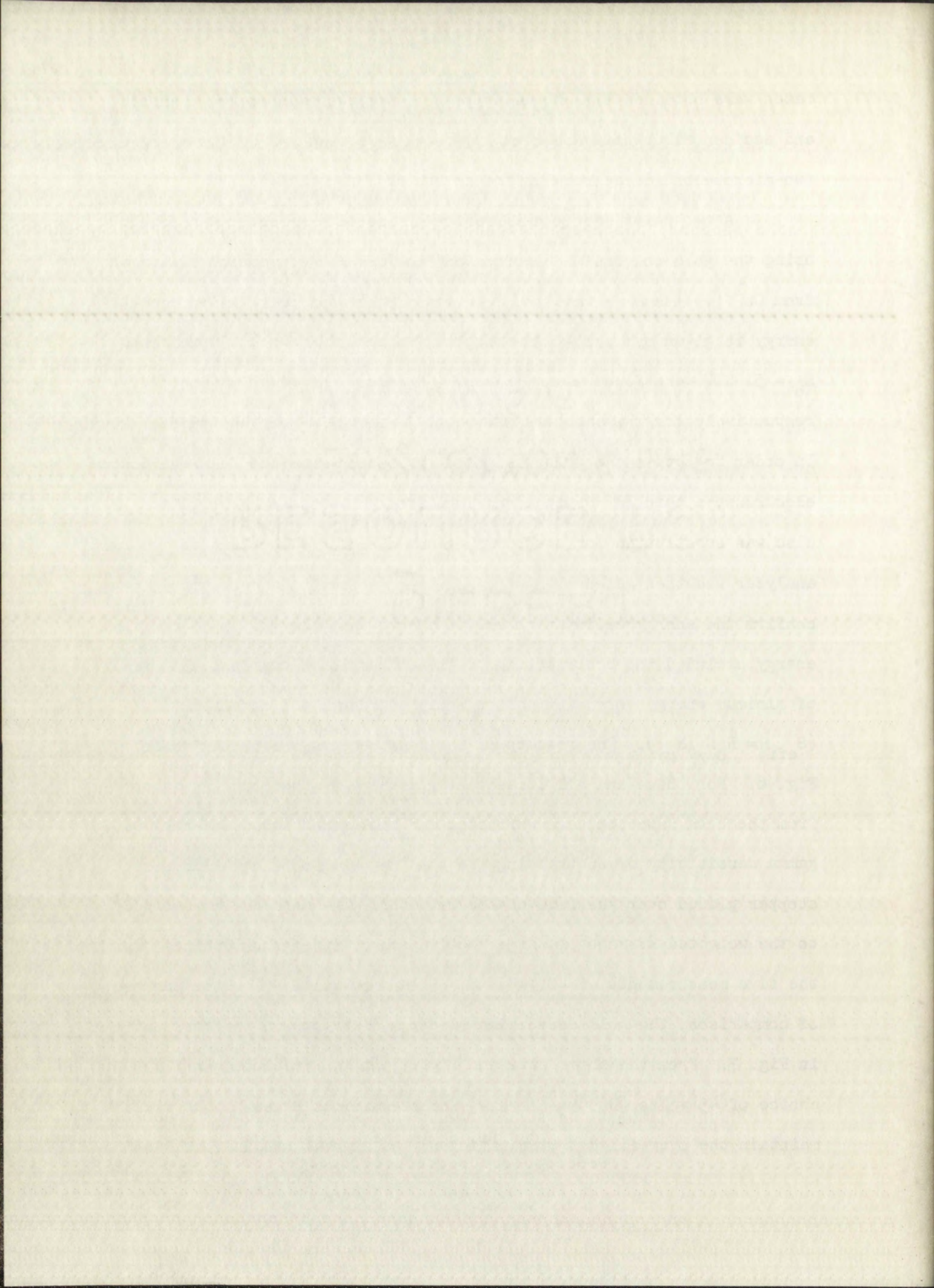
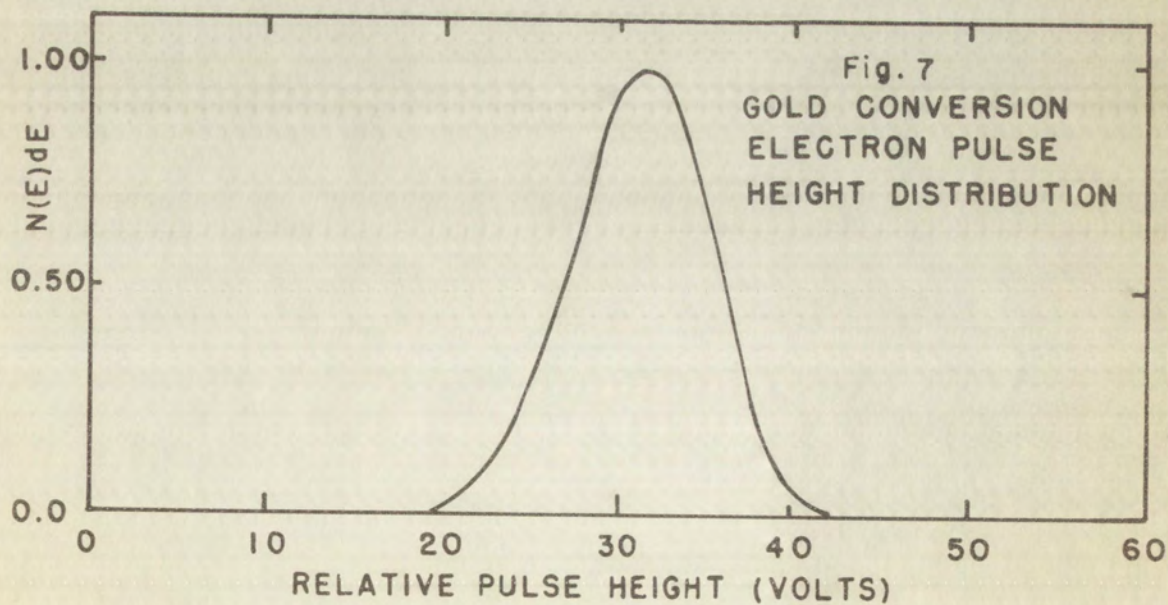
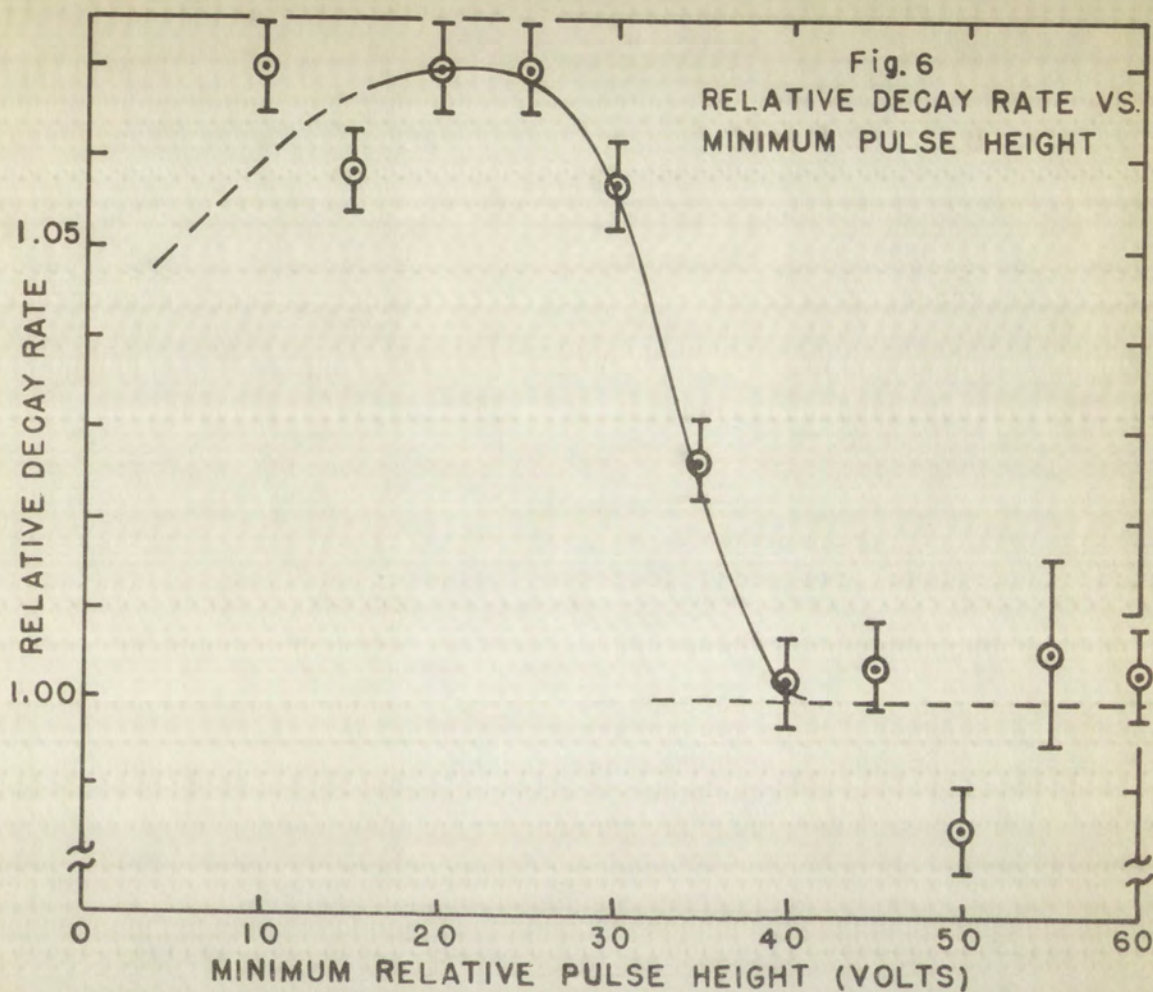


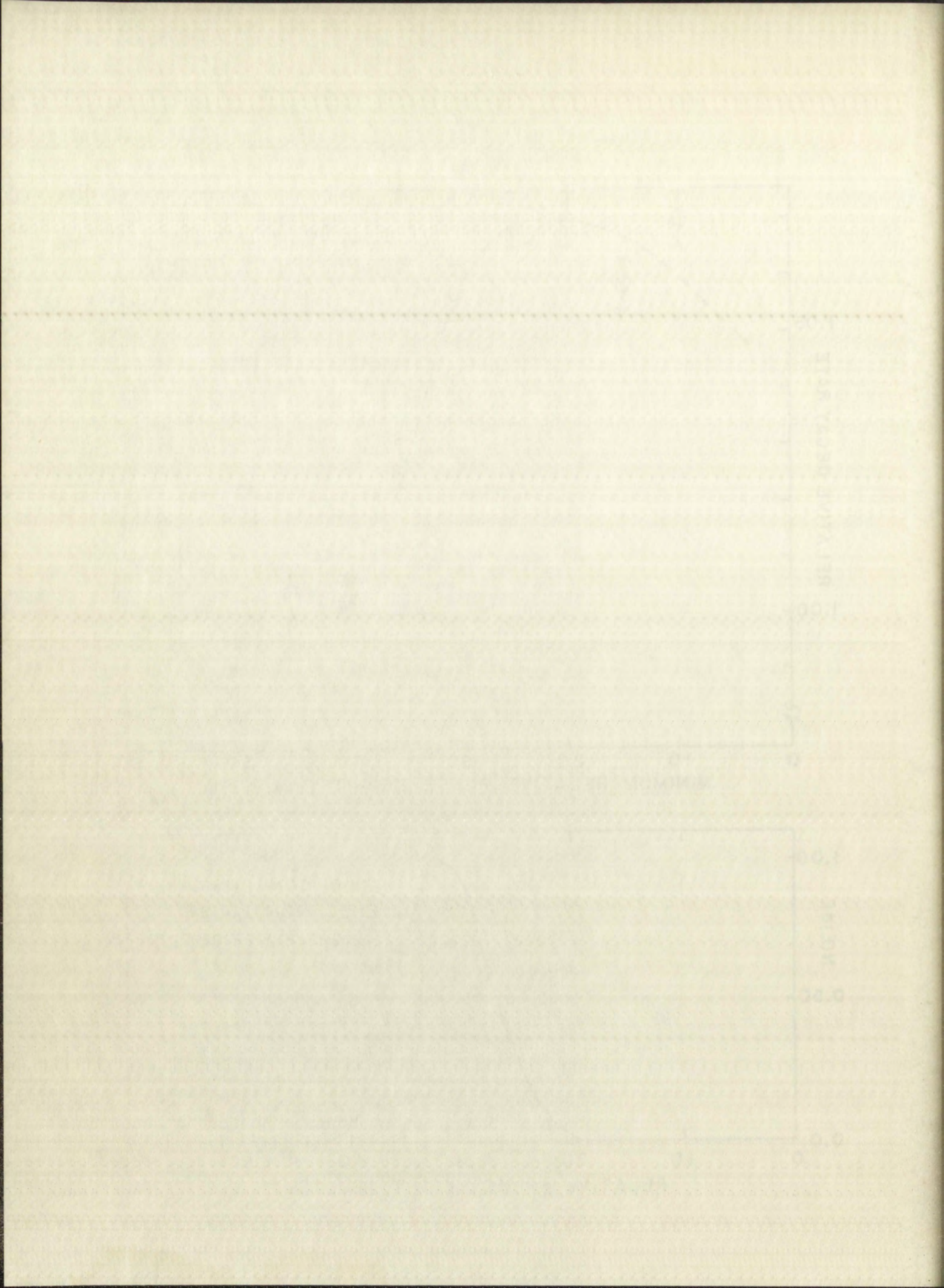
FIG. 2. BLOCK DIAGRAM OF THE ELECTRONIC EQUIPMENT

rates were obtained with no delay between the two coincidence channels and accidental coincidence counting rates were measured by inserting a two-microsecond delay between the channels.

A two point energy calibration of the beta detector was obtained using the gold conversion electron and the 624 KEV conversion electrons from Cs¹³⁷. Assuming that the relationship between pulse height and energy is given by: $(E - E_0) = KV$, the values of $K = 8.8 \text{ KEV/volt}$ and $E_0 = 51 \text{ KEV}$ were found using 329 KEV (32 volts) and 624 KEV (66 volts) respectively for the energies of the Au¹⁹⁸ and Cs¹³⁷ conversion electrons. In order to obtain the pulse height distribution from the fold conversion electrons, a thin NaI crystal shielded from the betas by a beryllium disc was substituted for the normal gamma detector. The hundred channel analyzer was then gated using the gold x-rays from this detector. To confirm the energy calibration and to insure that the choice of minimum energy excluded the contribution of the conversion electrons, a curve of minimum energy versus effective source strength was obtained ($S_{\text{eff}} = N_{\beta} N_{\gamma} / N_{\beta\gamma}$). The results of the measurements are presented in Fig. 6. For these and all subsequent measurements the counting rates from the beta detector were corrected for background and above-minimum gamma sensitivity by subtracting the counting rate obtained with a beta stopper placed over the face of the detector. The data are normalized to the weighted average of the effective source strengths obtained from the five measurements at 40, 45, 50, 55, and 60 volts. For the purpose of comparison, the gold conversion electron distribution is presented in Fig. 7. From the above data and Fig. 8, it was concluded that a choice of 45 volts ($E(\beta) = 411 \text{ KEV}$) for the minimum pulse height would maintain the over-all detector efficiency as high as possible and insure







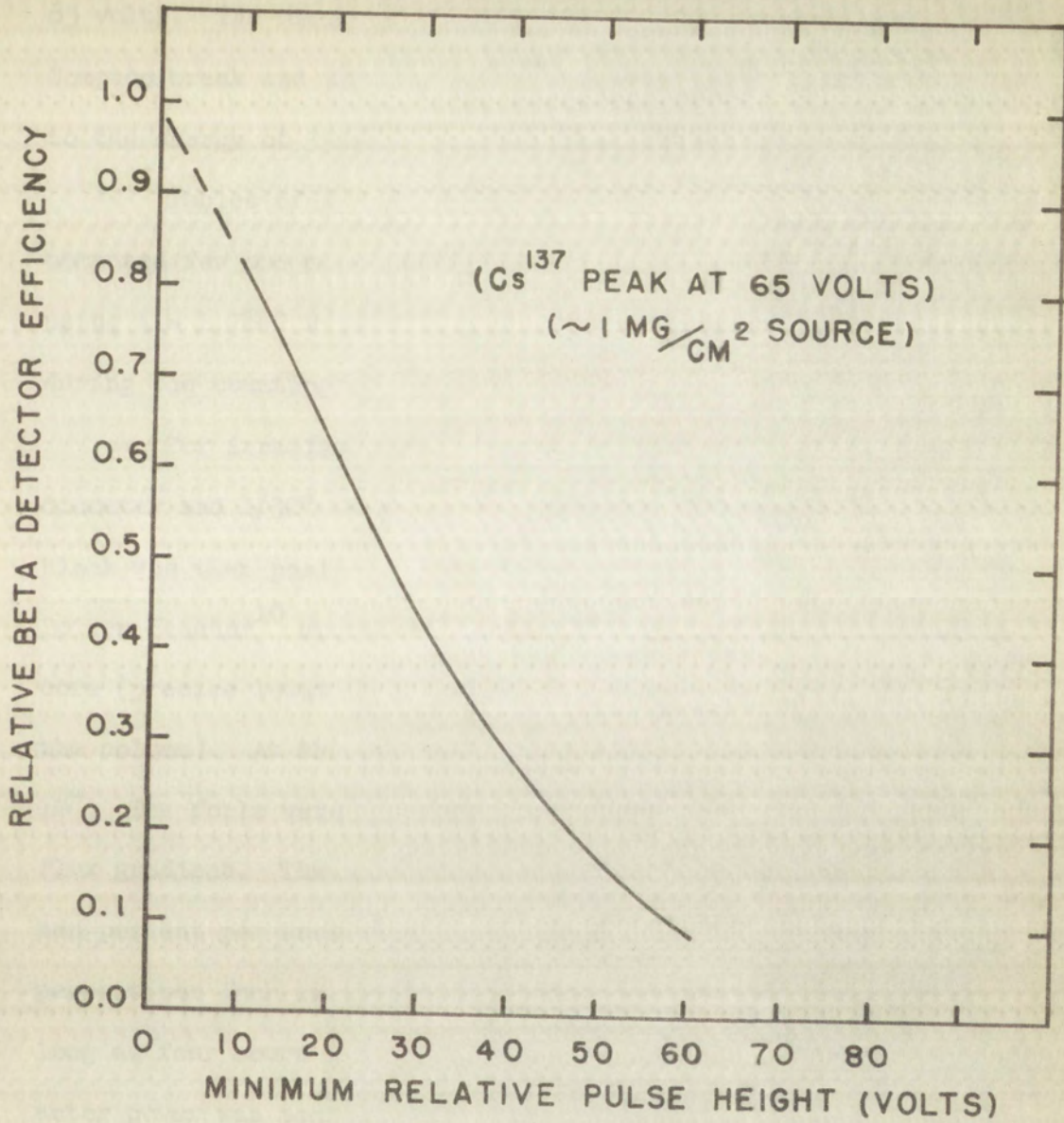


Fig. 8—RELATIVE AU¹⁹⁸ BETA DETECTOR EFFICIENCY



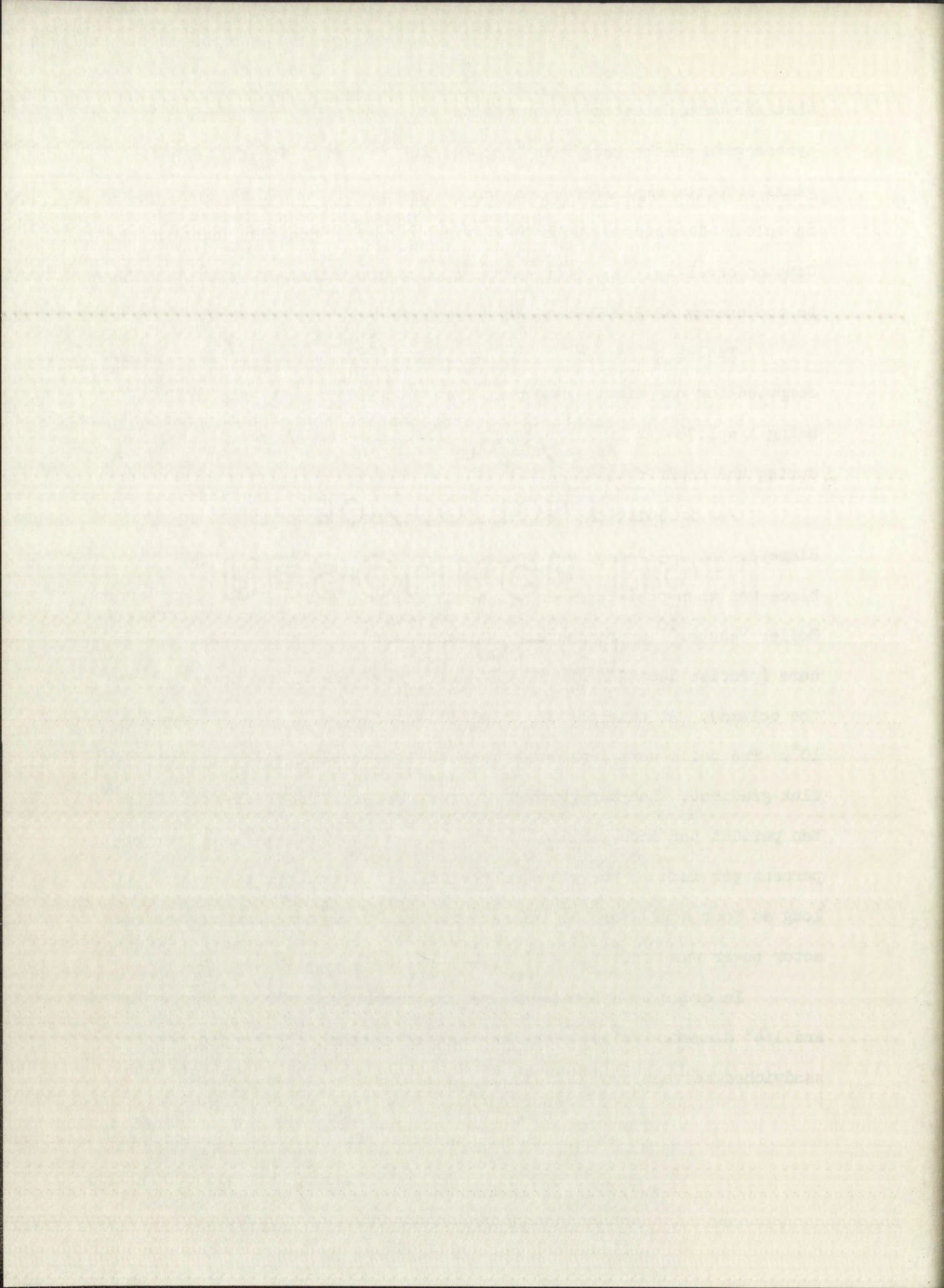
Fig. 3. Relationship between ...

that the beta detector was insensitive to conversion electrons. Frequent system gain checks were made with the Cs¹³⁷ source. The gain of the gamma detector amplifier was adjusted to give the Au¹⁹⁸ photopeak at 65 volts. The minimum pulse height was chosen as 50 volts (between the Compton break and the lower energy edge of the photopeak) corresponding to the energy of 330 KEV.

Tables of λt_0 , $e^{\lambda t_0}$, $e^{-\lambda t_0}$, $(1 - e^{-\lambda t_0})$, and $\lambda t_0 / (1 - e^{-\lambda t_0})$ were computed for one minute intervals from 0 to 200 hours by the MANIAC using $\lambda = 1.7842 \times 10^{-4}$ per minute. All data were corrected for decay during the counting time.

For irradiation, the foils were placed, unmounted, in a 3/4" diameter and 1/32" deep depression machined in a graphite block. The block was then positioned in the South Thermal Column of the Water Boiler Reactor¹⁰ approximately 63 inches from the center of the reactor core (precise location was obtained with reference to the outer end of the column). At this position the gold-cadmium ratio is greater than 10^4 . The foils were irradiated with their axes parallel to the principal flux gradient. The unperturbed neutron flux gradient is approximately ten percent per inch parallel to the axis of the foil and less than one percent per inch in the plane of the foil. The exposure times were as long as four hours for the thinnest foils. During irradiation, the reactor power was monitored with a parallel plate fission chamber.

In order to estimate the return probability, $\beta(0)$, for the 3/4" and 1/4" diameter foils, circular discs of cadmium, .030" thick, sandwiched between two .001" foils, were also irradiated.



CHAPTER V

DATA AND CONCLUSIONS

Table 1 on the following page presents a summary of the data for the relative activity per gram as a function of thickness for 3/4" and 1/4" diameter foils. The entries marked "stack" designate that a stack of .001" foils was used to obtain the nominal thickness. After irradiation, the foils from the stack were counted individually. The data were corrected for the variation of the detector efficiency as a function of foil thickness. It was found that the relative detector efficiencies could be approximately represented by an exponential absorption curve with:

$$\mu_{\beta} = 4.2 \text{ cm}^2/\text{g} \quad \text{and} \quad \mu_{\gamma} = 0.27 \text{ cm}^2/\text{g} \quad .$$

The appropriate averages were calculated (assuming a uniform source) yielding:

$$(1 + \overline{gh}) = 1.02 \text{ for } t = 450 \text{ mg/cm}^2 \quad ;$$

$$(1 + \overline{gh}) = 1.005 \text{ for } t = 255 \text{ mg/cm}^2 \quad .$$

No correction for counting rate effects were applied since, for the source strengths (10^5 d/s) and detection efficiencies employed, the counting rate correction, $\tau_{SC}(F)$, was less than 2×10^{-3} . The graphs of specific activity as a function of foil thickness are presented in Fig. 9. The indicated errors represent only counting statistics. The error resulting from variation of foil position, foil weight, foil impurities, and the evaluation of the corrections to the source strength

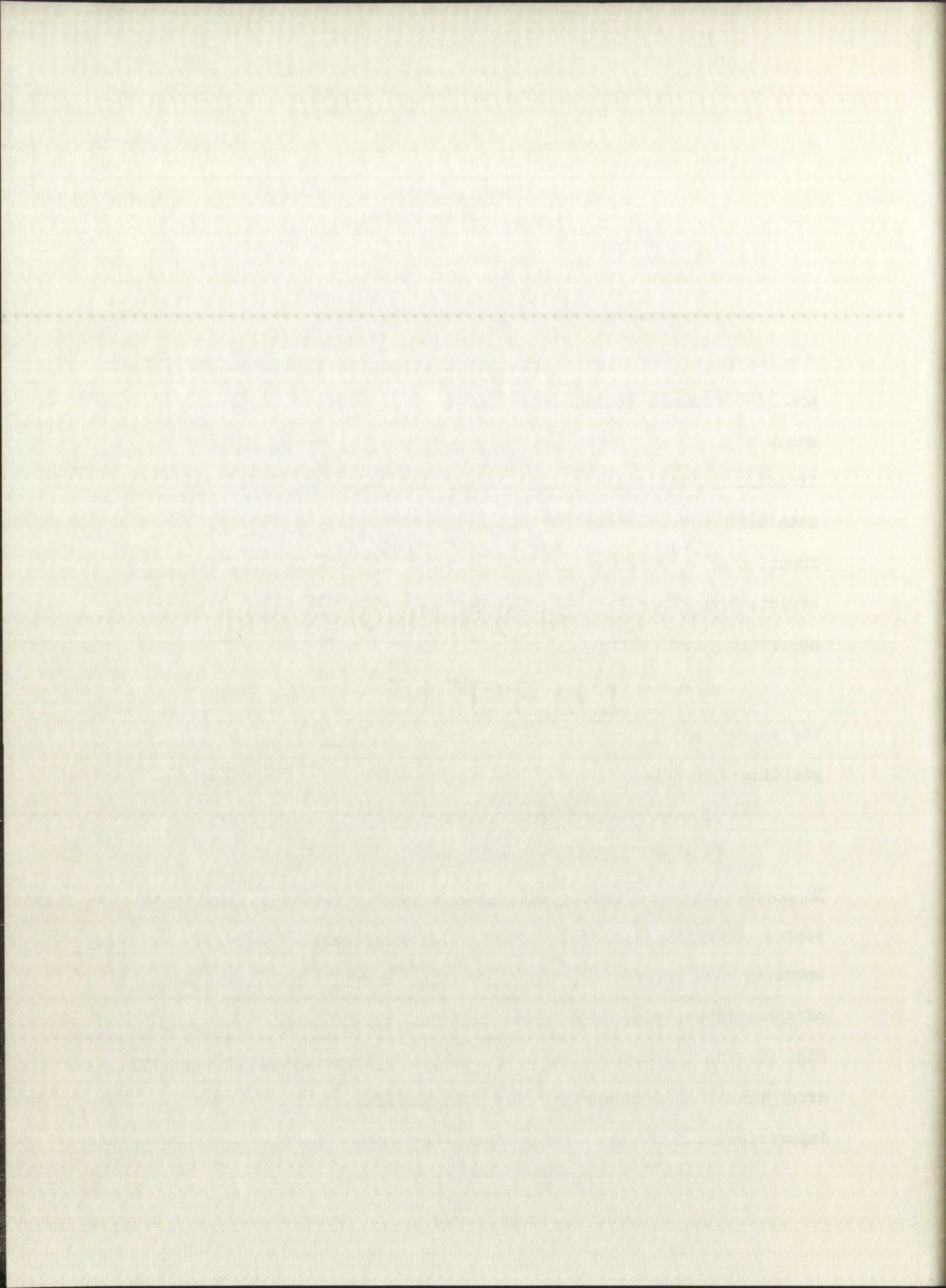


TABLE 1
DATA SUMMARY

MG/CM ² (Average)	y(3/4")*	Nominal Thickness (inches)	MG/CM ² (Average)	y(1/4")*	Nominal Thickness (inches)
1.81	.988	.	24.3	.981	.0005
1.85	1.001	.	54.5	.970	.001
1.36	1.011	.	149	.906	.003
4.75	.995	.	243	.888	.005
14.4	.993	.	449	.838	.010
50.6	.946	.001	$\beta/(1 - \beta) = .05$		
158	.903	.003(Stack)			
159	.899	.003			
269	.859	.005(Stack)			
255	.871	.005			
370	.822	.007(Stack)			
493	.767	.010			
$\beta/(1 - \beta) = .14$					

*y is equal to the activity/mg/neutron monitor count divided by the average of the activity/mg/neutron monitor count for the three thinnest 3/4" foils.

The error in y due to counting statistics (standard deviation) is between 0.5% and 1.0%.

The error in y due to error in x is
 is between 0.5% and 1.5%

x	y	$\frac{dy}{dx}$	$\frac{\Delta y}{y}$
100	100	1.00	1.00%
110	110	1.10	1.10%
120	120	1.20	1.20%
130	130	1.30	1.30%
140	140	1.40	1.40%
150	150	1.50	1.50%
160	160	1.60	1.60%
170	170	1.70	1.70%
180	180	1.80	1.80%
190	190	1.90	1.90%
200	200	2.00	2.00%

The error in y due to error in x is
 is between 0.5% and 1.5%

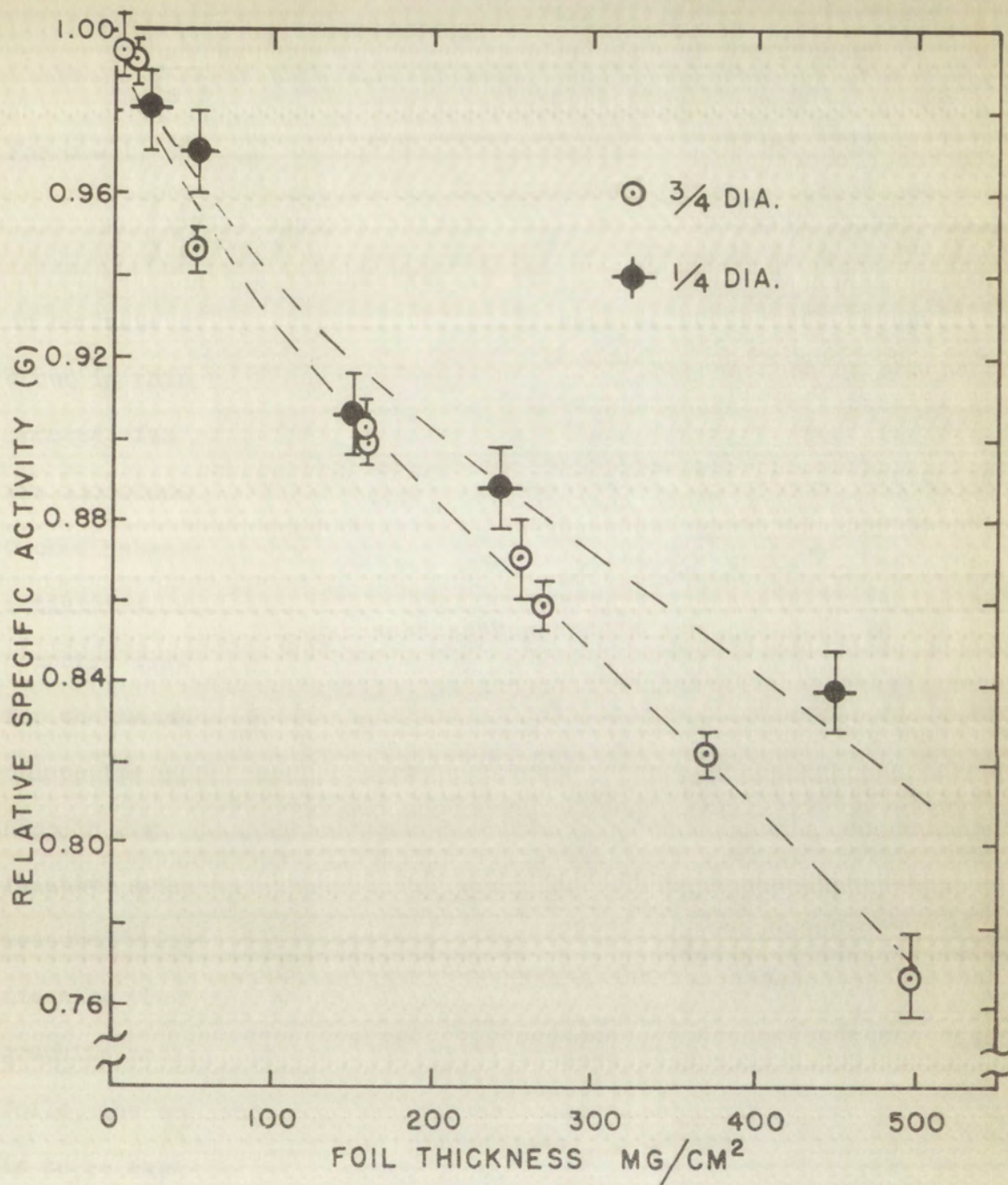
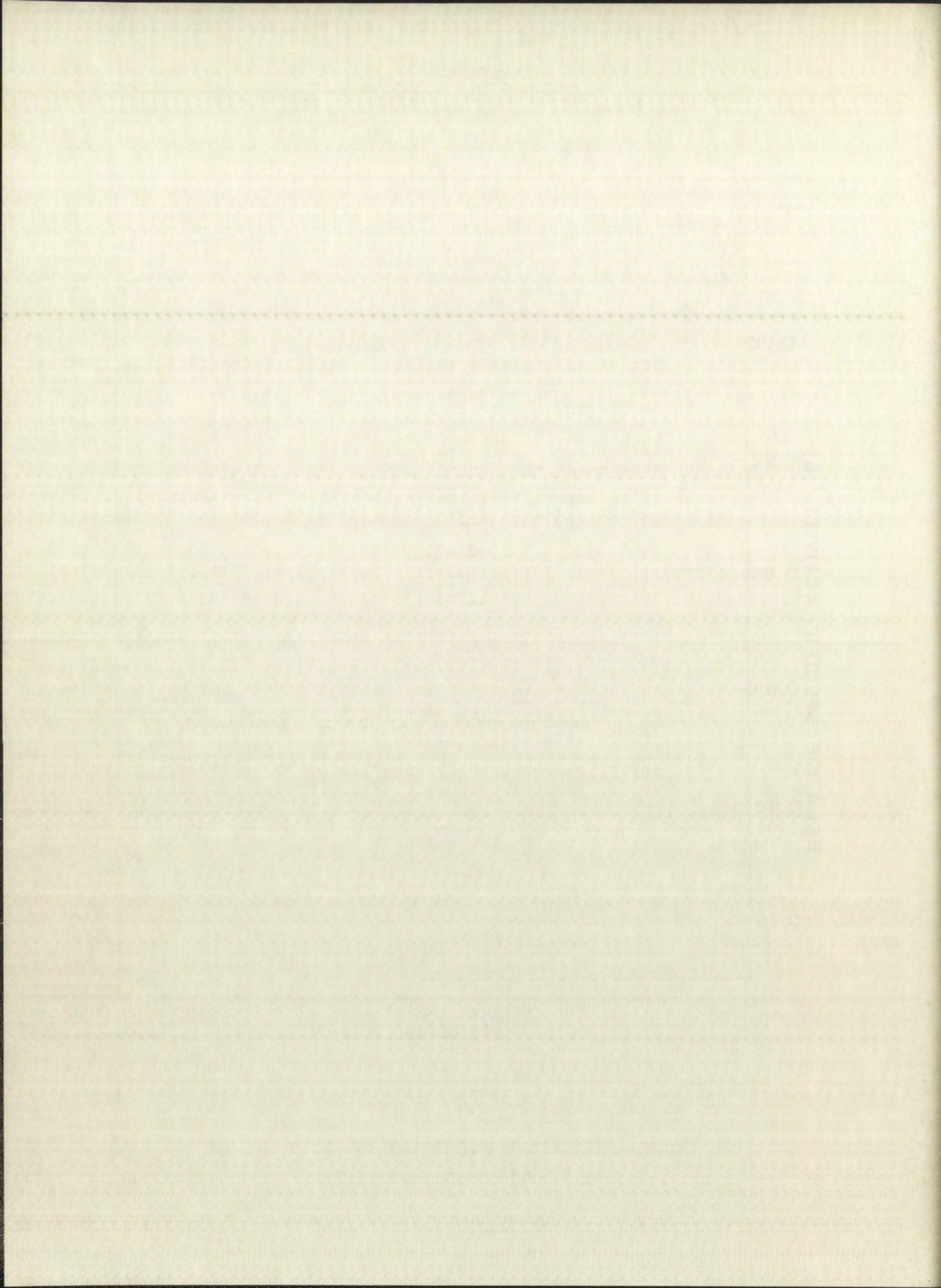


Fig. 9— RELATIVE ACTIVITY OF GOLD FOILS IRRADIATED IN GRAPHITE



is estimated to be one percent.

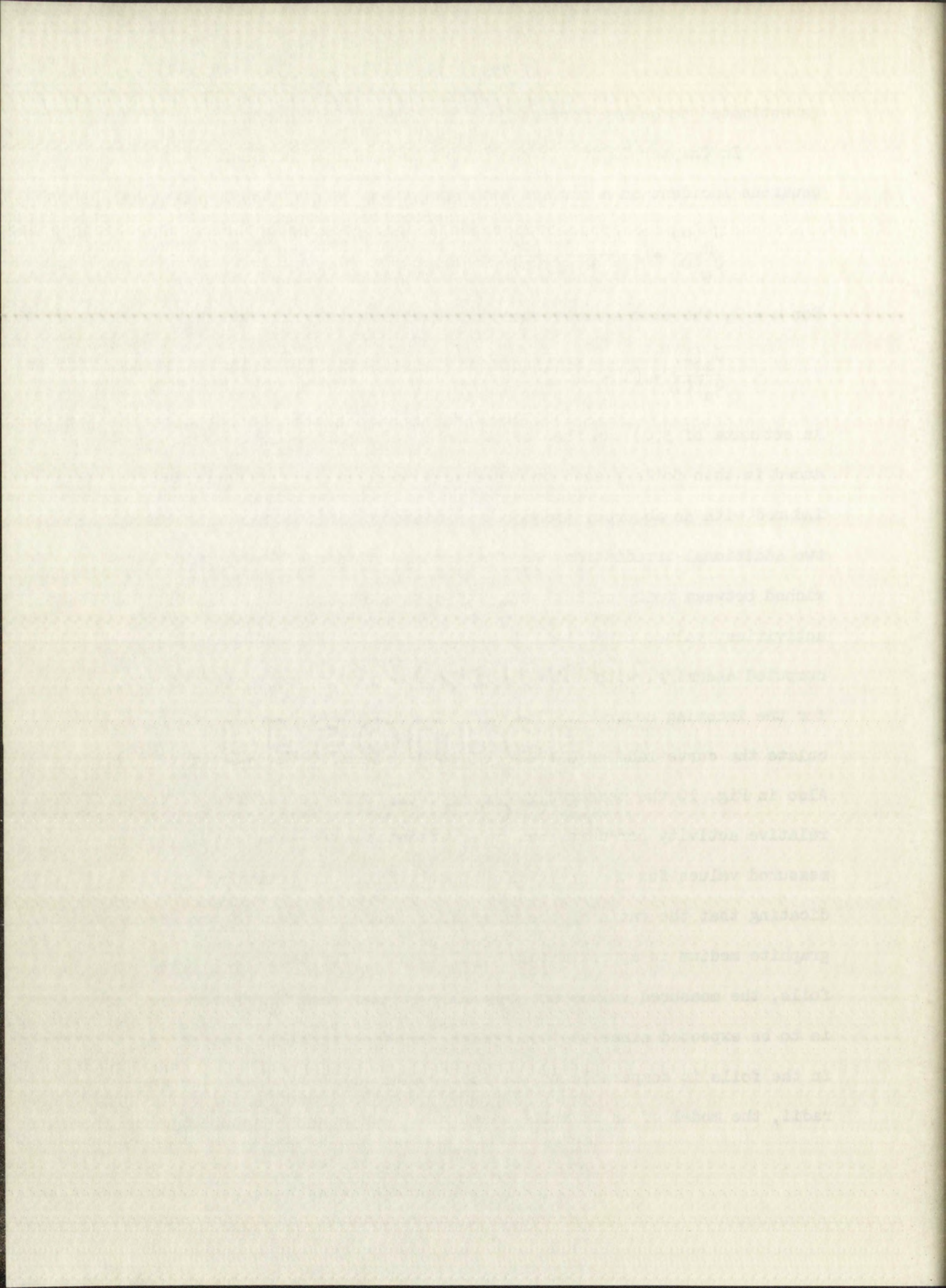
In Chapter II it was shown that the ratio of the number of neutrons incident on a surface with and without absorption is given by:

$$\frac{J_a(\alpha)}{J_a(0)} = \frac{(1 - \beta(0))}{1 - \beta(\alpha)(1-\alpha)} \quad .$$

For $\alpha = 1$, the expression reduces to:

$$\frac{J_a(1)}{J_a(0)} = (1 - \beta(0)) \quad .$$

An estimate of $\beta(0)$ can then be obtained by comparing the activity induced in thin foils placed over a black absorber with the activity induced with no absorber present. As mentioned in the preceding chapter, two additional irradiations were performed with a piece of cadmium sandwiched between foils of 1/4" and 3/4" diameter. From the ratio of activities, values of $\beta/(1-\beta)$ as indicated in the tables ($\beta = \beta(0)$) were computed assuming, with and without absorber, an isotropic distribution for the incoming neutrons. The value for the 3/4" foil was used to calculate the curve labeled $G_M/(1 + \alpha_M'(.14))$ in Fig. 10 ($\alpha_M' = 1 - f_0(\Sigma_0 t)$). Also in Fig. 10 the measured response of the foils is compared to the relative activity per unit area of an infinite sheet (Chapter II). The measured values for the 3/4" foils closely follow the function G_M , indicating that the ratio of the edge effect and the effect of the adjacent graphite medium is approximately equal to one. For the smaller diameter foils, the measured values are generally greater than G_M . This behaviour is to be expected since the absorption mean free path ($1/\Sigma_0 = .174$ cm) in the foils is comparable to the foil radius (.317 cm). For the small radii, the model of an infinite sheet will require appreciable edge



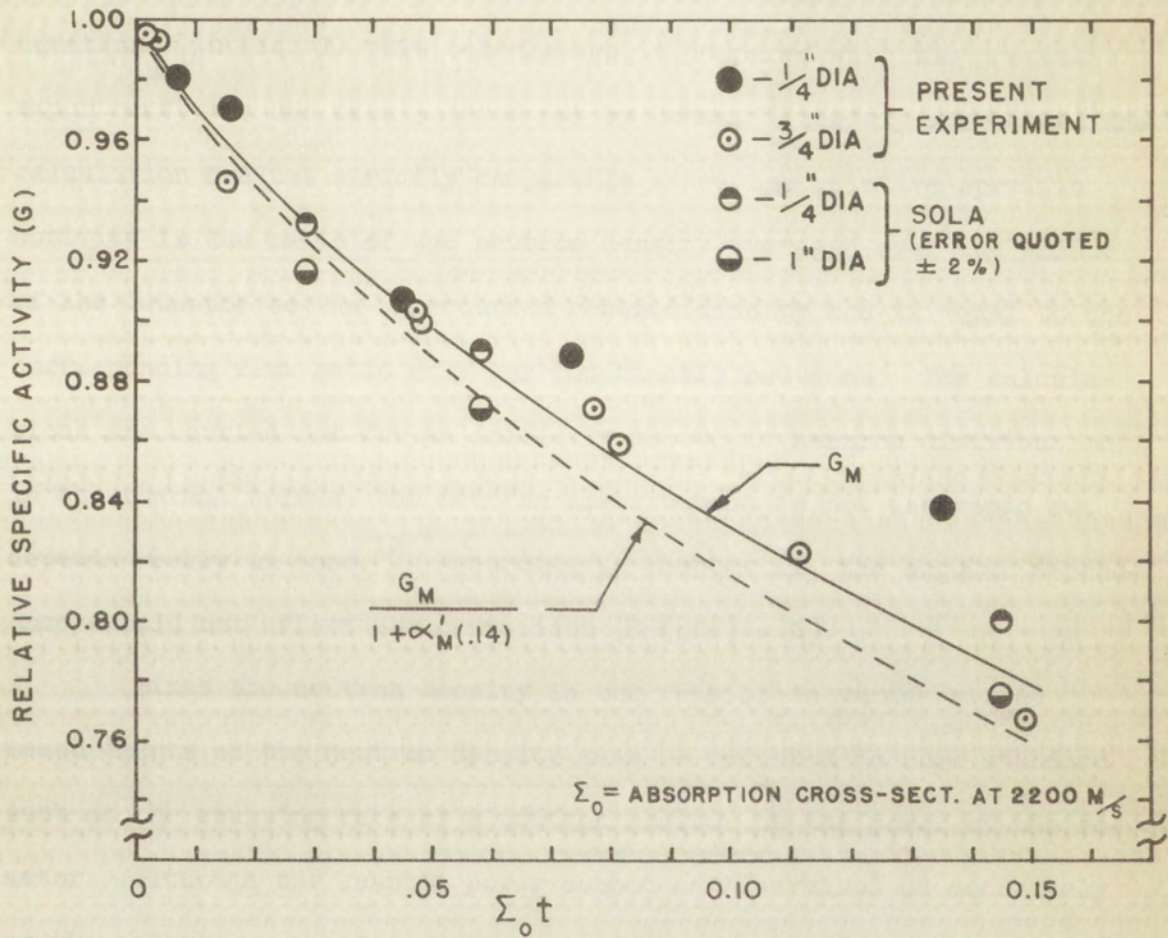
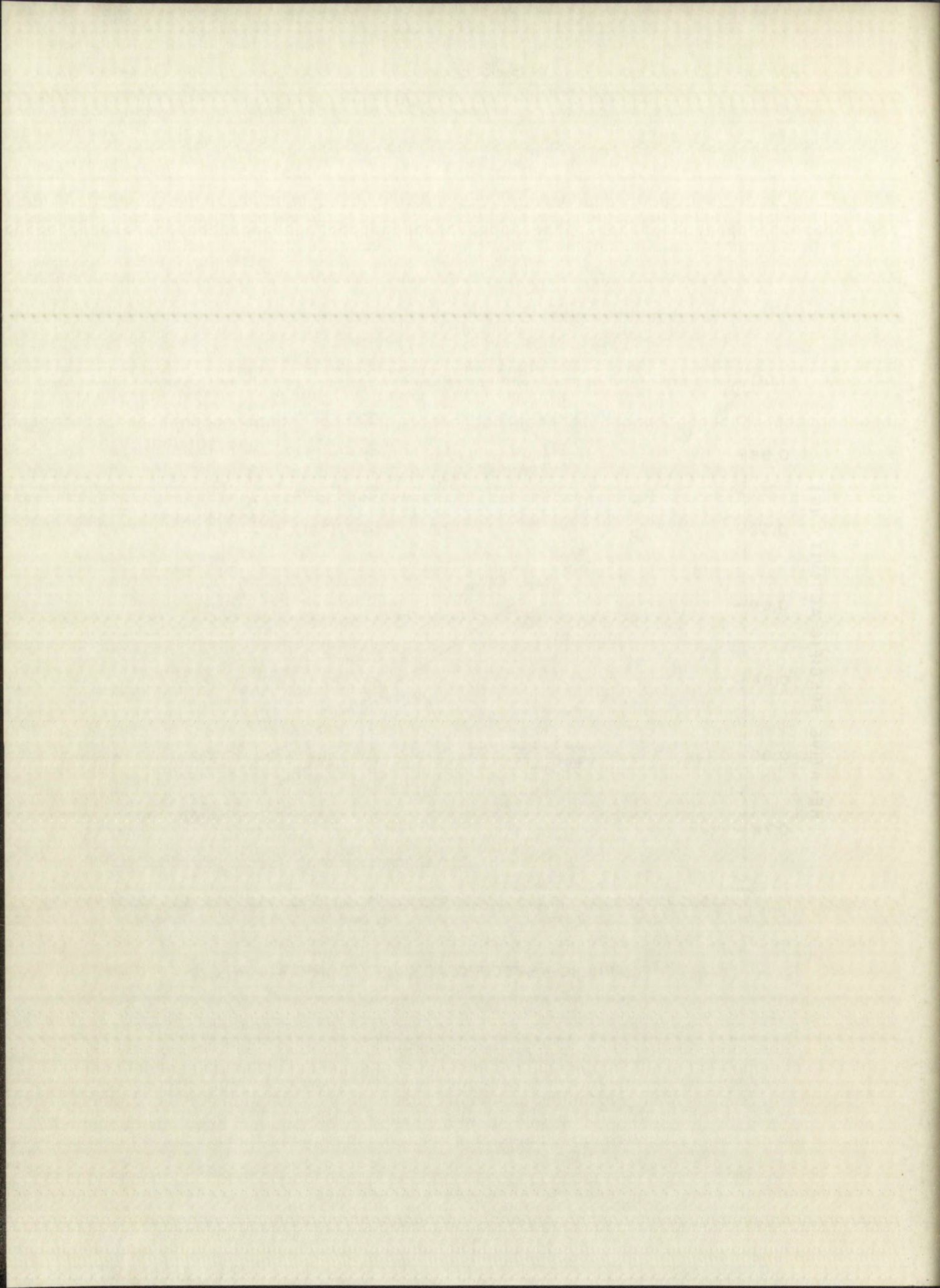


Fig. 10—SPECIFIC ACTIVITY COMPARISON



correction and less correction for the effect of the adjacent medium. Data taken from the measured values reported by Sola⁵ are also presented. To avoid confusion of points on the graph, only the values for .002", .004", and .010" (.001" \sim 48.3 mg/cm²) are given.

The average scalar flux relative to the unperturbed scalar flux for coin shaped detectors in graphite has been obtained by Dalton and Osborn⁶ from a numerical solution of the monoenergetic transport equation. In Fig. 11 this calculation is compared with the present experiment. As has been pointed out by Hanna,¹¹ the experiment and the calculation are not strictly comparable since the relative specific activity is the ratio of the neutron density averaged over the volume of the detector to the unperturbed neutron density and is equal to the corresponding flux ratio only for monokinetic neutrons. The calculations are carried out for an initially isotropic neutron distribution; in the thermal column, the neutron distribution is not isotropic but depends weakly on $\cos\theta$.¹² According to Chapter II, the angular dependence should not affect the comparison ($R_{\ell}(\text{odd}) = 0$).

Since the neutron density in the reactor is variable, the measurements of the neutron density must be referred to some standard such as the counting rate of a neutron monitor or the power of the reactor. Although the reactor power cannot be determined as accurately as the counting rate of a neutron monitor, the proportionality between the neutron density in the thermal column and the reactor power remains constant and therefore provides a convenient standard for routine irradiations. When accuracy is required, a neutron monitor may be calibrated and subsequent irradiations performed in terms of the counting rate of

Faint, illegible text, possibly bleed-through from the reverse side of the page. The text is mirrored and difficult to decipher.

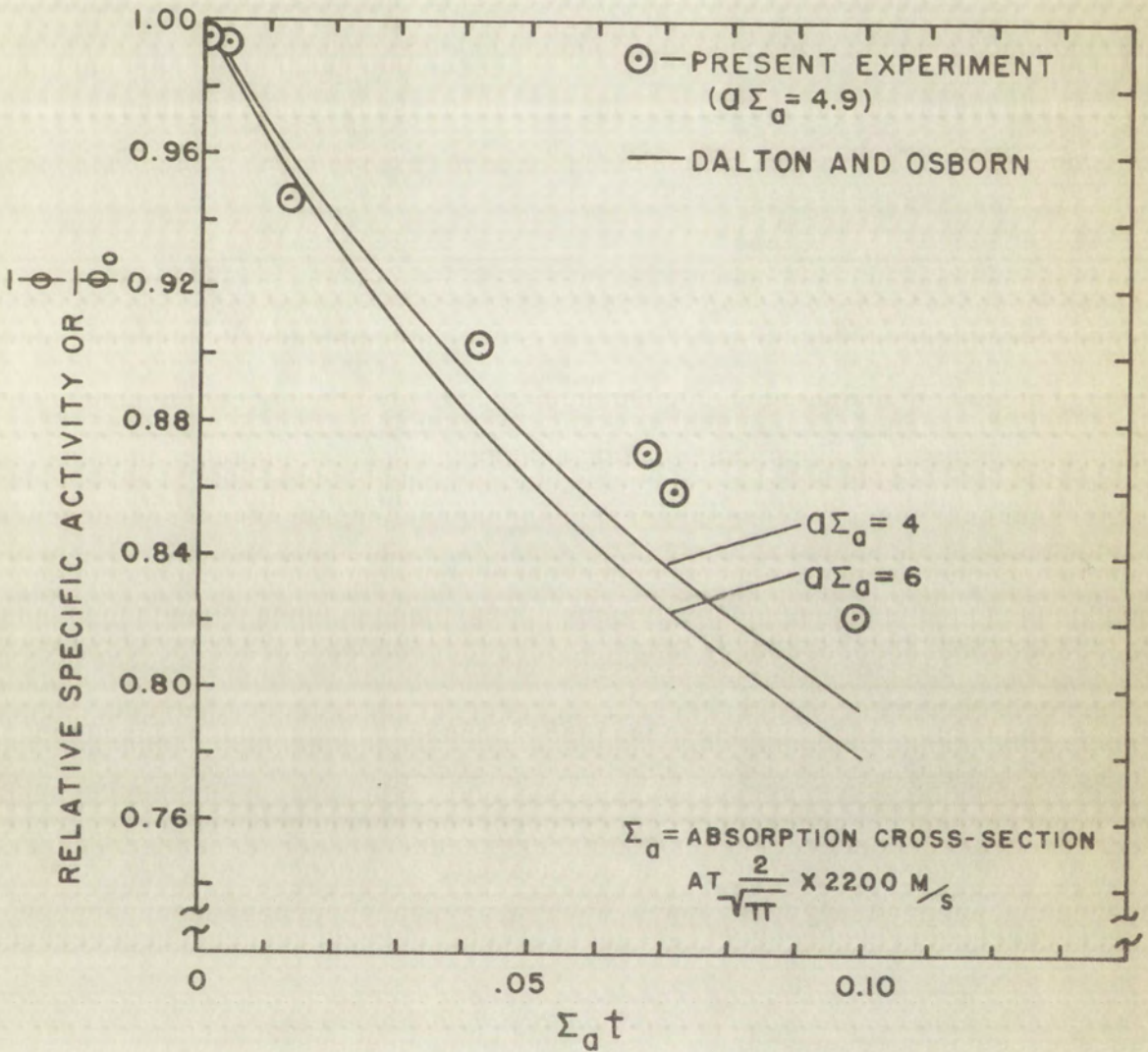
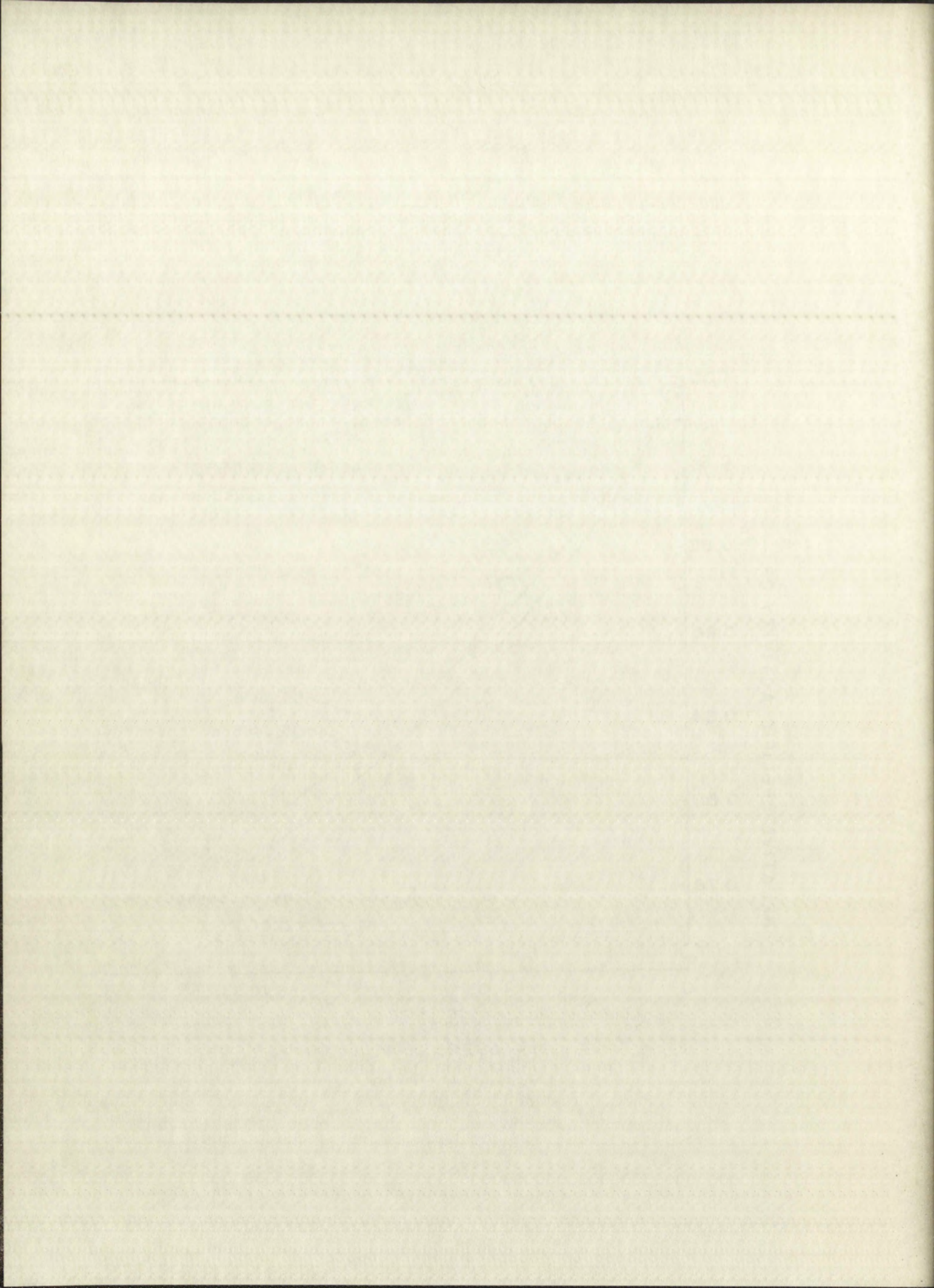


Fig. 11 — AVERAGE FLUX COMPARISON



the monitor. The average of the absolute activity of the three thinnest foils was used to obtain a calibration of a parallel plate fission chamber. The results of the calibration as well as the neutron density referred to the reactor power are given below. For convenience the neutron density multiplied by the velocity, $v_0 = 2200$ m/sec, is given.

At nineteen inches from the end of the South Thermal column

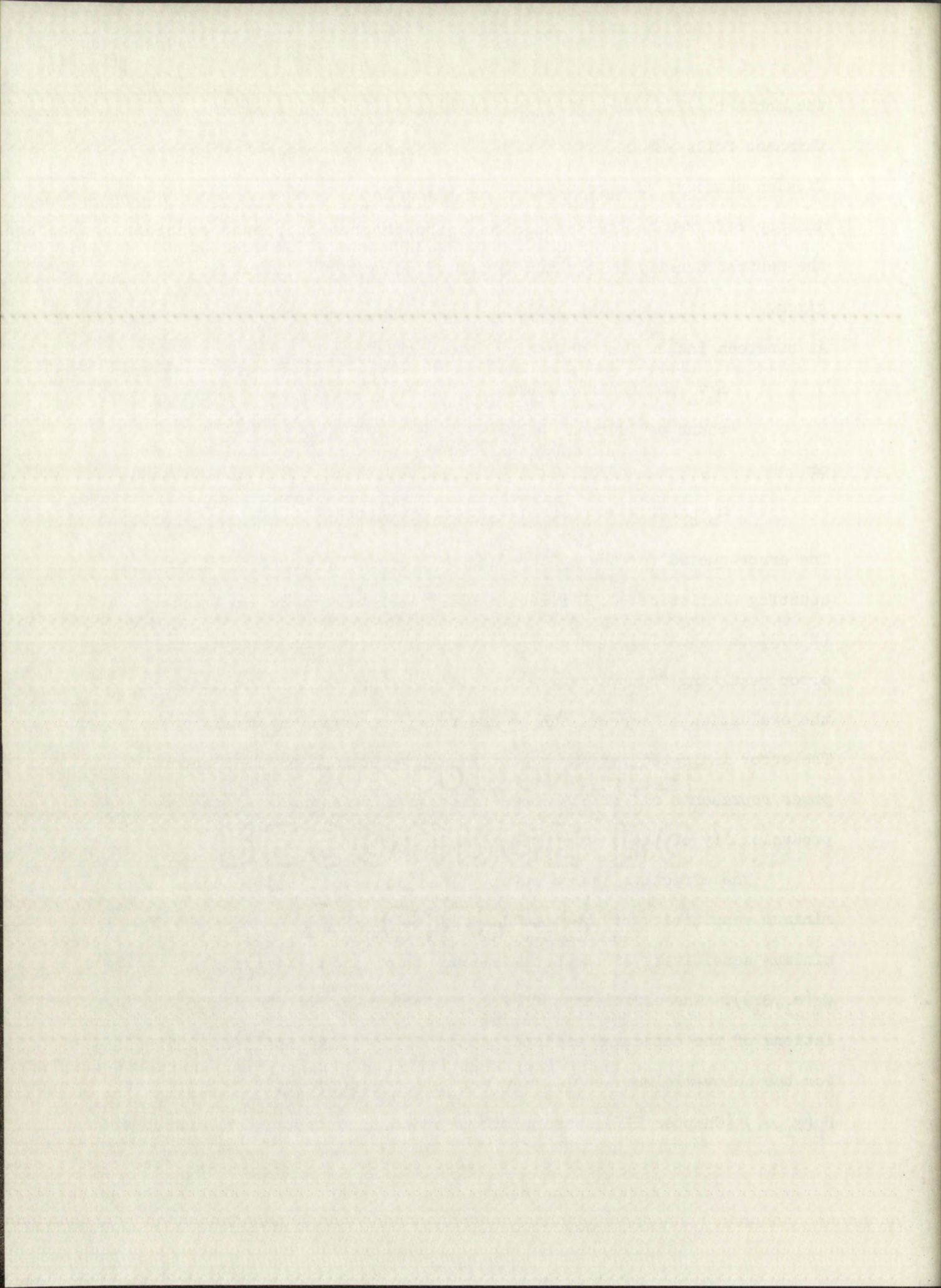
$$\begin{aligned} n_0 v_0 \text{ per neutron monitor} \\ \text{count per second} &= 1.60 \pm 0.03 \times 10^5 \end{aligned}$$

or

$$n_0 v_0 \text{ per kilowatt} = 7.0 \pm 0.4 \times 10^7 .$$

The error quoted for the calibration of the monitor counter reflects: counting statistics (0.5% for each foil); foil weight determination ($\pm 0.3\%$ for each foil); cross section ($\pm 0.3\%$); and an estimate of the error resulting from variation of foil position, foil impurities, and the evaluation of corrections to the source strength and cross section. The error indicated for the neutron density referred to the reactor power represents all of the above errors plus an estimate of the reproducibility of the reactor power calibration.

The effective source strength was corrected for the above-minimum sensitivity of the beta detector to γ_2 ($Q_\gamma(\gamma_2)$), and the below-minimum sensitivity of the beta detector to γ_1 and e_1 ($Q_\beta(\gamma_1, \beta_1)$, $Q_\beta(e_1, \beta_1)$). The efficiency, $Q_\gamma(\gamma_2)$, was obtained from theoretical calculations of the detection efficiency of NaI.^{13,14} To obtain the correction for the below-minimum sensitivity to γ_1 , the quantities, $P_\beta(\gamma_1)$ and $P_\beta(\gamma_1, e_1)$ (Chapter III), were obtained by assuming that the interaction



of γ_1 with the beta detector is the result of Compton collisions in the plastic scintillator.

Thus:

$$P_{\beta}(\gamma_1) = e^{-\mu_c x} = .20$$

and

$$P_{\beta}(\gamma_1, \beta_1) = .27 \text{ (numerical integration requiring the sum of the pulse heights to exceed the minimum) .}$$

Since the conversion electron distribution is so close to the minimum energy, the below-minimum sensitivity to e_1 was obtained by assuming $P_{\beta}(e_1)P_{\beta}(\beta_1, e_1) = 1$. Inasmuch as the foils used for the calibration were very thin, variation in efficiency because of source thickness was neglected. In addition to effects of source thickness, the efficiency of a detector for different parts of the source will vary because of the change in solid angle; and, provided the detectors are not completely black to the radiation, because of the change in the angle of incidence of the radiation from the source. Both effects are functions of the distance of an incremental area of the source from the axis of the source. The correction, \overline{gh} , is not expected to be appreciable since, because of the small solid angle subtended, both effects are small for the beta detector. One may obtain an estimate of \overline{gh} by expressing the variations, for each detector, as a series depending on the distance, \underline{r} , of an incremental area of the source from the axis of the source. A first approximation may be obtained by assuming the variation is entirely the result of variation in solid angle. Utilizing the series given by Jaffey¹⁵ (first two terms) for the solid angle subtended by a circular disc from an off axis point one obtains $\overline{gh} = 1.3 \times 10^{-4}$. The assumption was made that the variation in sensitivity because of angle of incidence

Faint, illegible text at the top of the page, possibly a header or introductory paragraph.

Main body of faint, illegible text, appearing to be several paragraphs of a document or report.

is comparable to the solid angle variation and no correction was applied for the variation in sensitivity over the volume of the source. Combining all of the above effects yields the relationship between the effective and actual source strength:

$$S_{\text{eff}} = (1.017) S_0 .$$

The gold cross section correction factor (1.005) was taken from values published by Westcott.¹⁶ For this correction, the effective neutron temperature was assumed to be 20°C and the contribution to the activation from epicalcium neutrons neglected.

The model of the infinite sheet and the cylindrical absorber imbedded in a scattering medium provide a convenient conceptual basis for considering the activation of a foil shaped detector. The effects of the adjacent medium and the energy and angular distributions of the incident neutrons may be separated; the relative importance of each may then be ascertained. The effect of the adjacent medium has been considered by monoenergetic, diffusion theory (Bothe³), transport theory (Ritchie-Eldredge,¹⁷⁺ Skyrme⁴) and single scattering return probability (Meister¹⁸⁺). The change in activation because of the adjacent medium has been measured directly by Meister⁷ (paraffin, graphite). The numerical solutions of the monoenergetic transport equation given by Dalton and Osborn furnish the most complete data available. However it is difficult to decide how to include the effects of the neutron energy distribution so that the activation of the detector may be obtained from the calculations of the average flux. The separate evaluation (including

⁺The g function defined in these papers differs from the definition given here. For comparable neutron distributions the difference amounts to approximately a factor of two ($\alpha \sim 2(1/2 - E_3(\Sigma_0 t))$).

... compared to the full width at half maximum ...
 for the variation in activation energy ...
 and actual source strength.

$$E_{act} = E_0 + kT \ln \left(\frac{A_0}{A} \right)$$

values obtained by ...
 activation energy was assumed to be ...
 activation from ...

The model of the ...
 included in a ...

for considering the ...
 of the adjacent ...
 incident ...

then be ...
 allowed by ...
 (Richardson-Dushman) ...
 (Richardson-Dushman) ...

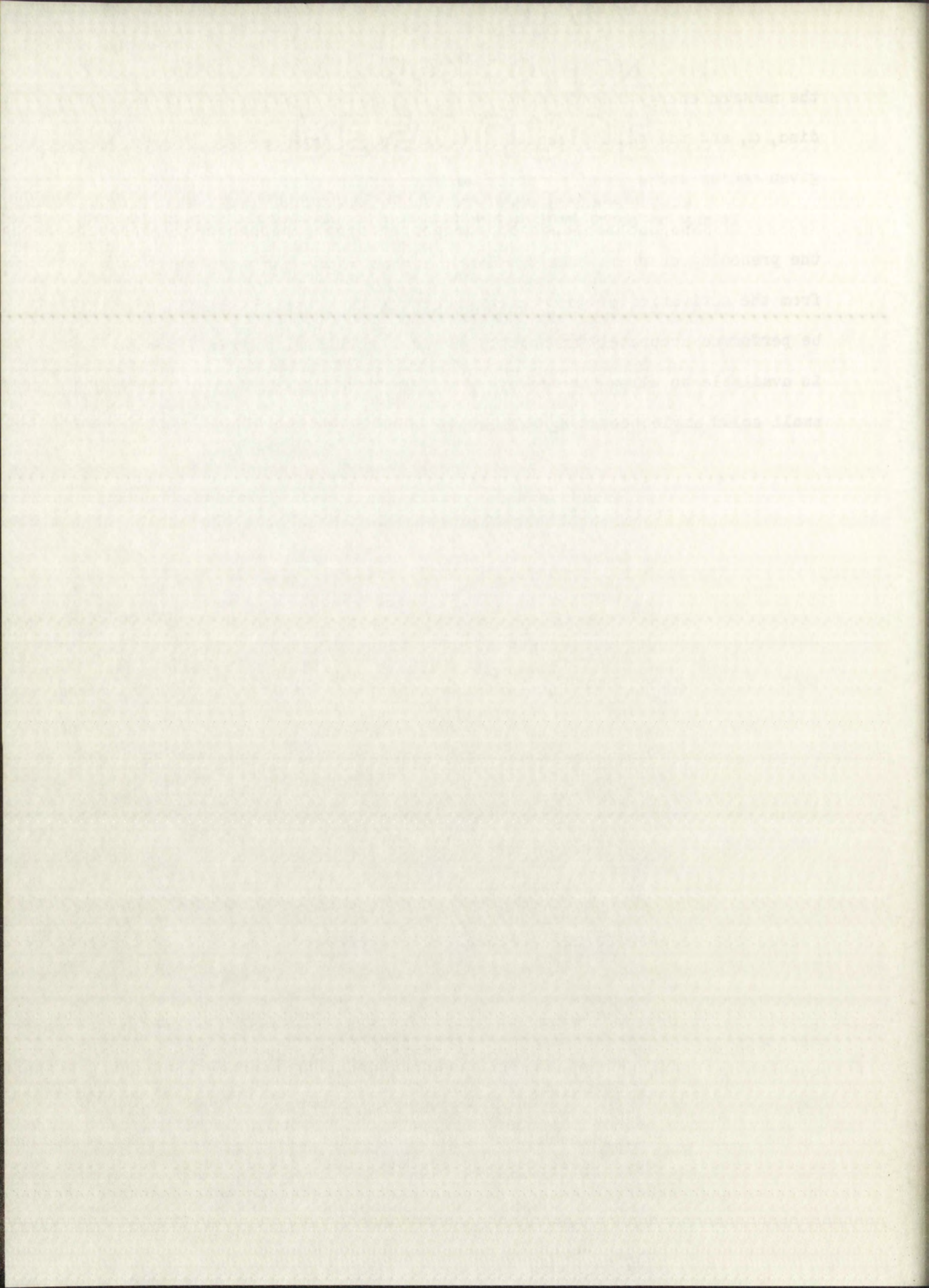
has been ...
 practical ...
 Hinton and ...

is difficult to ...
 distribution so ...
 the calculation of ...

The ...
 given ...
 to approximately ...

the neutron energy distribution) of the capture probability of a finite disc, α , and the return probability, $\beta(0)$ or if possible $\beta(\alpha)$, for the given medium and size of detector would be of interest.

It may be concluded from the above data and the discussion in the preceding chapters that the determination of the neutron density from the activation of gold foils, utilizing the proposed methods, may be performed accurately and simply provided sufficient neutron intensity is available to allow the use of relatively thin foils and an inefficient, small solid angle, counting system.



APPENDIX A

Section 1. Probability a neutron traverses the distance l without interaction.

Divide the distance l into $N = l/\Delta l$ equal lengths (N very large). The probability that the neutron survives the first interval Δl without interaction is $(1 - \Sigma\Delta l)$. The interaction probability is the same for each interval so the chance that the neutron traverses the entire length l without interaction is given by:

$$P(l) = (1 - \Sigma\Delta l)^N = (1 - \Sigma\Delta l)^{l/\Delta l} .$$

Expanding the expression on the right yields:

$$\begin{aligned} (1 - \Sigma\Delta l)^{l/\Delta l} &= 1 - \Sigma\Delta l(l/\Delta l) + l/\Delta l (l/\Delta l - 1) (\Sigma\Delta l/2!)^2 \\ &- l/\Delta l(l/\Delta l - 1) (l/\Delta l - 2) (\Sigma\Delta l/3!)^3 + \dots . \end{aligned}$$

For vanishingly small Δl one obtains:

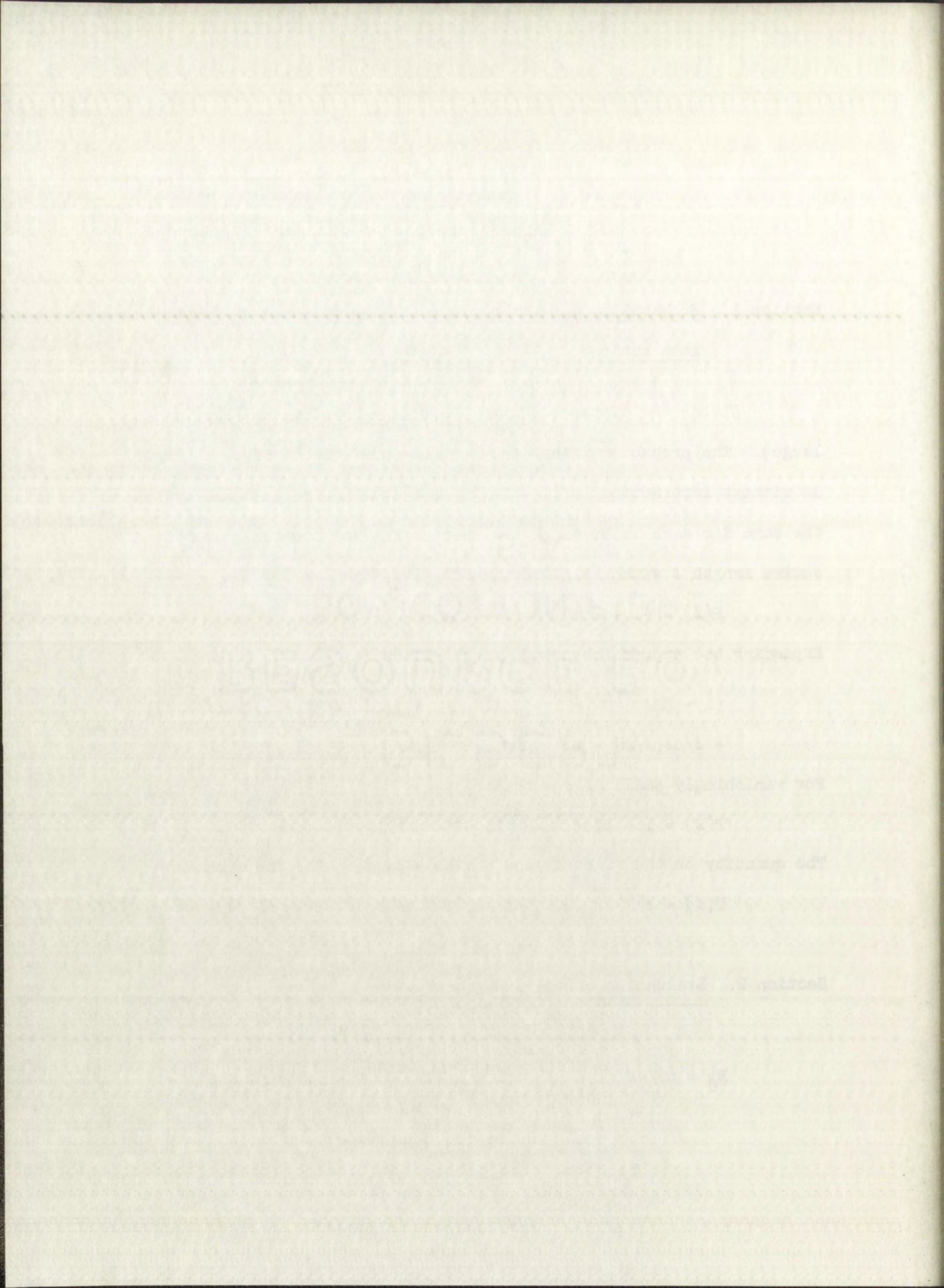
$$P(l) = 1 - \Sigma l + (\Sigma l)^2/2! - (\Sigma l)^3/3! + \dots .$$

The quantity on the right is the series expansion for the exponential.

$$P(l) = e^{-\Sigma l} .$$

Section 2. Evaluation of the integral R_θ .

$$R_\theta = nv/4\pi \int_0^\pi \int_0^{2\pi} (1 - e^{-\Sigma t/|\cos\theta|}) |\cos\theta| \sin\theta d\theta d\phi .$$



$$R_{\theta} = nv/4\pi \int_0^{\pi/2} (1 - e^{-\Sigma t / \cos\theta}) \cos\theta \sin\theta d\theta$$

$$= nv [1/2 - \int_0^{\pi/2} e^{-\Sigma t / \cos\theta} \cos\theta \sin\theta d\theta] .$$

Let $u = \cos\theta$.

$$R_{\theta} = nv [1/2 - \int_1^{\infty} \frac{e^{-\Sigma tu}}{u^3} du] ,$$

$$= nv [1/2 - E_3(\Sigma t)] .$$

Integrating twice by parts gives:

$$R_{\theta} = nv [1 - e^{-\Sigma t} (1 - \Sigma t) - (\Sigma t)^2 E_1(\Sigma t)] .$$

Section 3. Evaluation of R_M in terms of the Zahn integral.

$$R_M = \int_0^{\infty} \int_0^{\pi/2} \frac{4n_0}{\sqrt{\pi}} (v/v_0)^3 \exp[-(v/v_0)^2]$$

$$\times (1 - \exp[-\Sigma_0 t v_0 / v \cos\theta]) \cos\theta \sin\theta d\theta dv .$$

Let $u = v^2/v_0^2$.

$$R_M = \frac{2}{\sqrt{\pi}} n_0 v_0 \int_0^{\infty} \int_0^{\pi/2} u e^{-u} (1 - e^{-\Sigma_0 t / v_0 u \cos\theta}) \cos\theta \sin\theta d\theta du .$$

Let $y = u \cos^2\theta$, $dy = du \cos^2\theta$.

$$R_M = \frac{2 n_0 v_0}{\sqrt{\pi}} \int_0^{\infty} \int_0^{\pi/2} \frac{y}{\cos^3\theta} e^{-y/\cos^2\theta} (1 - e^{-\Sigma_0 t / \sqrt{y}}) \sin\theta d\theta dy .$$

$$f(x) = \int_0^x (x-t)^2 dt$$

$$f'(x) = \int_0^x 2(x-t) dt$$

Let $y = x-t$

$$f''(x) = \int_0^x 2 dt$$

$$f'''(x) = \int_0^x 2 dt$$

The general form of the function is

$$f(x) = \frac{1}{6}x^3 + C_1x^2 + C_2x + C_3$$

Section 2. Evaluation of \int in terms of the \int and \int

$$f(x) = \int_0^x \frac{1}{\sqrt{t}} dt$$

Let $y = \sqrt{t}$, then $t = y^2$

$$dy = \frac{1}{2\sqrt{t}} dt$$

$$f(x) = \int_0^{\sqrt{x}} \frac{1}{y} \cdot 2y dy$$

$$f(x) = 2 \int_0^{\sqrt{x}} 1 dy$$

$$f(x) = 2y \Big|_0^{\sqrt{x}} = 2\sqrt{x}$$

Let $\omega = y/\cos^2\theta$, $d\omega = 2y/\cos^3\theta \sin\theta d\theta$.

$$R_M = \frac{n_o v_o}{\sqrt{\pi}} \int_0^\infty \int_y^\infty (1 - e^{-\Sigma_o t/\sqrt{y}}) e^{-\omega} d\omega dy$$

$$= \frac{n_o v_o}{\sqrt{\pi}} \int_0^\infty e^{-y} (1 - e^{-\Sigma_o t/\sqrt{y}}) dy$$

$$= \frac{n_o v_o}{\sqrt{\pi}} [1 - \int_0^\infty e^{-y - \Sigma_o t/\sqrt{y}} dy] .$$

$$R_M = \frac{n_o v_o}{\sqrt{\pi}} (1 - f_o(\Sigma_o t)) .$$



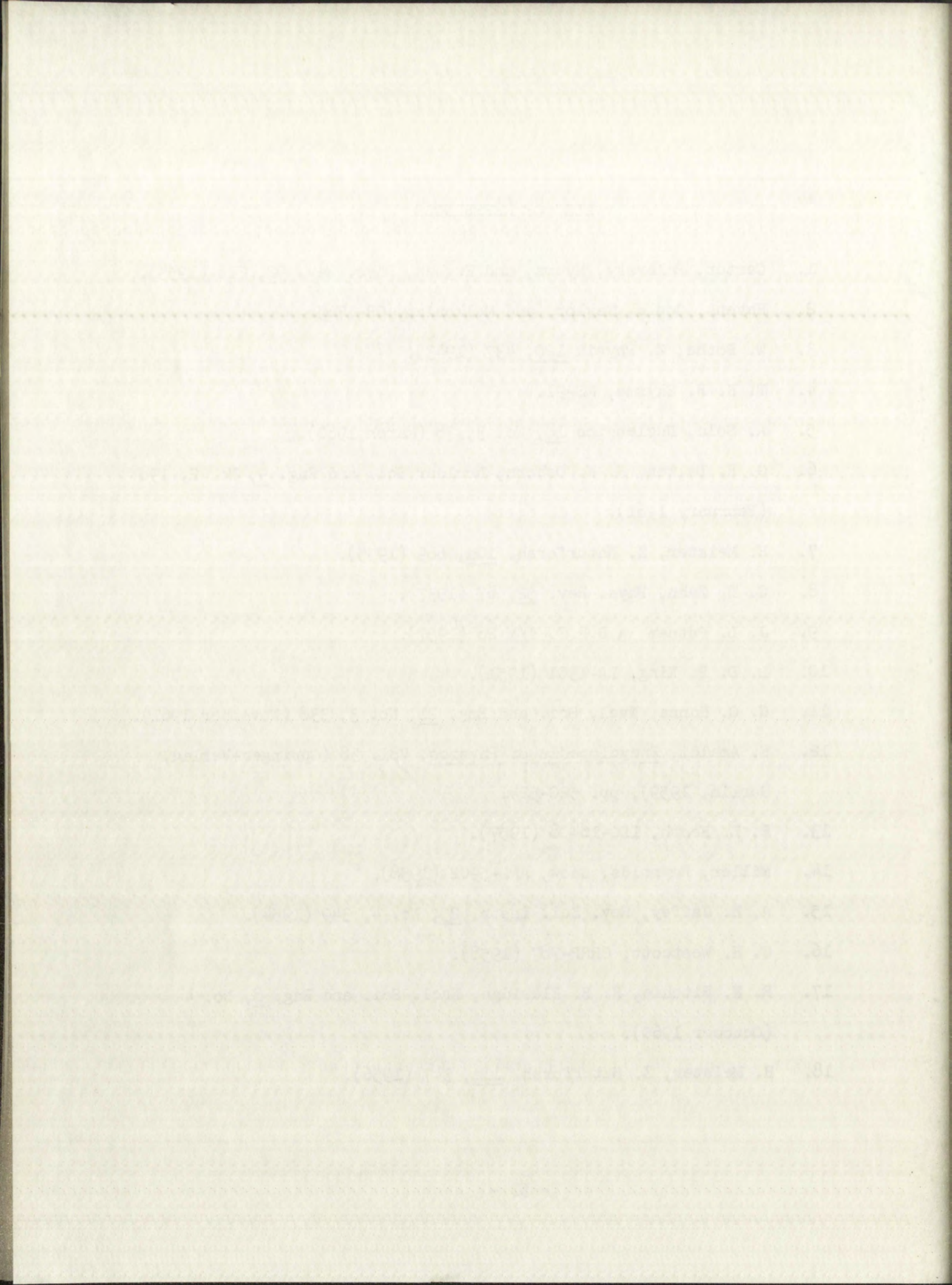


GEORGE BOND

1871

LIST OF REFERENCES

1. Carter, Palevsky, Myers, and Hughes, Phys. Rev. 92, 716 (1953).
2. Havens, Gould, Taylor, and Melkonian, CR-1765.
3. W. Bothe, Z. Physik 120, 437 (1943).
4. T. H. R. Skyrme, MS-91.
5. A. Sola, Nucleonics 18, No. 3, 78 (March 1960).
6. G. R. Dalton, R. K. Osborn, Nuclear Sci. and Eng. 9, No. 2, 198 (February 1961).
7. H. Meister, Z. Naturforsch. 10a, 669 (1955).
8. C. T. Zahn, Phys. Rev. 52, 67 (1937).
9. J. L. Putnam, A.E.R.E. 1/M 26 (1957).
10. L. D. P. King, LA-1301 (1951).
11. G. C. Hanna, Nucl. Sci. and Eng. 11, No. 3, 338 (November 1961).
12. E. Amaldi, Encyclopedia of Physics, Vol. 38 (Springer-Verlag, Berlin, 1959), pp. 520-524.
13. R. L. Heath, IDO-16408 (1957).
14. Miller, Reynolds, Snow, ANL-5902 (1958).
15. A. H. Jaffey, Rev. Sci. Instr. 25, No. 4, 349 (1954).
16. C. H. Westcott, CRRP-787 (1958).
17. R. H. Ritchie, H. B. Eldridge, Nucl. Sci. and Eng. 8, No. 4 (October 1960).
18. H. Meister, Z. Naturforsch. 11a, 347 (1956).



ADDED NOTE

The Subcommittee on Neutron Standards and Measurements of the Nuclear Science Committee of the National Research Council has been considering the problem of the measurement of neutron flux and density utilizing foil activation techniques. At a meeting held in Gainesville, Florida on November 13 and 14, 1961, methods were proposed for calculating the foil edge effect, and for comparing the calculations of Dalton and Osborn to the experimentally measured specific activity as a function of thickness. Unfortunately, the information (unpublished) concerning the proposed methods was received too late to be considered in this work.

